Professional Paper

SMARTS2, A Simple Model of the Atmospheric Radiative Transfer of Sunshine:

Algorithms and performance assessment

FSEC-PF-270-95
December 1995

Christian Gueymard

Florida Solar Energy Center
1679 Clearlake Road
Cocoa, Florida 32922-5703

A Research Institute of the University of Central Florida

Simple Model for the Atmospheric Radiative Transfer of Sunshine (SMARTS2)

Algorithms and performance assessment

Christian Gueymard

ABSTRACT

An upgraded spectral radiation model called SMARTS2 is introduced. The solar shortwave direct beam irradiance is calculated from spectral transmittance functions for the main extinction processes in the cloudless atmosphere: Rayleigh scattering, aerosol extinction, and absorption by ozone, uniformly mixed gases, water vapor, and nitrogen dioxide. Temperature-dependent or pressure-dependent extinction coefficients have been developed for all these absorbing gases, based on recent spectroscopic data obtained either directly from the experimental literature or, in a preprocessed form, from MODTRAN2, a state-of-the-art rigorous code. The NO_2 extinction effect, in both the UV and visible, is introduced for the first time in a simple spectral model. Aerosol extinction is evaluated using a two-tier Angström approach. Parameterizations of the wavelength exponents, single-scattering coefficient, and asymmetry factor for different aerosol models (proposed by Shettle and Fenn, Braslau and Dave, and also in the Standard Radiation Atmosphere) are provided as a function of both wavelength and relative humidity. Moreover, aerosol turbidity can now be estimated from airport visibility data using a function based on the Shettle and Fenn aerosol model.

An improved approximation to the extraterrestrial solar spectrum, treated at 1 nm intervals between 280 and 1700 nm, and 5 nm intervals between 1705 and 4000 nm, is based on recent satellite data in the UV and visible. The total irradiance between 280 and 4000 nm (1349.5 W/m^2) is obtained without scaling and is in good agreement with the currently accepted value of the solar constant (1367 W/m^2). Incident diffuse radiation and global radiation for any plane orientation at ground level are also calculated by the model, with provision for both multiple scattering effects and ozone absorption intricacies in the UV. SMARTS2 also has an optional circumsolar correction function and two filter smoothing functions which together allow the simulation of actual spectroradiometers. This facilitates comparison between modelled results and measured data.

Detailed performance assessment of the model is provided. It consists of prediction comparisons between the proposed model and rigorous radiative transfer models for different specific atmospheric conditions in the UV, visible, and near IR. High quality measured datasets in the UV and in the intervals 290–620 nm and 300–1100 nm are also used to validate the model by direct comparison. The resultant overall accuracy appears a significant improvement over existing simplified models, particularly in the UV. Therefore, SMARTS2 can be used in a variety of applications to predict full terrestrial spectra under any cloudless atmospheric condition.

CONTENTS

LIST OF TABLES

LIST OF FIGURES

1. INTRODUCTION

Spectral solar irradiance models are needed in a variety of applications spread among different disciplines such as atmospheric science, biology, health physics and energy technology (photovoltaic systems, high performance glazings, daylighting, selective coatings, etc.). In particular, Nann and Bakenfelder (1993) describe 12 possible uses of spectral radiation models for solar energy systems and buildings applications. Two types of spectral irradiance models may be used to predict or analyze solar radiation at the Earth's surface: sophisticated rigorous codes and simple transmittance parameterizations. A well known example of the first kind is the LOWTRAN family, which originated more than 20 years ago. It has been recently supplanted by an even more detailed code called MODTRAN (Anderson et al.,1993; Berk et al., 1989). This type of model considers that the atmosphere is constituted of different layers, and thus uses reference or measured vertical profiles of the gaseous and aerosol constituents.

Because of the required detailed inputs, execution time, and some output limitations, rigorous codes such as MODTRAN are not appropriate for all applications, particularly those in engineering. Most of the latter needs are presently filled by parameterized models which are relatively simple compared to MODTRAN. A number of these simple models have appeared in the literature since the early '80s (Bird, 1984; Bird and Riordan, 1986; Brine and Iqbal, 1983; Gueymard, 1993a; Justus and Paris, 1985; Matthews et al., 1987; Nann and Riordan, 1991). These models are based on Leckner's landmark contribution (1978). For computerized engineering calculations, SPCTRAL2 (Riordan, 1990), based on Bird (1984) and Bird and Riordan (1986), and SUNSPEC (McCluney and Gueymard, 1993), based on Gueymard (1993a), are frequently used. They both use Leckner's functions, at least for the determination of water vapor, mixed gases, and ozone absorption.

Much fundamental knowledge on gaseous absorption has been added since Leckner's work, so that a detailed reexamination of his approach now appears justified. Furthermore, data of higher spectral resolution are now available, improving the detail in those spectral regions where gaseous absorption changes rapidly with wavelength. Finally, it appeared necessary to undertake a detailed performance assessment of the model to guarantee its validity under most atmospheric conditions. Such an evaluation is an important part of the development of a radiation model, but few simple spectral models have been assessed as they ought to be. In fact, it appeared during the course of this study that most of the existing models could make incorrect predictions, both at short wavelengths and at large zenith angles.

This report develops the derivation of SMARTS2, an extensive revision of SMARTS1, a spectral model used to calculate direct beam and diffuse radiation (Gueymard, 1993a). There are nine main objectives and achievements in this study.

- Improve the extraterrestrial spectrum used (accuracy and resolution)
- Increase the spectral resolution of the transmittance calculations
- Introduce more accurate transmittance functions for all the atmospheric extinction processes, with consideration for temperature and humidity effects
- Add nitrogen dioxide (NO_2) to the list of absorbers, for the first time in this type of model
- Include highly accurate absorption coefficients from recent spectroscopic data
- Allow the calculation of diffuse irradiance in the UV and visible without the need for preliminary radiance calculations
- Add the capability to estimate the circumsolar enhancement factor for realistic comparison with radiometric data
- Add the flexibility to smooth the output irradiances using simulated radiometric filters
- Carefully assess the performance of the model against both reference radiative transfer models and high quality measured data.

2. SOLAR SPECTRUM

Whereas SMARTS1 and MODTRAN use the WRC85 extraterrestrial spectrum (Wehrli, 1985), SMARTS2 uses a modified spectrum. As no single recent dataset covers the whole spectrum, a composite of different datasets had to be devised in the same way as the original WRC85 spectrum. This new spectrum is justified for several reasons.

(i) Some problems were discovered in the WRC85 spectrum, including anomalous dips around 940, 1270, and 2300 nm [personal communications with Claus Fröhlich, 1992, Eric P. Shettle, 1993, and Bo-Cai Gao, 1994; see also Green and Gao (1993) and Gao and Green (1995)].

(ii) New high altitude balloon and satellite data have been published recently, particularly in the UV.

(iii) To obtain good resolution for subsequent applications, wavelength intervals needed to be both constant and small (see Section 7).

Between 280 and 412 nm, recent satellite data were obtained from Michael VanHoosier [personal communication, 1994]. They consist of the low-resolution version of measurements made on March 19, 1992 during a period of quiet sun with the SUSIM (Solar Ultraviolet Spectral Irradiance Monitor) instrument on board the Upper Atmosphere Research Satellite (UARS), as described by Brueckner et al. (1993). Data points listed at 0.25 nm intervals were reduced to a 1 nm step with a trapezoidal rule. The *total* irradiance between 280 and 412 nm is 123.34 W/m^2, which is close to the WRC85 value of 121.95 W/m^2. Although these two spectra have generally similar shapes, they do feature some noticeable differences, particularly in the 320-350 nm region. Figure 2.1a illustrates this, and also shows the older WRC81 spectrum at the resolution which is used in SPECTRAL2 and similar models.

Reference published spectra are used to construct the spectrum proposed here in the intervals 412-825 nm (Nicolet, 1989), and 825-2495 nm (Arvesen et al., 1969). The total irradiances in these spectral bands are 666.88 W/m^2 and 526.81 W/m^2, respectively. The WRC85 spectrum is used in the 2495-4000 nm interval only, and totals 32.43 W/m^2. The transition between the Nicolet and Arvesen spectra between 760 and 810 nm is smoothed using linear interpolation. Some probable outliers in the Nicolet spectrum were corrected in the 600-700 nm interval by comparison to the Arvesen et al. (1969) and Smith and Gottlieb (1974) spectra.

The total irradiance between 280 and 4000 nm is 1349.46 W/m^2, equivalent to the total WRC85 spectrum (1349.52 W/m^2), representing 98.72% of the solar constant of 1367 W/m^2. Although the two spectra happen to have identical total irradiances, an important difference between them is that the new spectrum does not revert to any renormalization to obtain the value of the solar constant, in contrast to the WRC85 spectrum. Figures 2.1b and 2.1c compare the new spectrum and those of the WRC in the visible and near IR.

The new spectrum (tabulated in the Appendix) has a total of 1881 wavelengths, at 1 nm intervals between 280 and 1700 nm, and at 5 nm intervals between 1705 and 4000 nm, with a transitional wavelength at 1702 nm. This is to be compared to 545 wavelengths for the downgraded WRC85 spectrum used in SUNSPEC and 122 wavelengths for the downgraded WRC81 spectrum used in SPCTRAL2.

The present resolution may be considered low by spectroscopists, just right by atmospheric physicists, or rather high by engineers. The 1 nm constant interval within the most important part of the spectrum is a good compromise between resolution and model complexity. The model's outputs (spectral transmittances and irradiances) can easily be downgraded afterwards if so desired by the user (see Section 7).

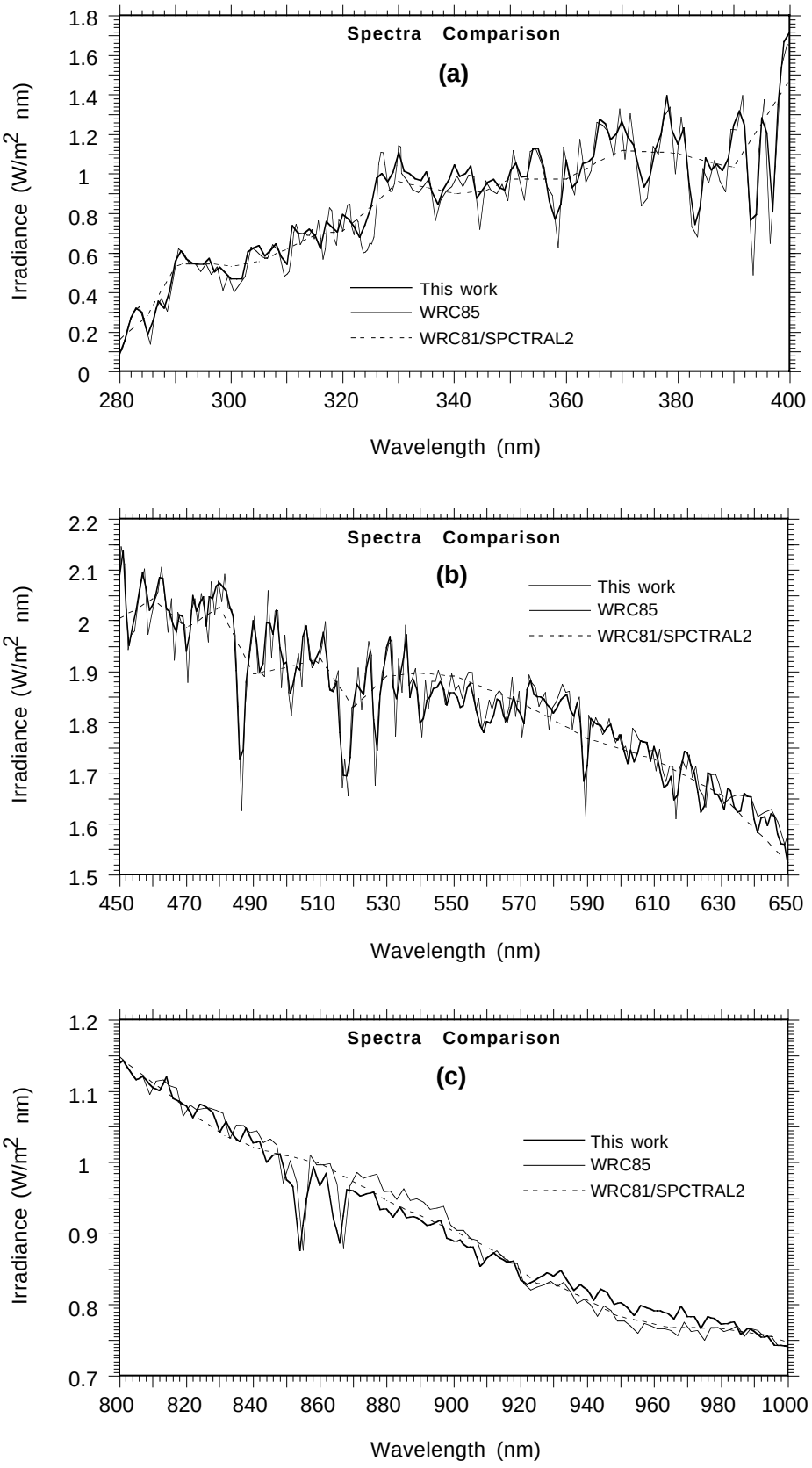

Fig. 2.1. Comparison of the solar spectrum used in SMARTS2 to other recent spectra for different bands. (a) 280–400 nm; (b) 450–650 nm; (c) 800–1000 nm.

3. REFERENCE ATMOSPHERES

Ten different reference atmospheres are proposed as defaults to the user. They consist of different vertical profiles of temperature, pressure, and of the concentrations of the main gases of the atmosphere. Six of these reference atmospheres are described by Anderson et al. (1986) and are also used in the LOWTRAN and MODTRAN families. Four supplementary atmospheres have been constructed for this work from other basic reference profiles (Anon., 1966). All profiles are defined with a vertical increment of generally 1 km. Table 3.1 lists the atmospheric parameters used for the first 4 km of the troposphere. Below this level, the atmospheric data (temperature, relative humidity, precipitable water, uniformly mixed gas abundance) may vary sharply with pressure and need to be interpolated. This is done in SMARTS2 using a four point Lagrange interpolation scheme for the vertical profile of each quantity listed above. The ozone and nitrogen dioxide total column abundances are also listed in Table 3.1, but only at *sea-level*. Because these constituents are normally largely concentrated in the stratosphere, their total abundance does not vary appreciably whenever the site altitude is below 4 km. For greater accuracy, a factor, C_t, can correct their total abundance at sea-level from the altitude, z, in km, using a linear fit based on the reference atmospheres' data:

$$C_t = 1 - 0.00898\, z\ . \tag{3.1}$$

A nominal or "effective" ozone temperature[1], T_{eo}, is defined as the weighted average of the concentration and temperature discretized profiles of the reference atmospheres (Anderson et al., 1986; Anon., 1966). This results in an average of 213 to 235.7 K for a sea-level site (Table 3.1). To approach actual conditions at any site and time, a correlation with the mean daily sea-level air temperature, T^*, obtained from the same dataset is considered:

$$T_{eo} = a_0 + a_1\, T^* \tag{3.2}$$

with a_0 = 332.41 K, a_1 = -0.34467 (summer) and a_0 = 142.68 K, a_1 = 0.28498 (winter). The use of a mean daily temperature instead of the instantaneous temperature, T, stems from the fact that the temperature at ground level is subject to daily fluctuations caused by solar heating of the ground and convection, and therefore decoupled from the less rapidly varying stratospheric temperature.

Relative humidity is tabulated for each level of the supplementary atmospheres (Anon., 1966). For the six primary reference atmospheres, it has been calculated from the mixing ratio of water vapor tabulated by Anderson et al. (1986), using the method described by Kneizys et al. (1980). Results appear in Table 3.1. (Relative humidity is an important "interactive parameter" that influences the size and optical properties of atmospheric aerosols, as will be shown in Section 4.2.6; it may also be used to estimate precipitable water, as mentioned in Section 4.2.5.)

Individual total column abundances are calculated in different ways. The total reduced thickness (in atm-cm) of O_3 and NO_2 is available for the six reference atmospheres considered in MODTRAN (Table 3.1). For the four supplementary atmospheres, new representative ozone values had to be proposed. The reference latitudes associated with these atmospheres (and indicated in Table 3.1) helped provide the needed ozone values, using average seasonal ozone distributions for the period 1957-75 (London, 1977) and the composite satellite data tabulated by Keating et al. (1990). Typical total NO_2 columns for the four supplementary atmospheres are selected from the limited data reviewed in Section 4.2.3.

---

[1] This effective temperature is only nominal—a temperature in name only—since the actual ozone molecules throughout the column's profile are not in thermodynamic equilibrium with each other. It is only a computational convenience, i.e., a single parameter description of a large-scale bulk system with substantial thermal gradient.

TABLE 3.1. Vertical profiles and effective pathlengths of ten reference atmospheres.
Key: USSA (U.S. Standard Atmosphere), MLS (Mid Latitude Summer), MLW (Mild Latitude Winter), SAS (Sub Arctic Summer), SAW (Sub Arctic Winter), TRL (Tropical), STS (Sub Tropical Summer), STW (Sub Tropical Winter), AS (Arctic Summer), AW (Arctic Winter), z (altitude), T_a (air temperature), T_{eo} (effective ozone temperature), p (pressure), RH (relative humidity).

Atmosphere		Vertical profiles				Effective pathlengths				
Latitude	z (km)	T_a (K)	T_{eo} (K)	p (mb)	RH (%)	O_2 (km)	CO_2 (km)	H_2O (cm)	O_3 (atm-cm)	NO_2 (atm-cm)
USSA	0	288.2	225.4	1013.3	45.5	4.9635	4.6854	1.419	0.3434	2.04E-4
45° N	1	281.7	223.4	898.8	48.7	3.9637	3.6853	0.899		
	2	275.2	221.3	795.0	51.8	3.1483	2.8836	0.566		
	3	268.7	219.4	701.2	50.6	2.4872	2.2449	0.326		
	4	262.2	217.7	616.6	50.0	1.9538	1.7389	0.193		
MLS	0	294.2	232.1	1013.3	75.7	4.9383	4.8866	2.927	0.3316	2.18E-4
45° N	1	289.7	229.7	902.0	65.6	3.9622	3.8792	1.727		
	2	285.2	227.3	802.0	54.8	3.1682	3.0651	1.024		
	3	279.2	224.9	710.0	45.0	2.5239	2.4089	0.561		
	4	273.2	222.4	628.0	38.8	2.0019	1.8849	0.325		
MLW	0	272.2	220.6	1018.0	77.0	5.0762	4.5566	0.855	0.3768	1.99E-4
45° N	1	268.7	218.7	897.3	70.4	3.9953	3.5658	0.549		
	2	265.2	217.0	789.7	65.4	3.1356	2.7789	0.346		
	3	261.7	215.4	693.8	56.7	2.4537	2.1555	0.188		
	4	255.7	213.9	608.1	49.8	1.9142	1.6630	0.104		
SAS	0	287.2	233.6	1010.0	74.9	4.9309	4.7057	2.079	0.3448	2.16E-4
60° N	1	281.7	231.7	896.0	69.8	3.9325	3.7118	1.316		
	2	276.3	229.6	792.9	69.7	3.1223	2.9148	0.836		
	3	270.9	227.5	700.0	65.0	2.4677	2.2784	0.483		
	4	265.5	225.4	616.0	60.3	1.9411	1.7724	0.280		
SAW	0	257.2	217.4	1013.0	80.4	5.0968	4.3277	0.424	0.3757	1.87E-4
60° N	1	259.1	216.1	887.8	69.3	3.9512	3.3635	0.295		
	2	255.9	214.8	777.5	69.9	3.0714	2.6003	0.193		
	3	252.7	213.5	679.8	65.6	2.3808	2.0009	0.107		
	4	247.7	212.1	593.2	60.4	1.8401	1.5315	0.057		
TRL	0	299.7	229.7	1013.0	74.9	4.9313	4.9539	4.117	0.2773	2.11E-4
15° N	1	293.7	226.9	904.0	72.3	3.9769	3.9407	2.494		
	2	287.7	224.3	805.0	74.2	3.1925	3.1198	1.441		
	3	283.7	221.8	715.0	47.8	2.5502	2.4572	0.735		
	4	277.0	219.6	633.0	34.7	2.0309	1.9237	0.432		
STS	0	301.2	224.5	1013.5	80.0	4.9006	4.9444	4.219	0.300	2.00E-4
30° N	1	293.7	221.5	904.6	65.0	3.9623	3.9412	2.593		
	2	288.2	218.8	805.1	60.0	3.1826	3.1254	1.695		
	3	282.7	216.4	714.8	60.0	2.5449	2.4660	0.998		
	4	277.2	214.1	633.1	50.0	2.0260	1.9359	0.604		
STW	0	287.2	221.2	1021.0	80.0	5.0198	4.8180	2.101	0.280	1.00E-4
30° N	1	284.2	218.3	906.4	70.0	4.0054	3.8100	1.218		
	2	281.2	215.7	803.5	50.0	3.1890	2.9977	0.709		
	3	274.7	213.4	710.7	45.0	2.5333	2.3443	0.369		
	4	268.2	211.2	626.8	35.0	2.0011	1.8234	0.209		
AS	0	278.2	235.7	1012.5	85.0	4.9733	4.6342	1.479	0.330	2.00E-4
75° N	1	275.6	232.9	895.0	75.0	3.9343	3.6494	0.965		
	2	273.0	230.3	790.2	65.0	3.1065	2.8618	0.615		
	3	268.4	228.0	696.7	60.0	2.4482	2.2332	0.343		
	4	261.9	225.9	612.5	55.0	1.9217	1.7341	0.195		
AW	0	249.2	213.0	1013.5	80.0	5.1357	4.1996	0.217	0.380	1.00E-4
75° N	1	252.2	210.4	884.1	65.0	3.9457	3.2454	0.150		
	2	250.9	208.1	772.1	60.0	3.0453	2.4954	0.093		
	3	245.4	206.0	672.7	55.0	2.3482	1.9077	0.051		
	4	239.9	204.1	584.3	50.0	1.8000	1.4517	0.029		

For water vapor, the incremental precipitable water, Δw, for an incremental atmospheric column of height Δz (normally 1 km) has been calculated from:

$$\Delta w = \rho_v \, \Delta z \tag{3.3}$$

where the water vapor density, ρ_v, is determined from the discretized humidity profile tabulated by Anderson et al. (1986) using the perfect gas laws. The total precipitable water above each level, w, is then obtained by Simpson's rule of integration, and expressed in g cm^{-2}, or equivalently in cm of height, as 1 cm^3 of condensed water has a mass of 1 g at standard temperature.
For O_2 and CO_2, the two most important absorbing gases, an effective reduced height, or scaled height, for a real (i.e., inhomogeneous) path has been obtained by scaling the actual density profiles with a Curtis-Godson approximation, in a way similar to Pierluissi and Tomiyama (1980) and Leckner (1978):

$$u_g = \int_z^\infty \left(\frac{p(h)}{p_0} \right)^n \left(\frac{T_1}{T(h)} \right)^m \left(\frac{\rho_a(h)}{\rho_{a0}} \right) dh \tag{3.4}$$

where $p(h)$, $T(h)$ and $\rho_a(h)$ are respectively the pressure, temperature and air density at level h, p_0=1013.25 mb, T_1 = 288.15 K, ρ_{a0} = 1.225 kg/m^3, and n and m are variable coefficients calculated for different gases and conditions by Pierluissi and Tsai (1987). They are taken here for O_2 and CO_2 as n = 0.9353 and 0.79, and m = 0.1936 and -1.3244, respectively. The scaled height u_g (in km) thus obtained for each gas is shown in Table 3.1.

Specific atmospheric conditions can be used instead of one of the reference atmospheres. If the site is not at sea level, it is necessary to correct eqn (3.2) for the difference between the sea-level and ground-level temperatures. This can be done roughly by extrapolating the selected atmospheric temperature profile as though the site were on a virtual tower having its base at sea-level. A pseudo-temperature gradient (in K/km) is fitted from the reference atmospheres as:

$$\Delta T = b_0 - b_1 \, T \tag{3.5}$$

where b_0 and b_1 are a function of the site altitude:

$$b_0 = \text{Min}\{49.42, \; 70.24 - 23.428 \, z + 2.523 \, z^2\} \tag{3.6a}$$

$$b_1 = \text{Min}\{0.1878, \; 0.26073 - 0.082424 \, z + 0.009098 \, z^2\}. \tag{3.6b}$$

This gradient can become negative at low temperatures because inversion layers appear near the surface in two of the reference cold atmospheres (SAW and AW). Such inversions frequently occur below 0°C as revealed by radiosonde soundings (Gueymard, 1994).

The numerical solution of eqn (3.4), obtained for the ten reference atmospheres and the data in Table 3.1, has been fitted to the O_2 and CO_2 scaled heights as a function of the site-level pressure, p, and temperature, T:

$$u_g = c_0 \, P^{c1} \, \theta^{c2} \tag{3.7}$$

where $P = p/p_0$, and $\theta = 288.15 \; / \; T$. The coefficients take the following values: for O_2, c_0 = 4.9293 km, c_1 = 1.8849, c_2 = 0.1815, and for CO_2, c_0 = 4.8649 km, c_1 = 1.9908, and c_2 = -0.697. If the site pressure is not known, it can be estimated from the site altitude and latitude according to the curve fit provided by Gueymard (1993b).

4. DIRECT BEAM RADIATION

Under cloudless sky conditions, direct beam radiation constitutes the major part of the incoming solar shortwave radiation, above about 400 nm. Moreover, its measurement can be used to derive information on probable atmospheric conditions (e.g., gaseous abundances and turbidity) by comparison with model calculations smoothed to approximate the instrument's spectral response. For these reasons, a major effort has been devoted to an accurate modeling of the individual *direct* transmittance functions. These functions are also used to then calculate *diffuse* radiation on a horizontal or tilted plane, as will appear in Section 5.

The beam irradiance received at ground level by a surface normal to the sun's rays (or "beam normal irradiance") at wavelength λ is given by

$$E_{bn\lambda} = E_{on\lambda}\, T_{R\lambda}\, T_{o\lambda}\, T_{n\lambda}\, T_{g\lambda}\, T_{w\lambda}\, T_{a\lambda} \tag{4.1}$$

where $E_{on\lambda}$ is the extraterrestrial irradiance corrected for the actual sun-earth distance and the other factors are the transmittances for the different extinction processes considered here: Rayleigh scattering, absorption by ozone, NO_2, uniformly mixed gases and water vapor, and finally, aerosol extinction. Note that NO_2 absorption in the UV and visible is introduced here for the first time in a simple spectral irradiance model. It is not yet considered in MODTRAN as of this writing. (The version used here, MODTRAN2, was kindly provided in August 1993 by Jim Chetwynd of Phillips Laboratory, Hanscom AFB.)

4.1 Sun's position and optical masses

The sun's apparent position is defined by its zenith angle and its azimuth. These angles are in turn obtained as a function of declination and hour angle through the algorithm described in the *Astronomical Almanac* (Nautical Almanac Office, 1992). It has been shown by Michalsky (1988) to have an accuracy better than 0.01° (for declination) which will be more than sufficient in the practical applications intended for SMARTS2.

Most simplified models use a single optical mass (usually the optical mass for air molecules or "air mass") to estimate the total slant path for all the extinction processes in the atmosphere. Different optical masses are considered here because each extinction process corresponds to a particular vertical concentration profile. Consideration of separate optical masses improves the model accuracy at large zenith angles, as they differ substantially above about 80°. The optical mass formulae have been fitted from the data rigorously calculated by Miskolczi et al. (1990). Other rigorous data at large zenith angles, from recent determinations including Mie scattering (Sarkissian, 1995; Sarkissian et al., 1995), were also added to better fit the optical masses of O_3 and NO_2; the NO_2 optical mass is further corrected in Section 4.2.3. The selected fitting function is similar to that proposed by Kasten (1965) and Kasten and Young (1989) but with better overall accuracy and the physical advantage of predicting a correct air mass of exactly 1.0 for a zenith sun:

$$m_i = [\cos Z + a_{i1}\, Z^{ai2}\, (a_{i3} - Z)^{a_{i4}}]^{-1} \tag{4.2}$$

where m_i stands for m_R (Rayleigh), m_a (aerosols), m_n (NO_2), m_o (ozone), m_g (mixed gases) or m_w (water vapor), Z is the zenith angle, and the coefficients a_{ij} appear in Table 4.1. The values of m_i for $Z = 90°$ are also indicated in Table 4.1, showing a wide dispersion between 16.6 and 71.4. In particular, the *air mass* thus calculated for $Z = 90°$ is 38.1361, in good agreement with the rigorously determined values, such as 38.1665 (Miskolczi et al., 1990) and 38.0868 (Kasten and Young, 1989).

Because of the model's capability to handle large zenith angles and optical masses, and the way the latter were defined in the first place (Young, 1974), it is stressed that the optical masses need to be used in conjunction with the *apparent* solar zenith angle, i.e., the true (astronomical) zenith angle minus refraction. Refraction is calculated according to the *Astronomical Almanac*, as a function of zenith angle, pressure, and temperature.

Situations for which the sun's disk is visible while its zenith angle is larger than 90° are rare but possible, e.g., at sunrise/sunset in mountainous areas with an open horizon, or as viewed from an airplane. To avoid numerical instability with eqn (4.2), the apparent zenith angle is limited to 91°, corresponding to a true astronomical angle of about 92°. This provision for solar depressions makes it possible to evaluate the diffuse irradiance just before sunrise or after sunset, when there is no direct radiation.

TABLE 4.1. Coefficients for the optical masses, eqn (4.2).

Extinction process	a_{i1}	a_{i2}	a_{i3}	a_{i4}	m_i @ Z=90°
Rayleigh	4.5665E–1	0.07	96.4836	–1.6970	38.136
Ozone	2.6845E+2	0.5	115.420	–3.2922	16.601
Nitrogen dioxide†	6.0230E+2	0.5	117.960	–3.4536	17.331
Mixed gases	4.5665E–1	0.07	96.4836	–1.6970	38.136
Water vapor	3.1141E–2	0.1	92.4710	–1.3814	71.443
Aerosols	3.1141E–2	0.1	92.4710	–1.3814	71.443

† For *stratospheric* NO_2 only; use the water vapor mass for *tropospheric* NO_2 and a weighted average for a combination of the two (see Section 4.2.3).

4. 2 Individual transmittances

4.2.1 Rayleigh scattering

The Rayleigh optical thickness has been calculated directly from its theoretical expression (see, for example, Kerker, 1969, and McCartney, 1976):

$$\tau_{R\lambda} = 24\pi^3 \frac{H_R}{N_0 \lambda^{-4}} \left(\frac{n_0^{\,2} - 1}{n_0^{\,2} + 2} \right)^2 \left(\frac{6 + 3\delta}{6 - 7\delta} \right) \tag{4.3}$$

where H_R is the atmospheric scale height (8.4345 km at 15°C), N_0 is the number density of molecules (2.547305E25 m^{-3} at 15°C), n_0 is the refractive index of air, δ is the depolarization factor, and λ is the wavelength. This equation has been reevaluated using the most recent determinations of δ (Young, 1981) and n_0 (Peck and Reeder, 1972), as recommended by Teillet (1990). Calculations were repeated every 2 nm between 250 and 1000 nm, and every 5 nm beyond 1000 nm. A least-squares curve fit was then used to develop the following equation[2] :

$$T_{R\lambda} = \exp(-\, m_R\, \tau_{R\lambda}) = \exp[-m_R\, P \,/\, (a_1\, \lambda^4 + a_2\, \lambda^2 + a_3 + a_4\, \lambda^{-2})] \tag{4.4}$$

where m_R is the optical air mass, P is the pressure correction defined earlier, a_1 = 117.2594 μm^{-4}, a_2 = -1.3215 μm^{-2}, a_3 = 3.2073E-4, and a_4 = -7.6842E-5 μm^2. Equation (4.4) fits the "exact" calculations obtained with eqn (4.3) with a deviation of 0.01% or less throughout the spectrum. This is an important improvement compared to a peak deviation of 3.4% at 540 nm (and larger

[2] Note that the wavelength unit is μm in all equations throughout this report even though units of nm are also employed in the text.

deviations beyond 2000 nm) for the frequently used Leckner equation (1978), and to an average deviation of about 1.5% for SPCTRAL2.

4.2.2 Ozone absorption

The Bouguer law is used to describe ozone absorption, i.e.,

$$T_{o\lambda} = \exp(-m_o\ \tau_{o\lambda}) \tag{4.5a}$$

where

$$\tau_{o\lambda} = u_o\ A_{o\lambda} \tag{4.5b}$$

is the ozone optical thickness, m_o its optical mass, u_o its reduced pathlength (in atm-cm), and $A_{o\lambda}$ its spectral absorption coefficient.

Ozone absorbs strongly in the UV, moderately in the visible, and slightly in the near infrared. Recent spectroscopic laboratory data from Daumont et al. (1992) are available for the Hartley-Huggins bands at 0.01 nm resolution. The original data [personal communication with Dominique Daumont] were smoothed in 1 nm steps, up to 344 nm. From 345 to 350 nm, data from Molina and Molina (1986) were downgraded from their original resolution of 0.5 nm. Between 351 and 355 nm, data from Cacciani et al. (1989) were used after smoothing to 1 nm. The same procedure was repeated between 356 and 365 nm, where the absorption coefficients were derived from the data in MODTRAN2 (based on unpublished data by Cacciani)[3]. The cut-off wavelengths of all these intervals were selected to reduce discontinuity at the blend between the different datasets.

A reference laboratory temperature, T_{ro} = 228 K, has been selected for all the datasets available to represent the basic absorption coefficients, $A_{o\lambda}(T_{ro})$. These coefficients are listed in the Appendix. Similar to Smith et al. (1992), a quadratic temperature correction is applied at other temperatures (if λ<344 nm), and particularly at the nominal ozone temperature:

$$A_{o\lambda}(T_{eo}) = \text{Max}\{0, A_{o\lambda}(T_{ro}) + c_1\ (T_{eo} - T_{ro}) + c_2\ (T_{eo} - T_{ro})^2\}. \tag{4.6}$$

(The Max function is used to avoid negative results, which may occur if T_{eo} is very low.)
The coefficients c_1 and c_2 were obtained by fitting the original datasets at 5 K intervals from 218 to 243K. Thus, for λ < 310 nm:

$$c_1 = (0.25326 - 1.7253\ \lambda\ + 2.9285\ \lambda^2) / (1 - 3.589\ \lambda) \tag{4.7a}$$

$$c_2 = (9.6635\text{E-}3 - 6.3685\text{E-}2\ \lambda\ + 0.10464\ \lambda^2) / (1 - 3.6879\ \lambda) \tag{4.7b}$$

and, for 310 ≤ λ ≤ 344 nm:

$$c_1 = 0.39626 - 2.3272\ \lambda\ + 3.4176\ \lambda^2 \tag{4.7c}$$

$$c_2 = 1.8268\text{E-}2 - 0.10928\ \lambda\ + 0.16338\ \lambda^2. \tag{4.7d}$$

In the visible (Chappuis band) and near infrared (Wulf band), recent data (Anderson, 1992, 1993)

---

[3] Note that MODTRAN2 outputs its results as a function of *wavenumbers* (in units of cm^{-1}), not wavelengths; a preliminary treatment of all MODTRAN2 results was therefore necessary to obtain the same wavelength intervals as used in SMARTS2.

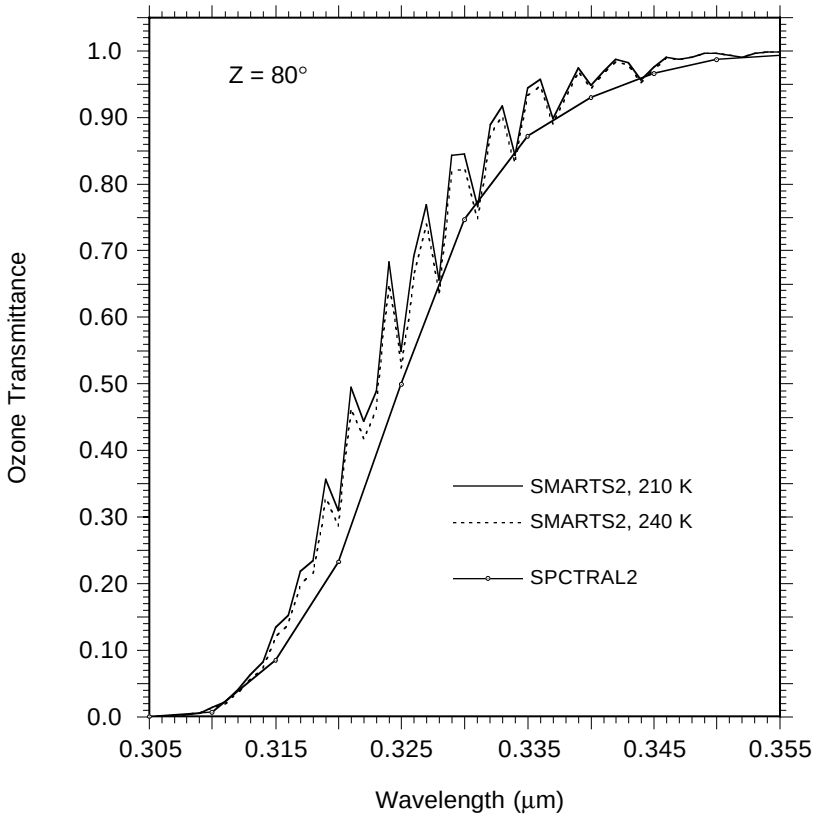

Fig. 4.1. Ozone transmittance predicted by SMARTS2 and SPCTRAL2.

were downgraded to 1 nm intervals from a dataset that will be used in future versions of MODTRAN (Shettle, 1994). The temperature effect here being less important than in the Hartley-Huggins band, a linear temperature correction is sufficient between 407 and 560 nm, and is obtained by interpolation between the two datasets for 228 and 240 K. The original data showed a significant temperature dependence up to 560 nm, and a negligible dependence between 560 and 762 nm. The following temperature correction is therefore applied only up to 560 nm:

$$A_{o\lambda}(T_{eo}) = \mathrm{Max}\{0, A_{o\lambda}(T_{ro})\,[1 + 0.0037083\,(T_{eo} - T_{ro})\exp[28.04\,(0.4474 - \lambda)]]\}. \qquad (4.8)$$

Finally, some very weak absorption bands are present above 3120 nm. The corresponding absorption coefficients were obtained by smoothing the MODTRAN2 transmittance results at 5 nm intervals up to 4000 nm.

The effect on the ozone transmittance of selecting two extreme nominal temperatures (210 and 240 K) is shown in Fig. 4.1 for a part of the Hartley-Huggins band. The jagged shape of these curves results from the detailed absorption structure characteristic of that band. At their peaks, these transmittances are significantly larger than SPCTRAL2 predictions, which use older absorption data and a coarser step (5 nm in this band).

4.2.3 Nitrogen dioxide absorption

Like ozone, NO_2 transmittance is modelled with Bouguer's law, i.e.,

$$T_{n\lambda} = \exp(-m_n\,u_n\,A_{n\lambda}) \qquad (4.9)$$

where m_n is the NO_2 optical mass, u_n its reduced pathlength (in atm-cm), and $A_{n\lambda}$ its spectral absorption coefficient. NO_2 is a highly variable atmospheric constituent which plays a key role in the complex ozone cycle, both in the stratosphere, where it is naturally present, and in the

troposphere, where its concentration may be high due to pollution. High concentrations of NO_2 over large cities are responsible in great part for the typical brown color of the pollution cloud (Husar and White, 1976). Total column measurements of NO_2 in an industrial city resulted in widespread values of u_n, ranging from 4.4E-5 to 1.3E-2 atm-cm, with a median of 1.66E-3 atm-cm (Schroeder and Davies, 1987). For comparison, the six most-used reference atmospheres (Anderson et al., 1986) list a total column of only about 2E-4 atm-cm NO_2 (Table 3.1). Actual long term measurements of the total NO_2 column for remote environments in both hemispheres show a typical seasonal pattern with a winter low of about 1E-4 atm-cm and a summer high of about 2E-4 atm-cm (Elansky et al., 1984; McKenzie and Johnston, 1984). Only a few other references discuss the variability of the tropospheric and/or stratospheric NO_2 abundances (Brewer et al., 1973; Coffey, 1988; Coffey et al., 1981; Elansky et al., 1984, 1994; Johnston et al., 1994; Kreher et al., 1995; McKenzie and Johnston, 1984; Mount et al., 1984; Noxon, 1978, 1979; Pommereau and Goutail, 1988; Solomon and Garcia, 1983; Song et al., 1994; Wofsy, 1978), so that the NO_2 climatology is still insufficiently known, particularly in urban environments.

The stratospheric and tropospheric NO_2 concentration profiles need also be considered. The stratospheric layer has a concentration profile similar to ozone in shape, whereas the tropospheric NO_2 is concentrated near the ground, similarly to aerosols. This has direct implication in the calculation of the NO_2 optical mass. Because no general optical mass formula for the highly variable vertical profile of NO_2 could be obtained from the literature, an approximation is now proposed. If only stratospheric NO_2 is present, m_n is calculated from eqn (4.2). Conversely, if the stratospheric NO_2 columnar height is negligible compared to its tropospheric counterpart, then the aerosol optical mass is used for the reason just explained. When the two layer loadings are of comparable magnitudes, an optical mass weighting is done similarly to the nominal NO_2 temperature described below.

The values of $A_{n\lambda}$ at different temperatures were derived from recent laboratory data (Davidson et al., 1988) in the 280-624 nm range and smoothed to 1 nm intervals from their original resolution (0.514 nm). Between 625 and 700 nm, data from Schneider et al. (1987) were used. As with ozone, a dependence of the absorption coefficients on the nominal NO_2 temperature is considered to extend the laboratory data. The reference temperature chosen here is T_{rn} = 243.2 K and the coefficients are listed in the Appendix for this temperature. For a nominal, or "effective", temperature T_{en}, the absorption coefficients are obtained as:

$$A_{n\lambda}(T_{en}) = \mathrm{Max}\{0, A_{n\lambda}(T_{rn})\,[1 + (T_{en} - T_{rn}) \sum_{i=0}^{i=5} f_i \lambda^i]\} \qquad (4.10)$$

where f_0 = 0.69773, f_1 = -8.1829, f_2 = 37.821, f_3 = -86.136, f_4 = 96.615, f_5 = -42.635, for $\lambda < 0.625$ μm, or else f_0 = 0.03539, f_1 = -0.04985, and $f_2 = f_3 = f_4 = f_5 = 0$.
Because of variations in the respective stratospheric and tropospheric concentrations of NO_2, its nominal atmospheric temperature is simply taken equal either to T_{eo} (for $u_n \leq$ 5E-4 atm-cm), or to T (when $u_n >$ 5E-3 atm-cm), or to their weighted mean between these limits.

The spectral transmittances for O_3 and NO_2 are compared in Fig. 4.2 for different total path-lengths, $m_o u_o$ and $m_n u_n$, respectively. These transmittances are almost equivalent in form but spectrally shifted when $m_n u_n$ is about a factor of 100 less than $m_o u_o$. This is equivalent to saying that NO_2 is about 100 times more efficient than ozone at absorbing radiation around their respective peak. However, it is also generally 20 to 10,000 times less abundant, so that its effect is significant, or more important than ozone, in polluted atmospheres only.

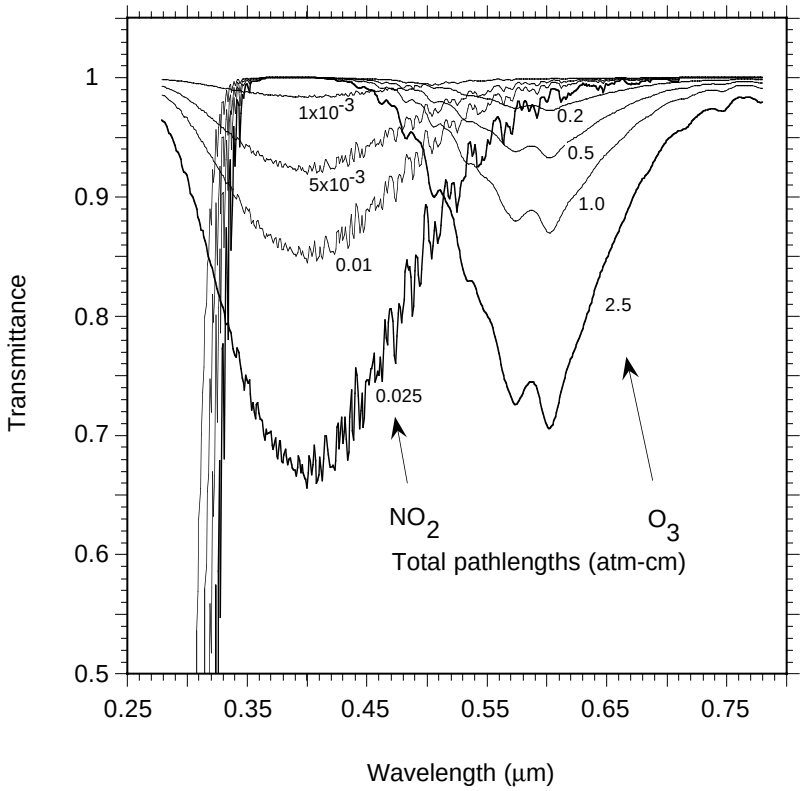

Fig.4.2. Ozone and NO_2 transmittances for different total pathlengths.

4.2.4 Uniformly mixed gas absorption

Some atmospheric constituents known as the "mixed gases" (principally O_2 and CO_2) have both a monotonically decreasing atmospheric concentration with altitude and significant absorption bands in the infrared. Using the analysis of Pierluissi and Tsai (1986, 1987), the mixed gas transmittance is defined as:

$$T_{g\lambda} = \exp[-(m_g\, u_g\, A_{g\lambda})^a] \tag{4.11}$$

where $m_g = m_R$ is the gas optical mass, $A_{g\lambda}$ is the spectral absorption coefficient, and u_g is the altitude-dependent gaseous scaled pathlength defined in Section 3. The value of u_g for O_2 is used below 1 μm and the value for CO_2 is used above, in accordance with their respective absorption spectra. The exponent a was obtained by averaging the data tabulated by Pierluissi and Tsai (1986, 1987): $a = 0.5641$ for $\lambda < 1$ μm, or else $a = 0.7070$. The values of $A_{g\lambda}$ (see the Appendix for their listing) were obtained by averaging MODTRAN2 transmittance results for different reference atmospheres, and inverting eqn (4.11). The mixed gas transmittance as obtained from eqn (4.11) for the Tropical reference atmosphere and a zenith angle of 80° is compared to other modelled values in Fig. 4.3. SMARTS2 and MODTRAN2 predictions are virtually indiscernible, as expected, whereas the cruder prediction of SPCTRAL2 is obvious. Note also the extremely sharp transition between 759 and 760 nm, where the transmittance drops from 0.97 to 0.08 for the modelled atmospheric conditions, due to strong absorption by O_2.

4.2.5 Water vapor absorption

In the near infrared spectrum, water vapor is by far the most important absorber. The accurate determination of its transmittance is therefore most important in this radiation model. Consequently, the functional form proposed by Pierluissi et al. (1989) has been slightly modified as follows:

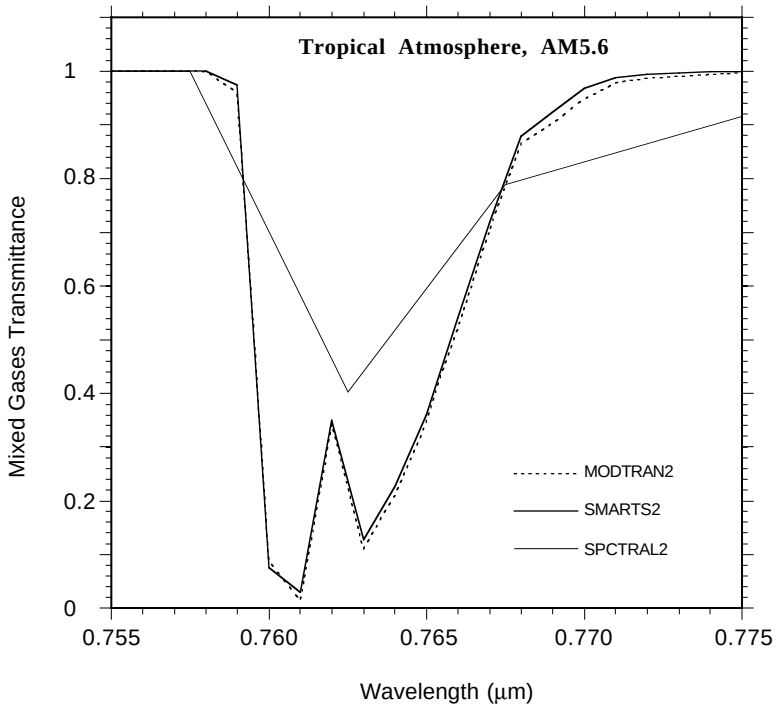

Fig. 4.3. Mixed gas transmittance in the visible.

$$T_{w\lambda} = \exp\{-[(m_w\, w)^{1.05}\, f_w^{\,n}\, B_w\, A_{w\lambda}]^c\} \tag{4.12}$$

where m_w is the water vapor optical mass, w the total precipitable water, c and n are wavelength-dependent exponents, B_w is a correction factor taking into account that the absorption process varies with the distance from the band center, and f_w is a pressure scaling factor that compensates for inhomogeneities in the water vapor pathlength by application of the Curtis-Godson approximation (Koepke and Quenzel, 1978; Leckner, 1978; Pierluissi et al., 1989). The latter factor is obtained similarly to the mixed gases reduced height, eqn (3.4), except that no temperature correction is necessary for water vapor in the visible and near infrared (see, e.g., Asano and Uchiyama, 1987; Ridgway and Arking, 1986; Tomasi, 1979):

$$f_w = k_w\,[0.394 - 0.26946\,\lambda\ + (0.46478 + 0.23757\,\lambda)\,P] \tag{4.13}$$

where $k_w = 1$ if $\lambda \leq 0.67$ μm, or else

$$k_w = (0.98449 + 0.023889\,\lambda)\,w^q \tag{4.14}$$

with

$$q = -0.02454 + 0.037533\,\lambda\,. \tag{4.15}$$

Exponents n and c in eqn (4.12) have been fitted from published data (Pierluissi et al., 1989) as:

$$n = 0.88631 + 0.025274\,\lambda - 3.5949\exp(-4.5445\,\lambda) \tag{4.16}$$

$$c = 0.53851 + 0.003262\,\lambda + 1.5244\exp(-4.2892\,\lambda) \tag{4.17}$$

The values of $A_{w\lambda}$ were obtained the same way as the $A_{g\lambda}$ previously, i.e., from MODTRAN2 results (see the Appendix for their tabulation). In MODTRAN2, both the selective band absorption and the continuum parameterizations have been improved over the previous versions of MODTRAN and LOWTRAN. The coefficients $A_{w\lambda}$ take both these two effects into consideration. It is important to note that MODTRAN2 absorption calculations are themselves based on HITRAN'92, the latest edition of a high resolution spectroscopic atlas for *line-by-line* calculations (Rothman et al., 1992). Although the relation between HITRAN'92 and SMARTS2 is indirect and involves some smoothing and downgrading, it should retain enough accuracy for the applications envisioned here.

The band wing correction factor, B_w, is introduced to improve the parameterization away from the absorption band centers in varying humidity conditions. It has been obtained by analyzing several MODTRAN2 runs for different combinations of zenith angles and atmospheres. It is parameterized as:

$$B_w = \mathrm{h}(m_w\, w)\, \exp(0.1916 - 0.0785\, m_w + 4.706\mathrm{E}\text{-}4\, m_w^2) \tag{4.18}$$

where

$$\mathrm{h}(m_w\, w) = 0.624\, m_w w^{0.457} \quad \text{if } A_{w\lambda} < 0.01, \text{ or} \tag{4.19a}$$

$$\mathrm{h}(m_w\, w) = (0.525 + 0.246\, m_w\, w)^{0.45} \text{ otherwise.} \tag{4.19b}$$

It should be noted that because of the introduction of B_w and f_w in eqn (4.13), the water vapor transmittance is not a simple function of the product $m_w\, w$, as it is in all simplified models, but rather a function of w, m_w, and p, as theory predicts (Gates and Harrop, 1963; Yamanouchi and Tanaka, 1985).

Precipitable water, w, needs to be carefully specified or accurately determined to obtain correct extinction calculations in the near infrared. For applications involving reference atmospheres, the precalculated values of Table 3.1 may be used. Alternatively, for applications involving real atmospheric conditions, w can be indirectly measured by different experimental methods or estimated by using empirical relationships between w and the surface temperature and humidity (e.g., Gueymard, 1994; Leckner, 1978).

Figure 4.4 compares the water vapor transmittance in the 940 nm band (also called the "ρστ band") as calculated by SMARTS2, MODTRAN2, and SPCTRAL2 for the U.S. Standard Atmosphere (w = 1.419 cm) and an air mass of 1.5 (corresponding to the ASTM and ISO standardized conditions (ASTM, 1987a; ISO, 1992). The difference between the predictions of SMARTS2 and MODTRAN2 is virtually indiscernible, whereas SPCTRAL2 is off by a significant margin in some wavelength intervals, due to its cruder resolution and older absorption data. Figure 4.5 displays the same comparison, but with the Tropical Atmosphere (w = 4.117 cm) and a solar zenith angle of 80° (m_w = 5.58). Because of the increased total water vapor slant path (23 cm for Fig. 4.5, compared to 2.13 cm in Fig. 4.4), the spectral transmittance is extremely low between 930 and 960 nm, and also SMARTS2 predictions appear slightly off in some intervals. However, this slight discrepancy would have been worse without the factor B_w in eqn (4.12).

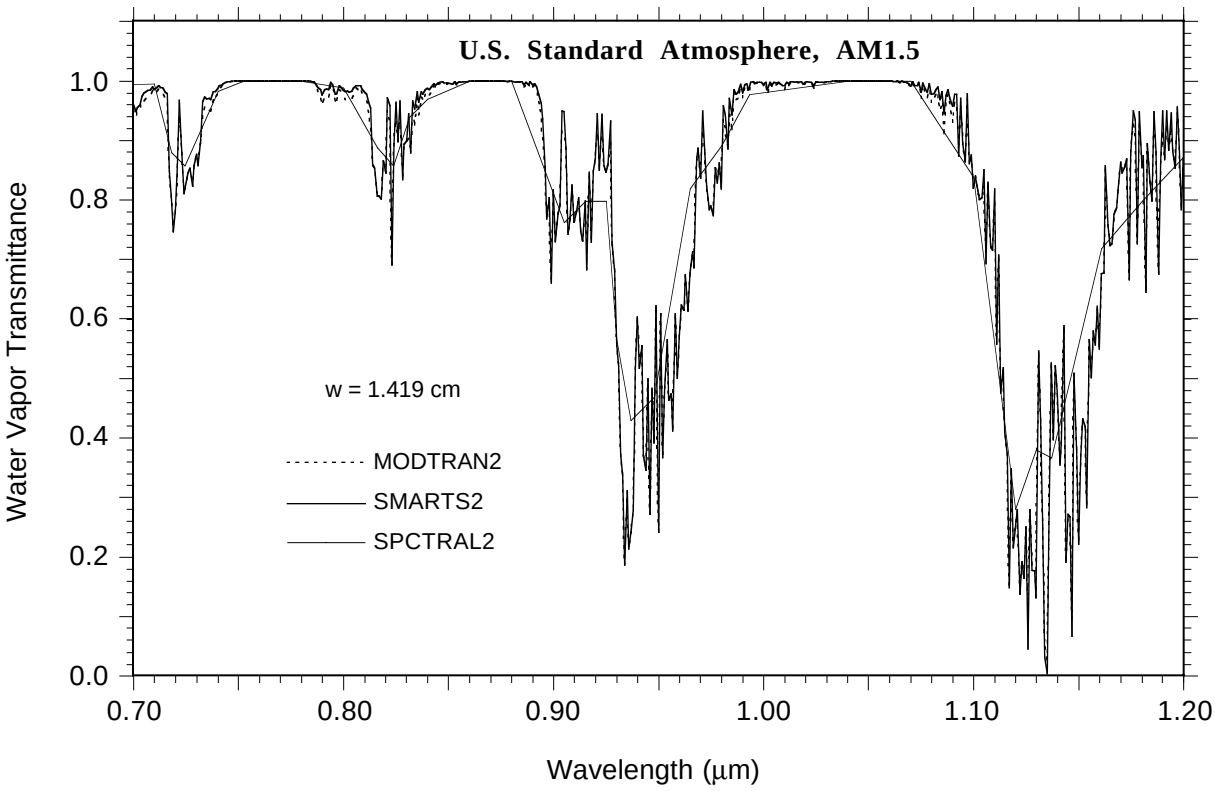

Fig. 4.4. Water vapor transmittance for the U.S. Standard Atmosphere and an air mass of 1.5.

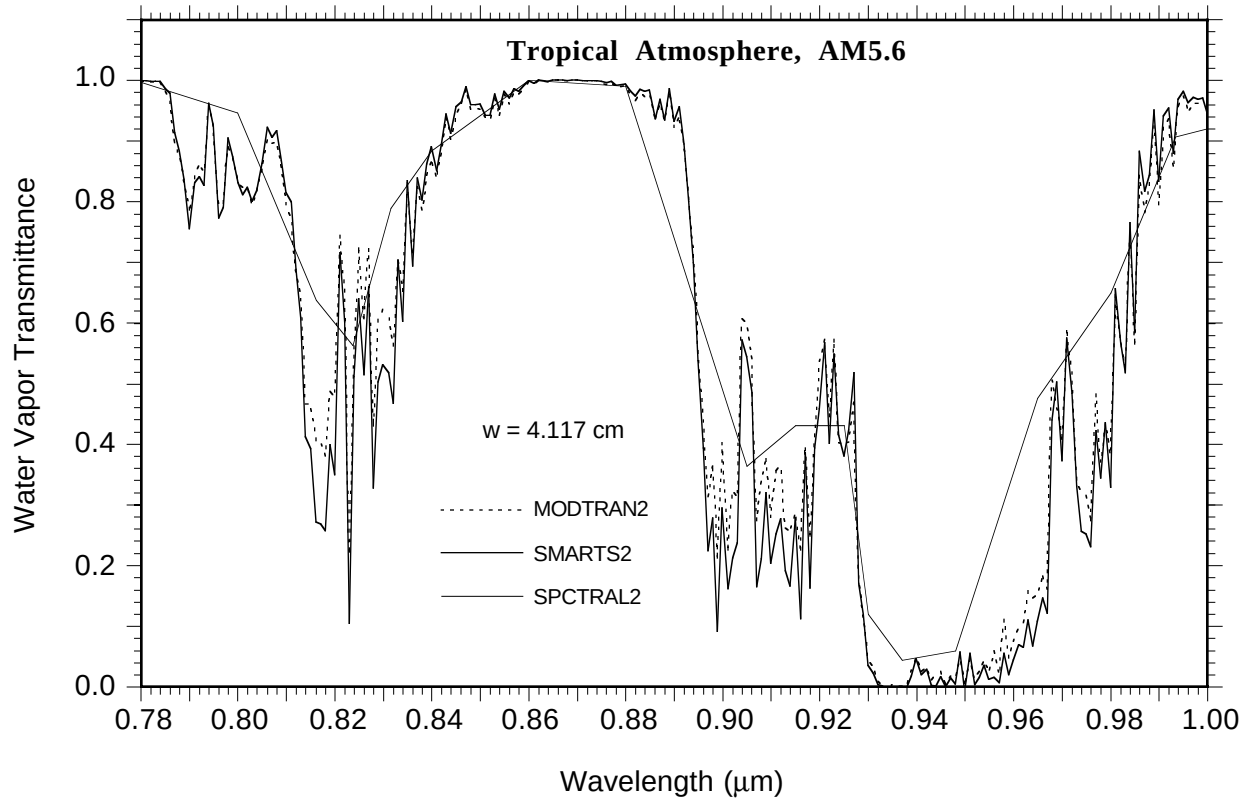

Fig. 4.5. Water vapor transmittance for a Tropical reference atmosphere and an air mass of 5.6.

4.2.6 Aerosol extinction

Spectral optical characteristics of both the tropospheric and stratospheric aerosols may change rapidly with time and with meteorological conditions. Although complete spectral determinations of the aerosol optical thickness would actually be needed for detailed modeling, such measurements are rare, and only broad climatological information is available in the general case, or only indirect estimates of turbidity based on visibility data.

This general lack of detailed aerosol data justifies the use of a simplified methodology, namely the modified Angström approach, which, as proposed by Bird (1984), considers only two different spectral regions, below and above λ_0 = 0.5 μm. The aerosol transmittance is obtained from the aerosol optical thickness, $\tau_{a\lambda}$, as:

$$T_{a\lambda} = \exp(-m_a\ \tau_{a\lambda}) \tag{4.20}$$

with

$$\tau_{a\lambda} = ß_i\ (\lambda/\lambda_1)^{-\alpha i} \tag{4.21}$$

where λ_1 = 1 μm, m_a is the aerosol optical mass, $\alpha_i = \alpha_1$ if $\lambda < \lambda_0$ and α_2 otherwise, and finally $ß_i = ß_1 = 2^{\alpha 2-\alpha 1}\ ß$ if $\lambda < \lambda_0$ and $ß_i = ß_2 = ß$ otherwise. Since $\tau_{a\lambda}$ is dimensionless in eqn (4.21), it is explicitly written as a function of a ratio, λ/λ_1.

Although turbidity is expressed here with the Angström coefficient, *ß* (defined at 1 μm), it can also be defined in terms of two alternate coefficients: Schuëpp's *B*, or the optical thickness τ_{a5} (both defined at λ_0). The correspondence between *ß*, *B* and τ_{a5} results from their respective definitions:

$$\tau_{a5} = 2^{\alpha 2}\ ß \tag{4.22}$$

$$B = \tau_{a5} / \ln 10. \tag{4.23}$$

Representative values of the wavelength exponents α_1 and α_2 have been obtained by linearly fitting (in log-log coordinates) the spectral optical coefficients of different reference aerosol models to eqn (4.21). This process is illustrated in Fig. 4.6 for a rural aerosol and shows that it is well described by the Angström model (α = 1.3), except in the UV. The four reference aerosols defined by Shettle and Fenn (1979), hereafter S&F, were used in LOWTRAN (starting with version 5) and MODTRAN, and their optical characteristics were tabulated for relative humidities between 0 and 99% in this cited report. The corresponding values of α_1 and α_2 obtained with the fitting technique explained above are given in Table 4.2. As it clearly shows, α_1 is always less than α_2, the average ratio α_1/α_2 is close to 0.7 for rural, urban, and maritime

TABLE 4.2. Wavelength exponents for different aerosol models (Shettle and Fenn, 1979).

Relative Humidity		0%	50%	70%	80%	90%	95%	98%	99%
Rural	α_1	0.933	0.932	0.928	0.902	0.844	0.804	0.721	0.659
	α_2	1.444	1.441	1.428	1.376	1.377	1.371	1.205	1.134
Urban	α_1	0.822	0.827	0.838	0.829	0.779	0.705	0.583	0.492
	α_2	1.167	1.171	1.186	1.229	1.256	1.252	1.197	1.127
Maritime	α_1	0.468	0.449	0.378	0.226	0.232	0.195	0.141	0.107
	α_2	0.626	0.598	0.508	0.286	0.246	0.175	0.098	0.053
Tropospheric	α_1	1.010	1.008	1.005	0.980	0.911	0.864	0.797	0.736
	α_2	2.389	2.379	2.357	2.262	2.130	2.058	1.962	1.881

aerosols at relative humidities ≤70%, and finally both α_1 and α_2 tend to decrease when relative humidity increases. This shows that the original Angström model (i.e, with $\alpha_1 = \alpha_2$ in eqn 4.21) is not appropriate for these reference aerosol models.

A fit of the data in Table 4.2 gives α_1 and α_2 from relative humidity and aerosol type:

$$\alpha_1 = (C_1 + C_2 X_{rh}) / (1 + C_3 X_{rh}) \quad (4.24a)$$

$$\alpha_2 = (D_1 + D_2 X_{rh} + D_3 X_{rh}^2) / (1 + D_4 X_{rh}) \quad (4.24b)$$

where coefficients C_i and D_i are found in Table 4.3 and

$$X_{rh} = \cos (0.9\, RH) \quad (4.25)$$

with an argument in degrees.

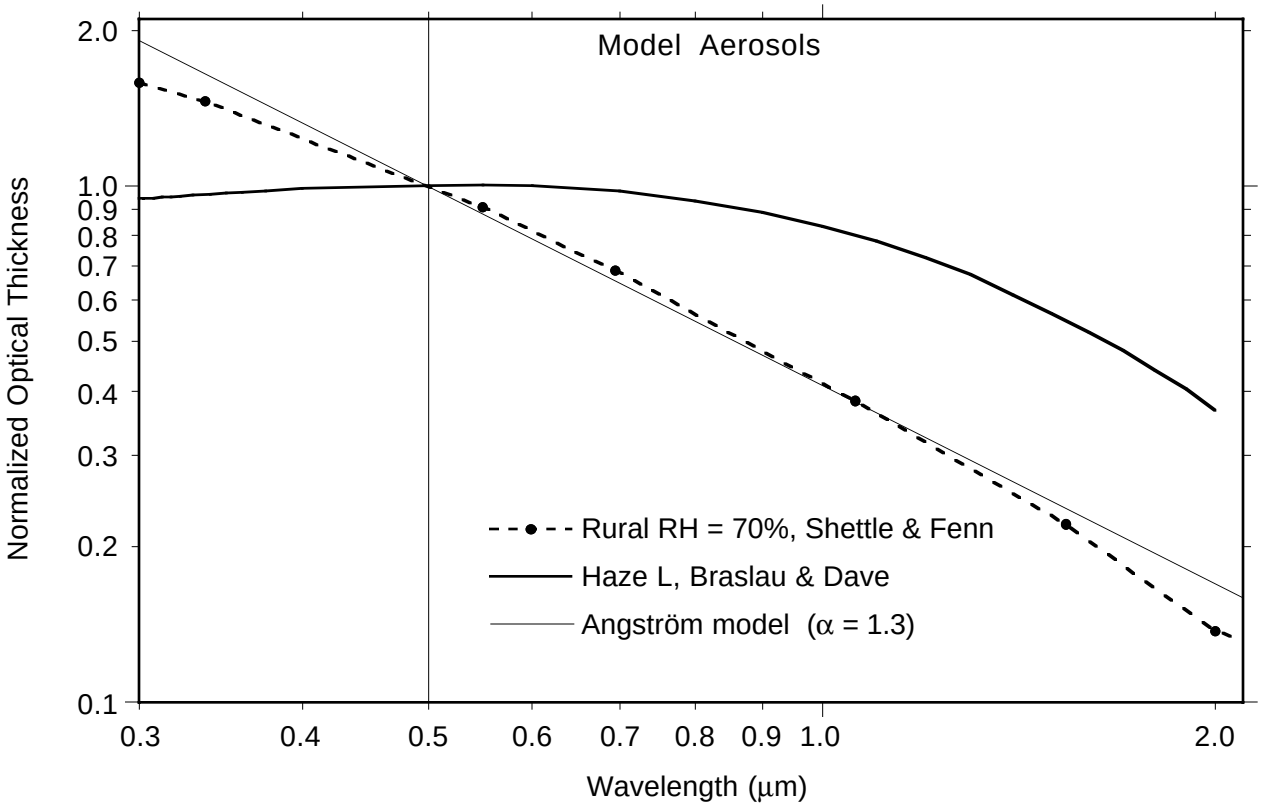

Fig. 4.6. Aerosol optical thickness (normalized to 0.5 μm) as a function of wavelength for selected aerosol models.

In the Braslau & Dave (hereafter B&D) atmospheric model (Braslau and Dave, 1973), no effect of relative humidity on the properties of the aerosol (of the *Haze L* type) is considered, which simplifies calculations. However, the aerosol optical thickness departs significantly from the Angström model, i.e., α actually varies considerably more with wavelength than this simple model predicts, as Fig. 4.6 illustrates. A significant gain of accuracy in the modeling of this relatively rare spectral behavior is obtained with the two-band split described by eqn (4.21). Using the same fitting technique as before, the resulting approximate values of α_1 and α_2 are -0.311 and 0.265, respectively. The negative sign of α_1 indicates that $\tau_{a\lambda}$ actually *decreases* with wavelength below about 500 nm, contrary to the "normal" behavior. A negative α_1 and a positive α_2 result in a flattened bell-shaped curve when plotting $\tau_{a\lambda}$ as a function of λ (Fig. 4.6).

Such a case may in fact be characteristic of maritime polar air masses, as observed in different circumstances by Weller and Leiterer (1988).

TABLE 4.3. Coefficients of eqn (4.24) for different aerosol models (Shettle and Fenn, 1979).

Coefficient	C_1	C_2	C_3	D_1	D_2	D_3	D_4
Rural	0.581	16.823	17.539	0.8547	78.696	0	54.416
Urban	0.2595	33.843	39.524	1.0	84.254	–9.1	65.458
Maritime	0.1134	0.8941	1.0796	0.04435	1.6048	0	1.5298
Tropospheric	0.6786	13.899	13.313	1.8379	14.912	0	5.96

A more recent and frequently used aerosol model is the preliminary standard known as the SRA (Standard Radiation Atmosphere) from IAMAP (1986). The relative humidity is here simply assumed to be below 70%, and thus without a direct effect on the optical characteristics of any of the three different aerosol types considered: continental, industrial and maritime. The average values of α_1, again obtained by linearly fitting the extinction coefficients, are respectively 0.940, 1.047 and 0.283, and those of α_2 are 1.335, 1.472 and 0.265. Data for other reference aerosols may be found elsewhere (d'Almeida et al., 1991), but some of the numerous tables this reference contains may be incorrect [personal communication with Eric P. Shettle, 1994].

If turbidity data are not available, it is possible to estimate the aerosol optical thickness from ground observations of visibility. When observing a standard target under ideal conditions[4], as assumed by the Koschmieder theory (1924), the farthest distance at which such a target can be observed provides a theoretical definition of the *meteorological range*, V_r, in km:

$$V_r = \ln(\varepsilon/C_t) / k_e = 3.912 / k_e \qquad (4.26)$$

where k_e is the total atmospheric extinction at 550 nm (close to the peak of the photopic curve). This extinction coefficient k_e (in km^{-1}) is the sum of the Rayleigh extinction coefficient, of the gaseous absorption coefficient (in case of absorbing gases in the line of sight, such as NO_2), and of the aerosol extinction coefficient. The latter is itself proportional to the aerosol optical thickness that is sought.

In practice, visibility (also called *visual range*, or more precisely, *prevailing visibility*) is reported at airports by human observers who use a few nonideal markers irregularly spaced. Various difficulties complicate the observation conditions[5], so that visibility thus obtained is only a crude estimate of the desired meteorological range. (See the analyses for non-standard viewing conditions by Allard and Tombach, 1981; Gordon, 1979; Gorraiz et al., 1986; and Horvath, 1971, 1981). Visibility is also generally skewed towards low values (Reiss and Eversole, 1978). According to the WMO recommendation, the most likely value for ε/C_t is 0.05, thus defining the

---

4 These conditions are: an ideal daytime observer threshold contrast ε = -0.02, a perfectly black target with an intrinsic contrast C_t = -1 as seen against the horizon, a perfectly homogeneous illumination, and perfectly homogeneous optical characteristics of the atmosphere.

5 For instance, (i) human vision is not a scientific instrument, (ii) visibility may not be the same in all directions, (iii) some gaseous absorption may be present and, moreover, not homogeneously distributed, (iv) ground relief may be an obstacle to distant markers. Their uneven distribution makes visibility a discontinuous function. Also, the markers may be non-black and seen in inhomogeneous illumination conditions, etc.

Meteorological Optical Range (MOR)[6]. Using eqn (4.26), the following formal relation between visibility or MOR, V, and meteorological range, V_r is obtained:

$$V_r = \eta\, V \tag{4.27}$$

where η is a constant resulting from the relative definitions of V and V_r, $\eta = \ln(0.02)/\ln(0.05) = 1.306$. But because of the fundamental disparity between the "practical" V and the "theoretical" V_r (as explained above), considerable spread can be expected in the exact value of η when dealing with *actual* observations of V. It has been observed to vary between 1.0 and 1.6, depending on local conditions (Gordon, 1979; Kneizys et al., 1980).

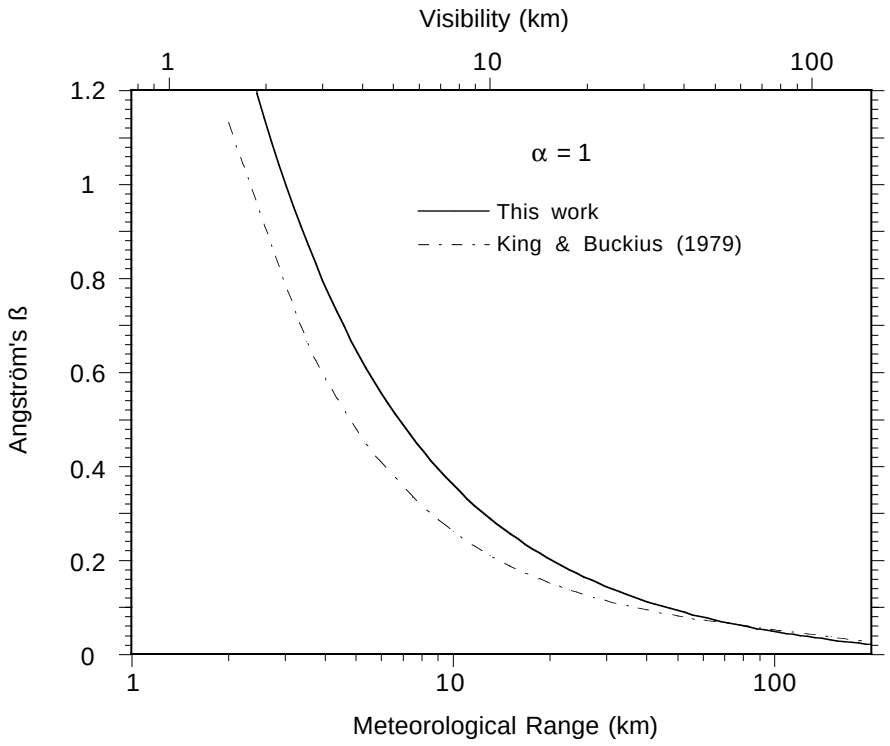

Fig. 4.7. Turbidity *vs* visibility and meteorological range.

MODTRAN2 was run for different meteorological ranges, reference aerosols and surface humidities to obtain the corresponding value of τ_{a5}, from which $ß$ and B can be obtained from eqns (4.22, 4.23). A fit of these data gives:

$$ß = 0.55^{\alpha_2}\,[1.3307\,(V_r^{-1} - V_m^{-1})^{0.614} + 3.4875\,(V_r^{-1} - V_m^{-1})] \tag{4.28}$$

where $V_m = 340.85$ km is the theoretical maximum meteorological range, obtained for a pure Rayleigh atmosphere corresponding to $ß = 0$. No additional dependence on the particular reference aerosol or its relative humidity could be isolated. Equation (4.28) is proposed here as a replacement for the King and Buckius equation[7] (1979), which was based on a now outdated aerosol model. The predictions of the two equations are compared in Fig. 4.7 which shows that eqn (4.28) predicts significantly larger turbidities for meteorological ranges below about 50 km.

---

[6] There is a great risk of confusion between Koshmieder's meteorological range and the WMO's MOR, as both definitions are frequently used and the terminology is not standardized.

[7] This equation was later incorrectly attributed to Selby and McClatchey in Iqbal's textbook (1983).

Figure 4.8 presents a comparison of the transmittances for S&F's rural aerosol and the USSA atmospheric conditions, as predicted by SMARTS2, MODTRAN2, and SPCTRAL2. The latter simply uses eqn (4.21) with $\alpha_1 = \alpha_2 = 1.14$ (i.e., the straight Angström model). Both SMARTS2 and SPCTRAL2 have been used with $\tau_{a5} = 0.3442$, a value that generates the same aerosol transmittance at 500 nm than a meteorological range of 25 km in MODTRAN2. It should be noted that the ASTM and ISO standards (ASTM, 1987a, 1987b; ISO, 1992) are based on $\tau_{a5} = 0.27$, a value said to correspond to $V_r = 25$ km according to both Bird et al. (1983) and to versions 4 or earlier of LOWTRAN—or incorrectly, to 23 km according to ASTM (1987a, 1987b) and ISO (1992). This correspondence between $V_r = 25$ km and $\tau_{a5} = 0.27$ results from the same outdated aerosol model used by King and Buckius and therefore does not appear appropriate anymore. MODTRAN2 uses a more recent and detailed aerosol model (Shettle, 1989; Shettle and Fenn, 1979) which explicitly considers the direct effect of humidity on the optical properties of aerosols; this is the same detailed reference aerosol model that has been used here to obtain Table 4.2, and eqns (4.24), (5.7), and (5.12). However, as partially illustrated in Fig. 4.8, MODTRAN2 evaluates the aerosol transmittance at only 13 wavelengths between 280 and 4000 nm, and linearly interpolates between these. Due to the actual curvature of the transmittance curve, this underestimates the aerosol transmittance if $\alpha > 0$ (the case of Fig. 4.8), or overestimates it otherwise, between the calculated reference points.

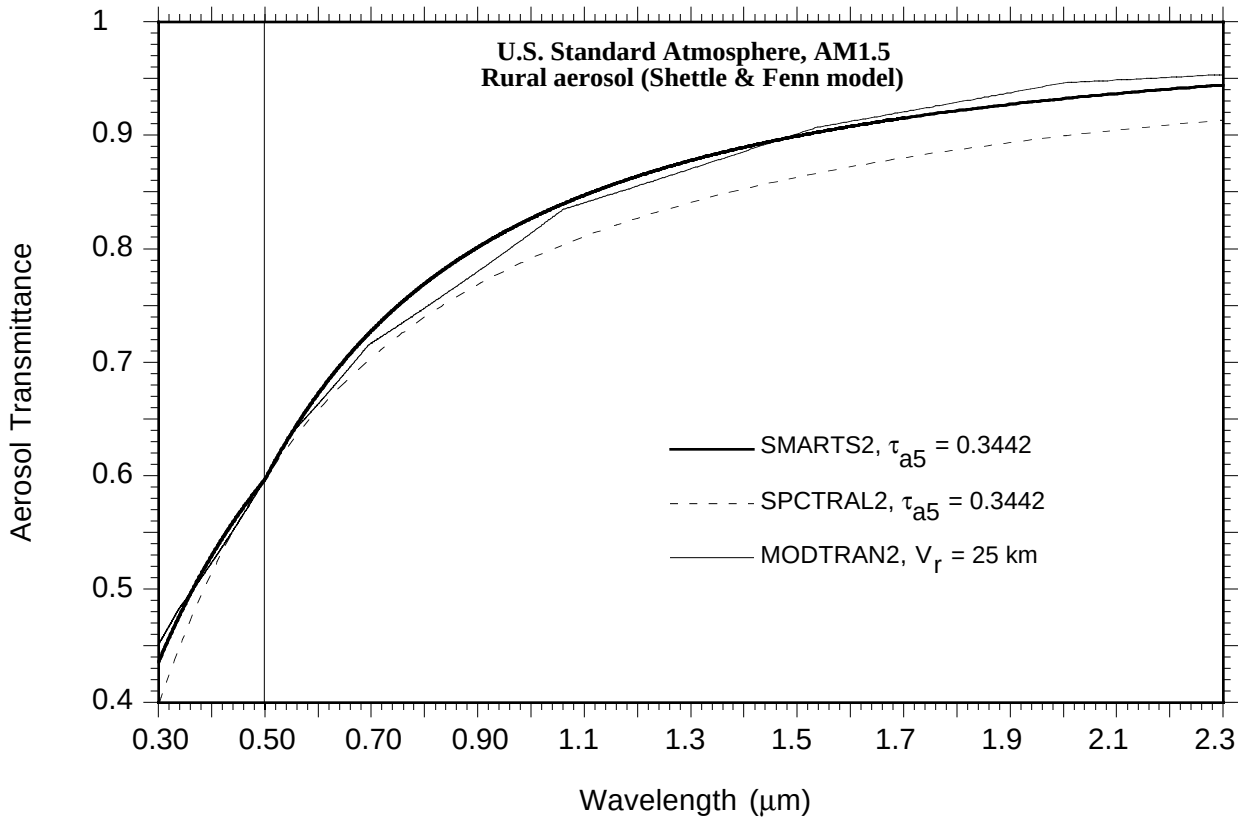

Fig. 4.8. Aerosol transmittance predicted by SMARTS2 and other models for a meteorological range of 25 km.

5. DIFFUSE RADIATION

Terrestrial diffuse radiation results from the complex radiance field of the sky and should theoretically be calculated as an integration of radiance over the whole sky vault. This is the approach used by rigorous codes (e.g., MODTRAN2; Bird and Hulstrom, 1982; Braslau and Dave, 1973; Dave and Halpern, 1976; Lenoble, 1985), but this method implies extensive computer calculations because radiance from a large number of sky elements needs to be evaluated first, and then integrated both spatially and spectrally. In the particular case of MODTRAN2 for example, one separate run is necessary for each sky element, and a minimum of a few hundred of these elements is necessary to perform an accurate numerical integration in clear skies. This precludes the use of such a method whenever a fast determination of diffuse irradiance is necessary, such as in engineering applications.

Simplified models (e.g., SPCTRAL2) obtain the diffuse irradiance from the same transmittance functions used to determine the direct beam irradiance. This simplified approach has some theoretical justification because what photons are not directly transmitted are scattered in all directions, and a roughly predictable fraction of these is directed downwards and constitutes the diffuse irradiance at ground level. This approach will be used here, with some refinements over the existing algorithms.

Diffuse irradiance is considered as the sum of three components—due to Rayleigh scattering, aerosol scattering and ground/sky backscattering. The first two components are corrected to take into account the multiple scattering effects, which are significant at shorter wavelengths.

5.1 Rayleigh component

The Rayleigh scattered component is calculated as:

$$E_{dR\lambda} = F_R\, E_{on\lambda}\, (1 - T_{R\lambda}^{0.9})\, \Gamma_{o\lambda}\, T_{n\lambda}\, T_{g\lambda}\, T_{w\lambda}\, T_{aa\lambda} \cos Z \qquad (5.1)$$

where $F_R = F_{R1} F_{R2}$ is the downward fraction of scattered radiation, $F_{R1} = 0.5$ is the downward scatterance for a single-scattering Rayleigh atmosphere. The correction factor for the multiple scattering effects of air molecules, F_{R2}, is obtained from Skartveit and Olseth (1988) as:

$$F_{R2} = 1 \text{ if } \tau_{R\lambda} < \tau_{Rm}, \text{ and} \qquad (5.2a)$$

$$F_{R2} = \exp\left[-\left(\frac{\tau_{R\lambda} - \tau_{Rm}}{\sigma_R} \right)^{0.72 + \cos Z} \right] \qquad (5.2b)$$

otherwise, where

$$\sigma_R = 3.65 - 2.3 \exp(-4 \cos Z) \qquad (5.3a)$$

$$\tau_{Rm} = 0.17\, [1 - \exp(-8 \cos Z)] \,. \qquad (5.3b)$$

All the transmittance functions in eqn (5.1) have been defined previously, except $\Gamma_{o\lambda}$ which will be discussed in Section 5.3, and the transmittance of the aerosol absorption process, $T_{aa\lambda}$, which is defined by:

$$T_{aa\lambda} = \exp[-m_a\, (\tau_{a\lambda} - \tau_{as\lambda})] \qquad (5.4)$$

where $\tau_{as\lambda} = \varpi_0 \tau_{a\lambda}$ is the optical thickness for aerosol scattering, and ϖ_0 is the single-scattering albedo. The latter is a fundamental optical characteristic aerosols (e.g., equal to 1.0 for a perfectly non-absorbing aerosol). For a real aerosol, it also normally varies with relative humidity and wavelength. The B&D reference absorbing aerosols, types C1 and D1 (Braslau and Dave, 1973), do not consider any humidity effect, therefore only the variation with wavelength has been fitted for it:

$$\varpi_0 = 0.9441 - 0.08817 \exp(1 - 3.3815\ \lambda) \tag{5.5a}$$

for $\lambda < 2$ μm, or else,

$$\varpi_0 = 0.8569 + 0.0436\ \lambda. \tag{5.5b}$$

Similarly for the SRA aerosol model (IAMAP, 1986):

$$\varpi_0 = \mathrm{Min}\left(0.99, \sum_{i=0}^{i=3} \phi_i \lambda^i\right) \tag{5.6a}$$

for $\lambda < 2$ μm, or, for $2 \le \lambda \le 4$ μm,

$$\varpi_0 = 1 - \frac{\upsilon_0 \exp[\upsilon_1(\lambda - \upsilon_2)]}{\{1 + \exp[\upsilon_1(\lambda - \upsilon_2)]\}^2} \tag{5.6b}$$

where the values of coefficients ϕ_i and υ_i are given in Table 5.1.

For the different reference aerosols of the S&F model (Shettle and Fenn, 1979), ϖ_0 is strongly dependent on both wavelength and humidity, as illustrated in Fig. 5.1 for the case of the urban aerosol. Because of the complex dependence on humidity and wavelength, the value of ϖ_0 is difficult to parameterize. It can be approximated with the same functions as in eqn (5.6) above, but with coefficients now dependent on relative humidity according to:

$$\phi_i = \sum_{j=0}^{j=2} \psi_{ij} RH_0{}^j \tag{5.7a}$$

for $i = 0$ to 3. Similarly,

$$\upsilon_i = \sum_{j=0}^{j=2} \psi_{ij} RH_0{}^j \tag{5.7b}$$

TABLE 5.1. Coefficients for the determination of the single-scattering albedo of the SRA aerosol model, eqn (5.6).

Aerosol type	Continental	Urban	Maritime
ϕ_0	8.4372E-01	6.4886E-01	9.6635E-01
ϕ_1	3.0206E-01	1.3465E-01	7.3464E-02
ϕ_2	-4.7838E-01	-3.0166E-01	-7.1847E-02
ϕ_3	1.5647E-01	8.3393E-02	1.9774E-02
υ_0	1.2853E-00	2.9784E-00	2.0006E-00
υ_1	1.4860E-00	6.1494E-01	7.1110E-00
υ_2	2.8357E-00	3.3122E-00	3.0136E-00

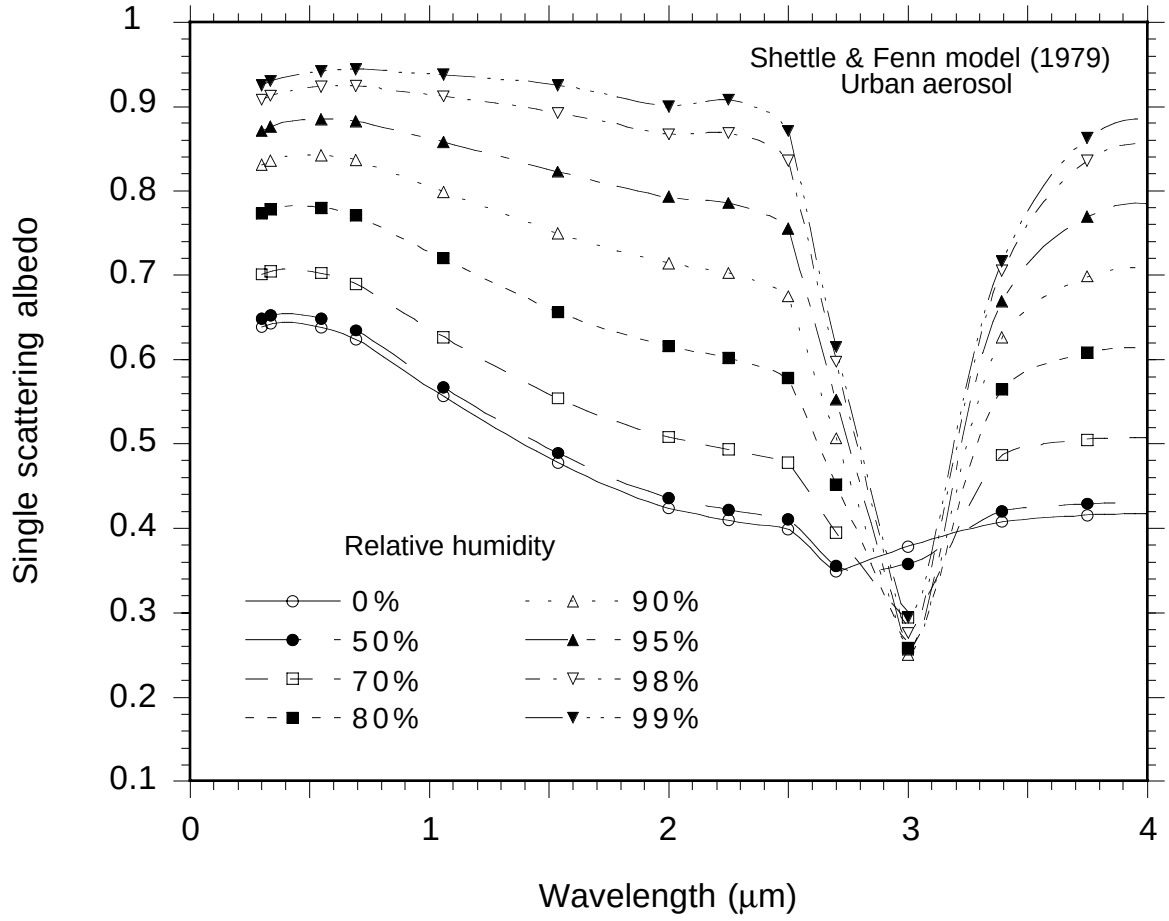

Fig. 5.1. Spectral single-scattering albedo of urban aerosol as affected by relative humidity.

for i = 0 and 2, and

$$\upsilon_1 = \exp(\psi_{11} + \psi_{12}\, RH_0 + \psi_{23}\, RH_0^2) \tag{5.7c}$$

with

$$RH_0 = \text{Max}\{RH, 50\}. \tag{5.7d}$$

The values of the coefficients ψ_{ij} are given in Table 5.2 for the different S&F reference aerosols.

5.2 Aerosol component

The aerosol-scattered irradiance is calculated as:

$$E_{da\lambda} = F_a\, E_{on\lambda}\, (1 - T_{as\lambda})\, \Gamma_{o\lambda}\, T_{R\lambda}\, T_{n\lambda}\, T_{g\lambda}\, T_{w\lambda}\, T_{aa\lambda} \cos Z \tag{5.8}$$

where $T_{as\lambda}$ is the transmittance for aerosol scattering, such that

TABLE 5.2. Coefficients for the determination of the single-scattering albedo of the Shettle & Fenn aerosol model, eqn (5.7).

Reference Aerosol	Rural	Urban	Maritime	Tropospheric
$\lambda < 2$ μm				
ψ_{00}	1.0151E-00	8.4946E-01	9.4016E-01	9.9926E-01
ψ_{01}	-6.0574E-03	-9.7903E-04	-3.5957E-04	-5.0201E-03
ψ_{02}	5.5945E-05	1.0266E-04	9.8774E-06	4.8169E-05
ψ_{10}	-1.2901E-01	-2.0852E-01	1.2843E-01	-5.5311E-02
ψ_{11}	2.1565E-02	1.2935E-02	1.2117E-03	1.8072E-02
ψ_{12}	-1.9500E-04	-9.4275E-05	-2.7557E-05	-1.6930E-04
ψ_{20}	2.0622E-01	3.9371E-01	-1.4612E-01	9.0412E-02
ψ_{21}	-3.1109E-02	-2.3536E-02	-8.5631E-04	-2.3949E-02
ψ_{22}	2.8096E-04	1.8413E-04	2.7298E-05	2.2335E-04
ψ_{30}	-8.1528E-02	-1.3342E-01	3.9982E-02	-3.9868E-02
ψ_{31}	1.0582E-02	7.3010E-03	3.7258E-04	7.5484E-03
ψ_{32}	-9.5007E-05	-5.7236E-05	-9.5415E-06	-6.9475E-05
$\lambda \geq 2$ μm				
ψ_{00}	3.0306E-00	7.5308E-00	-3.7748E-00	-4.4981E-00
ψ_{01}	1.2324E-01	-1.5526E-01	1.3631E-01	1.7798E-01
ψ_{02}	-6.4080E-04	1.0762E-03	-7.6824E-04	-9.9386E-04
ψ_{10}	1.0949E-00	-8.8621E-01	1.5129E-00	-5.0756E-00
ψ_{11}	5.4308E-03	-7.2508E-02	1.5867E-02	1.3536E-01
ψ_{12}	1.7654E-05	9.8766E-04	-1.2999E-04	-6.7061E-04
ψ_{20}	2.5572E-00	2.2092E-00	2.8725E-00	6.6072E-00
ψ_{21}	7.2117E-03	2.9849E-02	2.6098E-03	-8.1503E-02
ψ_{22}	-2.5712E-05	-2.2029E-04	-9.2133E-06	4.5423E-04

$$T_{as\lambda} = T_{a\lambda} / T_{aa\lambda} \tag{5.9}$$

and F_a is the fraction of the scattered flux that is transmitted downwards. Like F_R above, F_a is obtained as a product of a single-scattering fraction, F_{a1}, and a multiple-scattering correction factor, F_{a2}. The function F_{a1} is dependent on the aerosol asymmetry factor, g (see below for its estimation), according to Bird and Riordan (1986) and Justus and Paris (1987):

$$F_{a1} = 1 - 0.5 \exp[(a_{s0} + a_{s1} \cos Z) \cos Z] \tag{5.10a}$$

where

$$a_{s0} = [1.459 + (0.1595 + 0.4129 F_g) F_g] F_g \tag{5.10b}$$

$$a_{s1} = [0.0783 - (0.3824 + 0.5874 F_g) F_g] F_g \tag{5.10c}$$

$$F_g = \ln(1 - g). \tag{5.10d}$$

F_{a2} has been obtained indirectly by comparing the irradiances $E_{da\lambda}$ and $E_{dR\lambda}$, predicted by eqns (5.1) and (5.8), to those obtained by rigorous codes (Bird and Hulstrom, 1982; Dave and Halpern, 1976; Dave et al., 1975; Lenoble, 1985) for a combination of different atmospheric conditions and zenith angles. The following fit has been finally obtained:

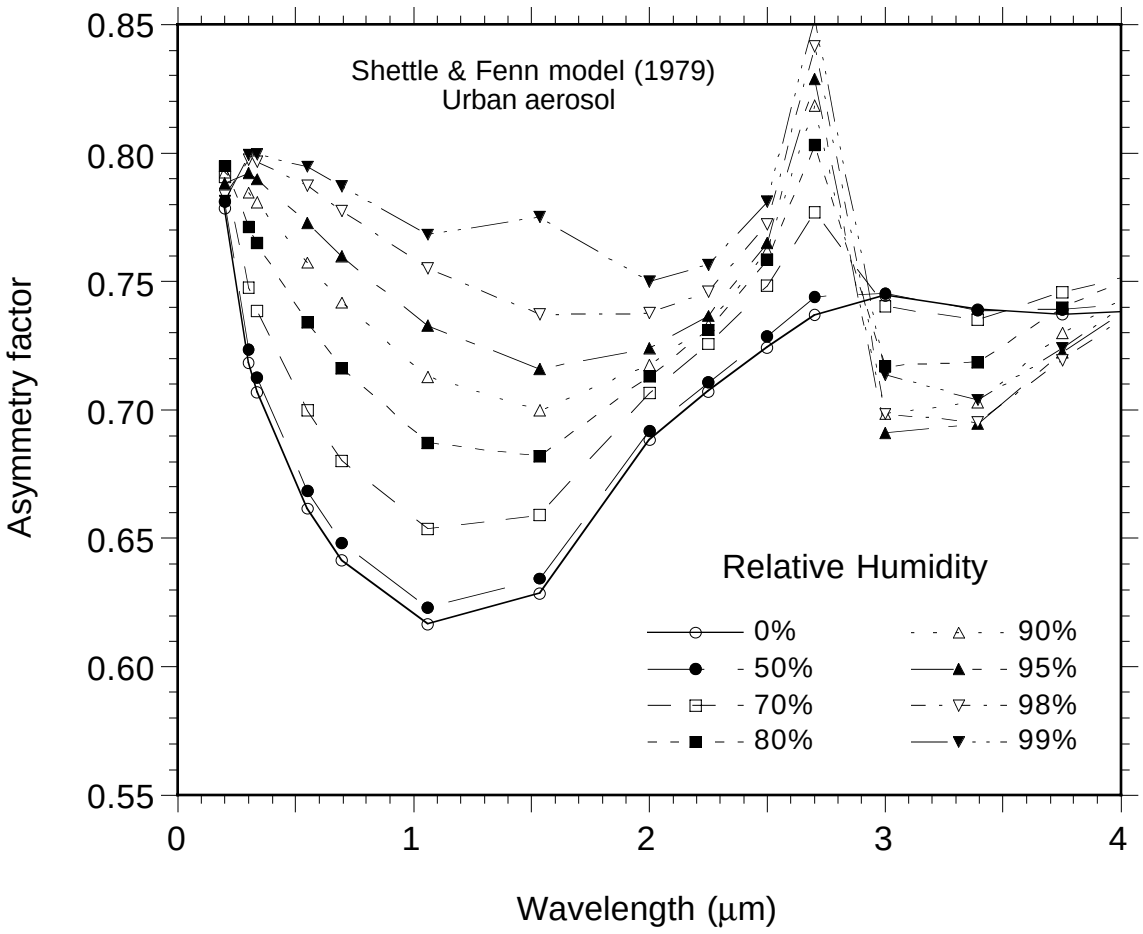

Fig. 5.2. Spectral asymmetry factor of urban aerosols as affected by relative humidity.

$F_{a2} = 1$ for $\tau_{as\lambda} \le 2$, or else (5.11a)

$$F_{a2} = \exp\left[-\left(\frac{\tau_{as\lambda} - 2}{\sigma_a}\right)^{\zeta}\right] \quad (5.11b)$$

where

$$\sigma_a = \text{Max}\{1, 3.5 - (4.53 - 0.82\ \tau_{as\lambda})\ \cos Z + (8.26 - 6.02\ \tau_{as\lambda})\ \cos^2 Z\} \quad (5.11c)$$

$$\zeta = -0.5 + \exp[0.24\ (\cos Z_0)^{-1.24}] \quad (5.11d)$$

$$\cos Z_0 = \text{Max}(0.05, \cos Z). \quad (5.11e)$$

The asymmetry factor is a key optical characteristic of aerosols and its spectral data have been tabulated in a few cases, e.g., d'Almeida et al. (1991), IAMAP (1986), and Shettle and Fenn (1979). An example of the variation of g with wavelength and relative humidity appears in Fig. 5.2 for the urban aerosol defined by Shettle and Fenn (1979). Neglecting the spikes in the near IR that occur at high humidity, the asymmetry factor of the reference aerosols defined in

IAMAP (1986) and in Shettle and Fenn (1979) can be parameterized as:

$$g = \mathrm{Max}(0.99, \sum_{i=0}^{i=4} k_i \lambda^i) \qquad (5.12a)$$

where the coefficients k_i are given in Table 5.3 for the SRA aerosol models. For the S&F humidity-dependent aerosol models, the coefficients k_i have been themselves regressed against relative humidity:

$$k_i = \kappa_{i0} + \kappa_{i1}\, RH_0 + \kappa_{i2}\, RH_0^2 \qquad (5.12b))$$

where the values of all coefficients are given in Table 5.4.

TABLE 5.3. Coefficients for the determination of the asymmetry factor of the SRA aerosol model, eqn (5.12a).

Aerosol type	Continental	Urban	Maritime
k_0	7.5141E-01	6.6851E-01	7.7876E-01
k_1	-3.5648E-01	-2.0657E-01	-1.3625E-01
k_2	2.9982E-01	1.4680E-01	1.6092E-01
k_3	-8.1346E-02	-4.0565E-02	-5.6749E-02
k_4	7.3038E-03	3.8811E-03	6.1178E-03

The Braslau & Dave aerosol models are based on Deirmendjian's "Haze L" aerosol type. From the detailed calculations summarized in Table B of Lenoble (1985) for this reference aerosol, its asymmetry factor is obtained as 0.8042. This value is assumed to hold at all wavelengths for the Braslau & Dave aerosol models.

TABLE 5.4. Coefficients for the determination of the asymmetry factor of the Shettle & Fenn aerosol model, eqn (5.12b).

Aerosol type	Rural	Urban	Maritime	Tropospheric
κ_{00}	7.5831E-01	6.5473E-01	7.7681E-01	7.7544E-01
κ_{01}	9.5376E-04	6.0975E-04	-2.7558E-03	-3.1632E-03
κ_{02}	-2.3126E-06	-4.3907E-05	-3.6350E-05	3.5770E-05
κ_{10}	6.5007E-02	1.0582E-02	-3.0700E-01	-2.3927E-03
κ_{11}	-1.9238E-02	-2.0473E-02	5.5554E-03	-3.8837E-03
κ_{12}	1.6785E-04	1.9499E-04	-4.0140E-05	2.8519E-05
κ_{20}	-2.5092E-02	7.2283E-02	1.1744E-01	-9.6464E-03
κ_{21}	1.5397E-02	1.3209E-02	3.7471E-04	5.8684E-04
κ_{22}	-1.3813E-04	-1.3393E-04	-1.5242E-06	-4.3942E-06
κ_{30}	-4.7607E-04	-3.3056E-02	-7.4695E-03	0
κ_{31}	-4.0963E-03	-3.0744E-03	-1.0596E-03	0
κ_{32}	3.6814E-05	3.1910E-05	6.5979E-06	0
κ_{40}	7.4163E-04	3.6485E-03	-1.3810E-03	0
κ_{41}	3.5332E-04	2.4708E-04	1.7037E-04	0
κ_{42}	-3.1460E-06	-2.5440E-06	-1.0431E-06	0

5.3 Effective ozone transmittance

An effective ozone diffuse transmittance for downward scattering, $\Gamma_{o\lambda}$, appears in eqns (5.1) and (5.8) instead of the direct ozone transmittance, $T_{o\lambda}$, that has been used in most simplified models since Leckner's work. It was found during the course of this work that the diffuse irradiance predicted by the existing simple models decreased too much with wavelength in the UV-B (below about 320 nm), where ozone absorption by far dominates all other extinction processes. This can be traced back to the concomitent decrease of $T_{o\lambda}$ with wavelength, which is so sharp below 300 nm that the resultant underprediction of diffuse irradiance by simple models even reaches *several* orders of magnitude, especially at large zenith angles. It therefore appears that the depleting effect of ozone on the downward diffuse radiation does not follow Bouguer's law.

The effective ozone transmittance has been obtained as the ratio between the reference diffuse irradiance, $E_{d0\lambda} = E_{dR\lambda} + E_{da\lambda}$, predicted by rigorous calculations in the UV (Bird and Hulstrom, 1982; Shettle and Green, 1974) and the equivalent quantity obtained by eqns (5.1) and (5.8) for $\Gamma_{o\lambda} = 1$. The following parameterization has been obtained:

$$\Gamma_{o\lambda} = \exp(-\gamma_1 \tau_{o\lambda}^{0.95} - \gamma_2 \tau_{o\lambda}) \text{ for } \tau_{o\lambda} \le 2 \tag{5.13a}$$

or else

$$\Gamma_{o\lambda} = \exp[-\gamma_3 - \gamma_4 (\tau_{o\lambda} - 2)] \tag{5.13b}$$

where

$$\gamma_1 = (-11.012 + 12.392\ m_o) / (1 + 0.23644\ m_o) \tag{5.13c}$$

$$\gamma_2 = 3.2656\ [1 - \exp(-0.46464\ m_o^{1.25})] - 0.965936\ \gamma_1 \tag{5.13d}$$

$$\gamma_3 = 1.93187\ \gamma_1 + 2\ \gamma_2 \tag{5.13e}$$

$$\gamma_4 = \exp(0.31045 + 0.001684\ m_o - 0.28549\ m_o^{-4}) \tag{5.13f}$$

and $\tau_{o\lambda}$ is defined in eqn (4.5b).

Figure 5.3 illustrates the wide variation of the ratio $\Gamma_{o\lambda} / T_{o\lambda}$ with m_o and $\tau_{o\lambda}$. It is apparent that this ratio is generally slightly below 1 for small values of $\tau_{o\lambda}$, as in the Chappuis and Wulf bands, but sharply increases for larger values in the UV-B part of the spectrum. It will be shown in Section 8 that the use of $\Gamma_{o\lambda}$ in eqns (5.1) and (5.8) results in physically reasonable estimates of diffuse UV irradiance, even at large zenith angles.

5.4 Backscattered component

Lastly, the backscattered component is calculated assuming an infinite series of interreflections between the ground and the atmosphere. This can be modelled as

$$E_{db\lambda} = \rho_{s\lambda}\ (\rho_{b\lambda} E_{bn\lambda} \cos Z + \rho_{d\lambda} E_{d0\lambda}) / (1 - \rho_{d\lambda} \rho_{s\lambda}) \tag{5.14}$$

where $\rho_{b\lambda}$ is the *zonal*[8] ground spectral reflectance for beam radiation, $\rho_{d\lambda}$ its counterpart for diffuse radiation, and $\rho_{s\lambda}$ is the sky overall reflectance. The difference between $\rho_{b\lambda}$ and $\rho_{d\lambda}$ is

[8] Zonal refers here to a characteristic area of 1-100 km^2 around the site (Gueymard, 1993b).

introduced here because most natural surfaces[9] exhibit non-Lambertian reflection characteristics to some degree. For a purely Lambertian surface, these reflectances would both reduce to $\rho_{g\lambda}$, the ground reflectance for global radiation. A discussion of the intricacies introduced by this non-Lambertian spectral model follows.

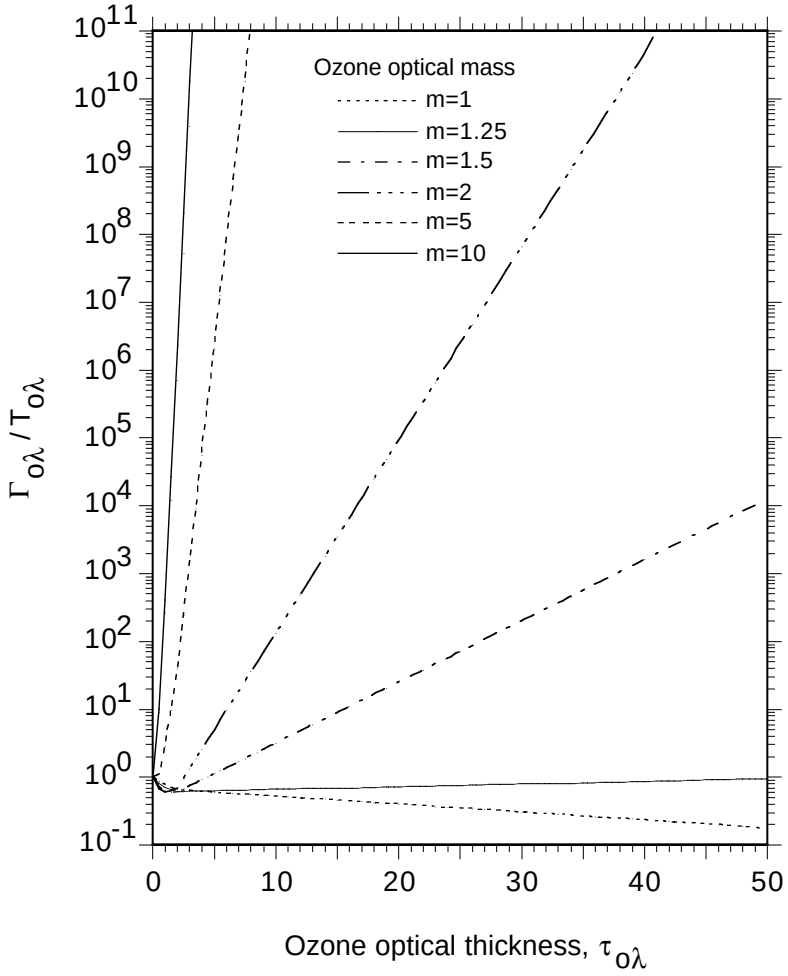

Fig. 5.3. Ratio $\Gamma_{o\lambda} / T_{o\lambda}$ as a function of $\tau_{o\lambda}$ and m_o.

Over continents, the monthly-average zonal ground albedo[10], ρ_g, defined as the *broadband* counterpart of $\rho_{g\lambda}$, varies between about 0.14 and 0.8. A discussion of zonal albedo, its sources, and a simple seasonal model for North America is presented by Gueymard (1993b). The broadband value is not a suitable substitute for the spectral value at *all* wavelengths because natural surfaces generally exhibit pronounced spectral selectivity (Bowker et al., 1985; Coulson and Reynolds, 1971). In particular, reflectances in the UV are generally significantly less than in the visible (Blumthaler and Ambach, 1988). A notable exception is snow (particularly when dry

9 The term surface is used loosely here to include "layer."

10 It is generally considered that *albedo* refers to the reflectance of a broad area (up to planetary scale) illuminated specifically by the sun (Iqbal, 1983). Broadband solar reflectance and albedo would thus be interchangeable terms. There are other interpretations as well. Kondratyev (1969) considers the term albedo applicable only to a purely diffuse reflection process. Forgan (1983) attempts to distinguish the spectral property (reflectance) from its broadband average (albedo). This latter distinction will be followed here, and the term "spectral albedo" avoided because any source (be it artificial or the sun) can be used to obtain reproducible *spectral* data, whereas a broadband value is fundamentally dependent on the particular source spectrum.

and fresh): its UV reflectance is larger than its broadband counterpart (Blumthaler and Ambach, 1988), but its reflectance beyond 1.25 μm is very low (Choudhury and Chang, 1979). These observations are also both predicted by theory (Wiscombe and Warren, 1980). A comparison of the spectral reflectances of some natural and artificial surfaces appears in Fig. 5.4. A large variability exists from one type of surface to the other, not to mention the variation from one sample to another for a single type. Only basalt exhibits a roughly constant reflectance over the spectrum, and is thus a rare surface which follows the assumption of a "constant albedo equal to 0.2" frequently used in solar energy applications.

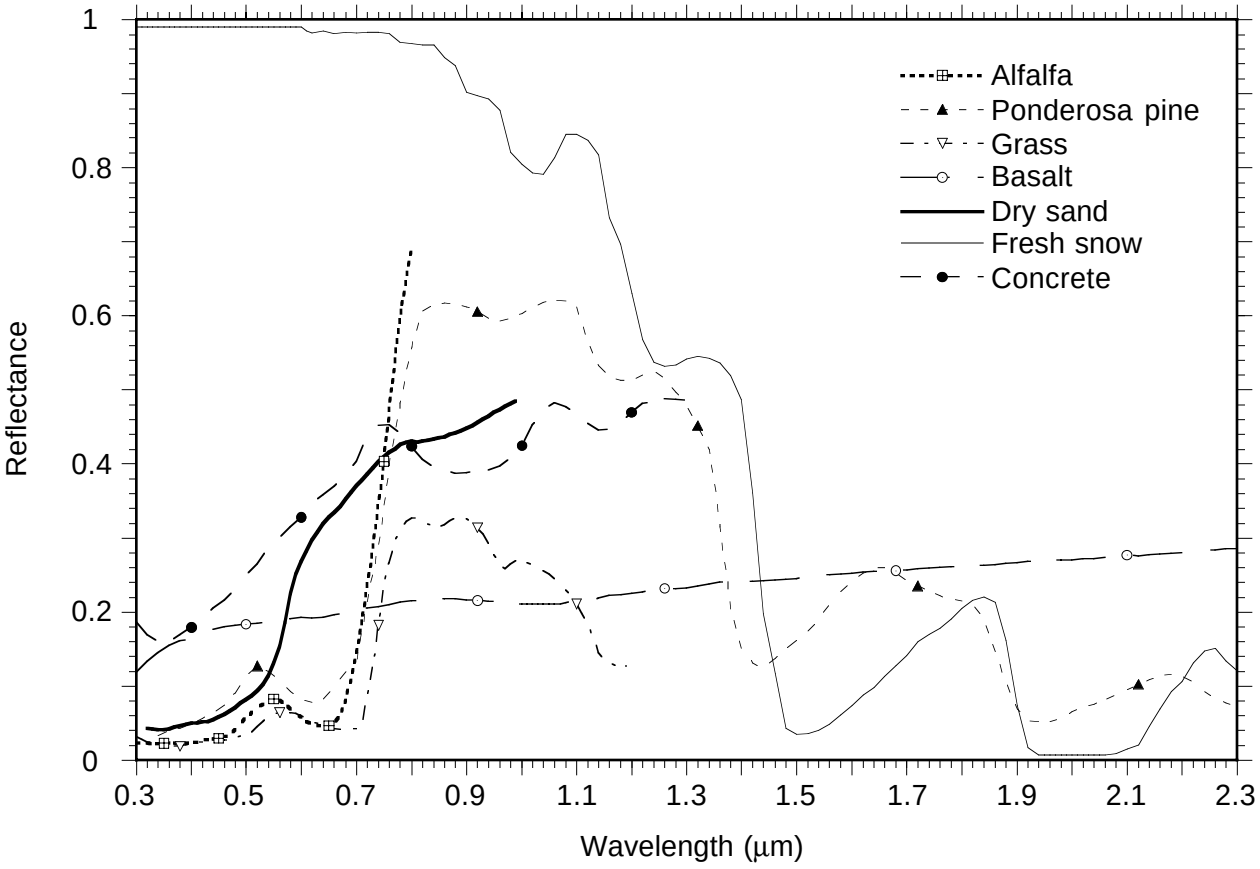

Fig. 5.4. Spectral reflectances of some ground covers (Bowker et al., 1985)

Besides the spectral variability of individual surface types, it is stressed that zonal reflectance is in fact defined as a reflectance averaged over a large area, and thus may differ significantly from the reflectance of each sub-area of land in the mosaic.

The characteristics of non-Lambertian reflectance are particular to each surface. Whereas some surfaces are nearly Lambertian, others, such as bodies of water, exhibit strong specular characteristics. Many studies have shown such an increase of ground albedo with zenith angle (see, for example, Kondratyev, 1969). Ideally, a non-Lambertian reflectance calculation should consider a spatial integration of the bidirectional reflectance. Spectral bidirectional reflectance data are almost nonexistant, and subject to considerable natural variation among samples, not to mention the large amounts of computer storage required, so that a more practical alternative is necessary. To approximate the slight non-Lambertian nature of most surfaces, a simple function, R_z, is used to correct the reflectance at *normal* incidence, $\rho_{b0\lambda}$, which will be calculated later

$$\rho_{b\lambda} = R_z \, \rho_{b0\lambda} \, . \qquad (5.15)$$

Two expressions for R_z are considered, and both are adapted from the "representative" functions that Larsen and Barkstrom (1977) proposed for land or snow. The expression for "land" surfaces is here extended to all natural surfaces except water, snow, and ice:

$$R_z = [1 - \cos Z \, \mathrm{Ln}(1 + 1/\cos Z)] / 0.307, \tag{5.16a}$$

with $R_z = 3.26$ for $Z = 90°$. The representative expression for snowy surfaces is:

$$R_z = (1 - 0.176 \cos Z) / 0.824. \tag{5.16b}$$

The diffuse reflectance can be obtained by integrating (5.15) over the hemisphere

$$\rho_{d\lambda} / \rho_{b0\lambda} = \int_0^{\pi/2} R_z \sin Z' \cos Z' \, dZ' / \int_0^{\pi/2} \sin Z' \cos Z' \, dZ' . \tag{5.17}$$

Substituting (5.16) into (5.17), a numerical integration gives $\rho_{d\lambda} / \rho_{b0\lambda} = 1.33$ for land surfaces and 1.07 for snowy surfaces, respectively.

The quantity $\rho_{b0\lambda}$ can be estimated from available reflectance data in two different ways. Under cloudy conditions with only diffuse radiation, $\rho_{b0\lambda}$ is obtained from the ratios just mentioned once $\rho_{d\lambda}$ is measured. Under cloudless conditions with low diffuse radiation and with a known zenith angle, $\rho_{b0\lambda}$ stems from the measurement of $\rho_{b\lambda}$ and eqn (5.15).

The reflectance of bodies of water is highly specular and is usually obtained from Fresnel's formula. Using spectral data for the index of refraction for both air (Peck and Reeder, 1972) and water (Hale and Querry, 1973), as well as a spectrally constant supplemental reflectance of 0.015 corresponding to the backscatter radiance emerging from below a deep water surface (estimated at 0.005–0.020, according to Katsaros et al., 1985), the spectral values of $\rho_{b\lambda}$ have been evaluated at 50 nm intervals for zenith angles between 0 and 90°. These results have been closely fitted with

$$\rho_{b\lambda} / \rho_{b0\lambda} = 1 + (0.001209 - 0.00010748 \, \lambda) \exp[(0.11087 + 0.0017729 \, \lambda) \, Z] \tag{5.18a}$$

$$\rho_{b0\lambda} = 0.039063 - 0.010104 \, \lambda + 0.0077394 \, \lambda^2 - 0.0021669 \, \lambda^3. \tag{5.18b}$$

Substituting (5.18a) into (5.17) and fitting the results by wavelength, the diffuse reflectance of water is then obtained as

$$\rho_{d\lambda} = 0.0803 - 0.00365 \, \lambda. \tag{5.19}$$

These water reflectances are in good agreement with other predictions and measurements provided in the literature (Cogley, 1979; Kondratyev, 1969).

Sky reflectance is calculated as

$$\rho_{s\lambda} = T^{\Delta}_{g\lambda} T^{\Delta}_{w\lambda} T^{\Delta}_{aa\lambda} T^{\Delta}_{n\lambda} \left[(1 - F^{\Delta}_{R})(1 - T^{\Delta}_{R\lambda}) S_{o\lambda} \sqrt{T^{\Delta}_{as\lambda}} + (1 - F^{\Delta}_{a})^{0.9} (1 - T^{\Delta 2}_{as\lambda}) \right] \tag{5.20a}$$

where quantities indicated by a superscript delta are for an *upward* illumination and are evaluated from their original equations (in Section 4) with the usual reference air mass of 1.66 for diffuse radiation, and

$$S_{o\lambda} = \exp[-(4.8344\mathrm{E}5 + 2.3088\mathrm{E}6 \, u_o) \, (\lambda - 0.38)^{5.8}] \tag{5.20b}$$

for $\lambda \leq 0.38$ μm, and $S_{o\lambda} = 1$ elsewhere.

The functional form of eqn (5.20a) differs significantly from that adopted in other simplified spectral models such as SPCTRAL2 (Bird, 1984; Brine and Iqbal, 1983; and Justus and Paris, 1985, 1987). These models tend to generate an incorrect sky reflectance in the UV because of their poor handling of the ozone diffuse transmittance, as revealed by the comparison of the predictions of eqn (5.20) to these models shown in Fig. 5.5.

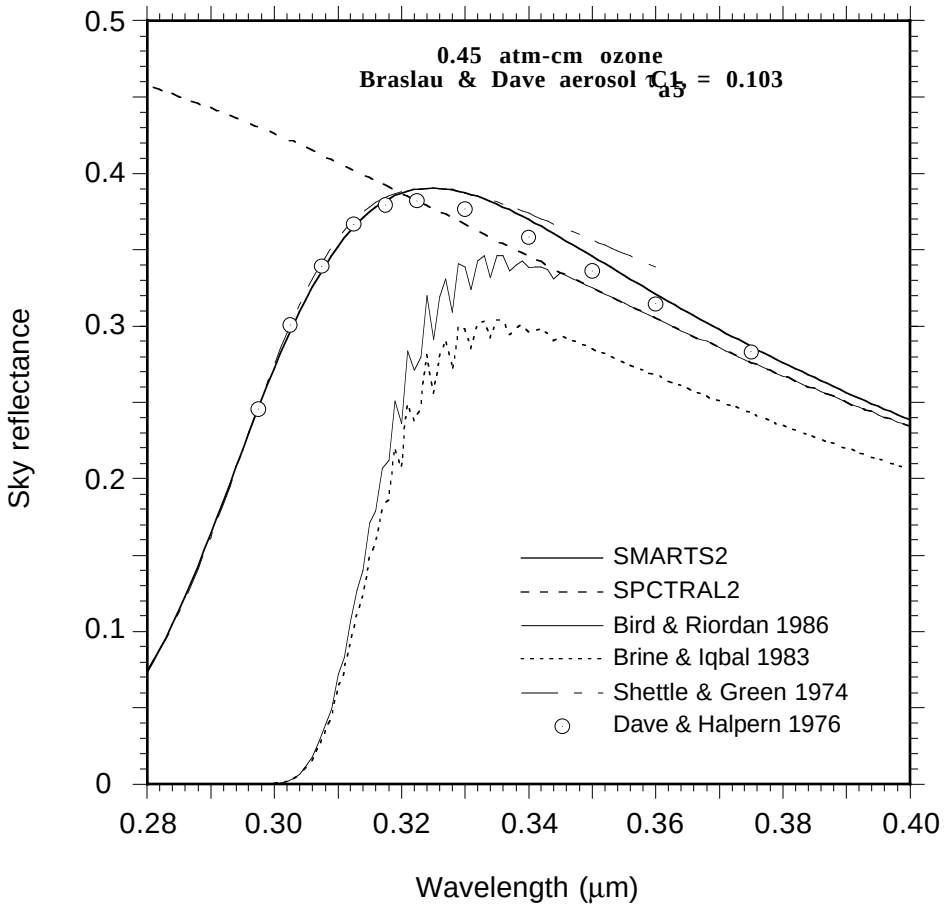

Fig. 5.5. UV sky reflectance predicted using different models.

Equations (5.20a) and (5.20b) have been adjusted so that the resulting UV sky reflectances are comparable to the rigorous calculations of Dave and Halpern (1976) and Shettle and Green (1974) for the typical range of values of the reduced ozone thickness, u_o. Shettle and Green (1974) have derived a simplified equation from their rigorous model to estimate sky reflectance below 360 nm, and it is also indicated on Fig. 5.5. This comparison shows that the predicted sky reflectance at 300 nm varies between an extremely low value of 0.0, according to Brine and Iqbal (1983) and Bird and Riordan (1986), and an extremely high 0.425, according to SPCTRAL2, with an intermediate, more likely value of 0.27 according to Shettle and Green (1974) and eqn (5.20a).

When the three diffuse irradiance components are determined from eqns (5.1), (5.8), and (5.14), the total diffuse irradiance can be obtained:

$$E_{d\lambda} = E_{dR\lambda} + E_{da\lambda} + E_{db\lambda}. \quad (5.21)$$

The global irradiance on a horizontal surface is then simply

$$E_{\lambda} = E_{bn\lambda} \cos Z + E_{d\lambda}. \quad (5.22)$$

TABLE 5.5. Backscattering amplification factors for different ground covers, zenith angles, and wavelengths.

Wavelength (nm)	300	325	400	500	600	700	800
Sky reflectance	0.3505	0.4392	0.3159	0.2079	0.1462	0.1085	0.0893
Z = 0°							
Direct/diffuse ratio	8.57E-01	8.35E-01	1.70E+00	2.91E+00	4.39E+00	5.92E+00	7.65E+00
Alfalfa	1.015	1.019	1.021	1.048	1.046	1.111	1.568
Ponderosa pine	1.012	1.023	1.043	1.095	1.065	1.102	1.454
Grass	1.020	1.020	1.019	1.027	1.047	1.032	1.260
Basalt	1.081	1.117	1.148	1.156	1.156	1.154	1.169
Dry sand	1.033	1.036	1.043	1.068	1.220	1.290	1.346
Fresh snow	1.987	2.412	2.228	2.007	1.903	1.825	1.817
Concrete	1.130	1.145	1.163	1.213	1.271	1.317	1.340
Reference surface	1.140	1.177	1.182	1.170	1.162	1.154	1.157
Z = 60°							
Direct/diffuse ratio	3.53E-02	2.54E-01	6.37E-01	1.34E+00	2.34E+00	3.12E+00	4.08E+00
Alfalfa	1.008	1.013	1.013	1.029	1.029	1.066	1.333
Ponderosa pine	1.007	1.016	1.026	1.057	1.041	1.061	1.266
Grass	1.011	1.013	1.011	1.016	1.029	1.019	1.153
Basalt	1.045	1.080	1.090	1.093	1.097	1.092	1.099
Dry sand	1.018	1.025	1.026	1.041	1.136	1.173	1.203
Fresh snow	1.550	1.965	1.745	1.603	1.560	1.491	1.480
Concrete	1.072	1.099	1.099	1.128	1.168	1.188	1.200
Reference surface	1.078	1.121	1.110	1.102	1.101	1.091	1.092
Z = 85°							
Direct/diffuse ratio	4.18E-19	5.89E-06	1.86E-03	3.00E-02	1.23E-01	2.75E-01	4.66E-01
Alfalfa	1.008	1.010	1.008	1.013	1.010	1.021	1.096
Ponderosa pine	1.007	1.012	1.016	1.025	1.014	1.019	1.077
Grass	1.011	1.011	1.007	1.007	1.010	1.006	1.044
Basalt	1.044	1.064	1.055	1.041	1.033	1.028	1.029
Dry sand	1.018	1.020	1.016	1.018	1.046	1.053	1.059
Fresh snow	1.531	1.769	1.456	1.265	1.188	1.152	1.138
Concrete	1.070	1.079	1.060	1.056	1.057	1.058	1.058
Reference surface	1.075	1.096	1.068	1.045	1.034	1.028	1.027

A backscattering amplification factor for diffuse radiation can be defined as the ratio of $E_{d\lambda}$, as obtained from eqn (5.21) for the actual ground reflectance, to that obtained for a non-reflective, ideally black reference surface, $E_{d0\lambda}$. This amplification factor is a function of the product $\rho_{g\lambda}$ $\rho_{s\lambda}$ and of the direct/diffuse ratio $R = (E_{bn\lambda} \cos Z)/E_{d0\lambda}$, which is a strong function of λ and Z. (For this particular calculation, all surfaces have been considered Lambertian for simplicity, so that $\rho_{b\lambda} = \rho_{d\lambda} = \rho_{g\lambda}$.) The amplification factor has been calculated for different wavelengths and a few samples of ground cover, the reflectance of which appeared in Fig. 5.4. A reference surface

with an ideal spectrally-independent reflectance of 0.2 has been added for comparison, as it is often used in solar energy calculations. Atmospheric conditions comparable to those in Fig. 5.5 have been used (USSA, 0.45 cm ozone, rural aerosol with $ß = 0.1$). Table 5.5 shows that the amplification factor is very low (about 1.015) in the UV and the visible for vegetation (alfalfa, Ponderosa pine, and grass). Yet, it is extremely high (e.g., 1.97 for $Z = 60°$) for fresh snow at 325 nm where sky reflectance is close to its maximum (Fig. 5.5), snow reflectance is considerable (0.99), and diffuse radiation is larger than direct radiation. This case is very important because the high amplification factor results in a substantial increase in UV-B and UV-A biological doses. The spectral dependence of the amplification factors is generally very different for natural ground cover and concrete, compared to the reference surface. Therefore, actual spectral field-measured reflectance data should be used instead of broadband estimates, wherever possible, for accurate irradiance calculations.

5.5 Radiation on tilted surfaces

For irradiances on non-horizontal surfaces, additional calculations are required because such surfaces receive diffuse radiation from only a part of the sky vault, while also receiving some reflected radiation from the foreground. The broadband CDRS model is used over most of the spectrum because it coincidentally gave good results when applied to spectral data (Gueymard, 1987). At short wavelengths, however, this broadband anisotropic model tends to overestimate the spectral sky diffuse radiation on inclined planes because the sky anisotropy is low or negligible in the UV (Dave and Furukawa, 1966; Schauberger, 1992). Therefore, the conventional isotropic model (Iqbal, 1983) for diffuse radiation is used there. The transition between the isotropic and anisotropic models is assumed here to be dependent on the ratio $\tau_{a\lambda}$ / $\tau_{R\lambda}$ for convenience because scattering by aerosols is strongly anisotropic (forward peaked), whereas Rayleigh scattering is essentially isotropic. This ratio then varies greatly with wavelength and turbidity. Ideally perfect isotropy holds when this ratio is lower than 0.5, and anisotropic scattering when it is larger than 1.5. Linear interpolation within this range is considered between the extremes. Thus, the global irradiance on a tilted surface, $E_{s\lambda}$, can be modelled as

$$E_{s\lambda} = E_{bn\lambda} \cos\vartheta + R_d E_{d\lambda} + \rho'_{g\lambda} R_r E_{\lambda} \quad (5.23a)$$

where $\rho'_{g\lambda}$ is the local reflectance of the ground (assumed horizontal) bordering the tilted surface, and ϑ is the angle of incidence of the sun's rays on the tilted surface, which can be obtained from

$$\cos\vartheta = \cos S \cos Z + \sin S \sin Z \cos(\chi - \chi_s) \quad (5.23b)$$

where S is the slope angle of the surface, χ_s its azimuth, and χ the sun's azimuth. The conversion factors, R_d and R_r, are such that:

$$R_d = (\tau_{a\lambda} / \tau_{R\lambda} - 0.5) R_{da} + (1.5 - \tau_{a\lambda} / \tau_{R\lambda}) R_{di}] \text{ for } 0.5 \le \tau_{a\lambda} / \tau_{R\lambda} \le 1.5, \quad (5.23c)$$

$$R_d = R_{di} \text{ for } \tau_{a\lambda} / \tau_{R\lambda} < 0.5, \text{ and } R_d = R_{da} \text{ for } \tau_{a\lambda} / \tau_{R\lambda} > 1.5$$

$$R_{di} = (1 + \cos S) / 2 \quad (5.23d)$$

$$R_r = 1 - R_{di} \quad (5.23e)$$

where R_{da} is obtained from S, Z, and ϑ according to Gueymard (1987).

As pointed out by Gueymard (1993b) and in the previous section, the reflectance of the *local* foreground, rather than the zonal reflectance used above to calculate the backscattered irradiance, should be used to calculate the reflected irradiance on a tilted plane. Spectral reflectance data for natural surfaces may be found in Blumthaler and Ambach (1988), Bowker et al. (1985), Choudhury and Chang (1979), Coulson and Reynolds (1971), Doda and Green (1980, 1981), Kriebel (1977), and Krinov (1953); see also Fig. 5.4. As cautioned above, the use of broadband albedo values in the UV part of the spectrum is generally not a valid simplification. Because most ground covers exhibit non-Lambertian reflection (see previous section), different reflectances have to be considered for direct and diffuse radiation. In the absence of bidirectional reflectance data, the following approximate formula is proposed to obtain $\rho'_{g\lambda}$:

$$\rho'_{g\lambda} = \{\rho_{d\lambda} E_{d\lambda} + [\rho_{b0\lambda} + (\rho_{b\lambda} - \rho_{b0\lambda}) \left|\cos(\chi - \chi_s)\right|] E_{bn\lambda} \cos Z\} / E_{\lambda} . \qquad (5.24)$$

6. CIRCUMSOLAR RADIATION

The direct beam radiation calculated so far comes ideally from the solar disk only. When comparing such *calculations* to measured data, it is important to take into account the circumsolar diffuse radiation that is also intercepted in the aperture (typically a 1–10° full angle) of an actual spectroradiometer, sunphotometer, or pyrheliometer. This circumsolar contribution is a function of the size distribution in the aerosol column and increases with turbidity and optical mass. The circumsolar radiance within the solar aureole decreases sharply with the angular distance from the sun's center (i.e., the scattering angle). Because the circumsolar irradiance from the sky is nonnegligible compared to the sun's direct beam irradiance, at least in certain conditions (Fröhlich and Quenzel, 1974; Grassl, 1971; Shah, 1978), a correction factor needs to be applied to the calculated spectral beam irradiance if a radiometer with a field of view larger than the solar disk is to be simulated.

The radiometer optical geometry is important for precise calculations. The "aperture" angle mentioned above corresponds to the "view angle", i.e., the full angle determined by the exterior aperture of the instrument as viewed from the *central point* of the receiver. The *opening angle*, ξ_o is defined as half this aperture angle. It is the most commonly reported characteristic of a radiometer's optical geometry. The *slope angle*, ξ_s, and *limit angle*, ξ_l, are the minimum and maximum half viewing angles, respectively, at which any beam will strike the receiver area directly, with $\xi_s < \xi_o < \xi_l$. This means that for an incidence angle, ξ, less than ξ_s, the receiver will be fully efficient (100% response), whereas for $\xi > \xi_l$ the receiver will ideally detect no signal (0% response). For intermediate incidences angles, the response will be partial, as described by the geometric penumbra function, $P(\xi)$, derived by Pastiels (1959) and used by others (e.g., Major, 1994):

$$P(\xi) = [a^2 (\phi - \sin\phi) + \mu - \sin\mu] / 2\pi \tag{6.1a}$$

where

$$\mu = 2 \arccos (y_1 - y_2) \tag{6.1b}$$

$$\phi = 2 \arccos [(y_1 + y_2) / a] \tag{6.1c}$$

$$y_1 = (b / 2) \tan\xi \tag{6.1d}$$

$$y_2 = [(a^2 - 1) / 2b] / \tan\xi \tag{6.1e}$$

$$a = (\tan\xi_l + \tan\xi_s) / (\tan\xi_l - \tan\xi_s) \tag{6.1f}$$

$$b = 2 (\tan\xi_l - \tan\xi_s). \tag{6.1g}$$

The calculation of the circumsolar correction factor is rather involved because the atmospheric scattering properties vary widely with both the aerosol optical characteristics and wavelength. The maximum circumsolar effect is known to occur around 0.4–0.5 μm, with negligible contributions in the infrared beyond 1.5 μm. A circumsolar correction factor, $F_{c\lambda}$, to be multiplied by the pure direct beam irradiance, is used to approximate the latter's experimental counterpart:

$$F_{c\lambda} = 1 + E_{dc\lambda} / E_{bn\lambda} \tag{6.2}$$

where $E_{bn\lambda}$ is defined in eqn (4.1), and the circumsolar irradiance, $E_{dc\lambda}$, results from the spatial integration of the spectral sky radiance within the total field of view of the radiometer. As the circumsolar radiance varies strongly with the scattering angle but only slightly with azimuth, the azimuthally averaged radiance that exists along the almucantar, $L_{a\lambda}(\xi)$, is conventionally used to

avoid a double angle integration over the aureole (Box and Deepak, 1979; 1981). The circumsolar irradiance detected by the radiometer is then (see, e.g., Major, 1994; Putsay, 1980, 1995a)

$$E_{dc\lambda} = 2\pi \int_0^{\xi_l} L_{a\lambda}(\xi) P(\xi) \sin\xi \cos\xi d\xi . \tag{6.3}$$

Because multiple scattering from aerosol particles is only marginal in the aureole, at least for scattering angles below 10° (Box and Deepak, 1978), it will be neglected here, thus symplifying calculations. The conventional single-scattering approximation to the almucantar radiance (Volz, 1987) will be used here, with the addition of two correction terms which explicitly include multiple scattering by *molecules* and backscattering after multiple reflections from the ground (Box and Deepak, 1979; 1981). The almucantar radiance will thus be expressed as:

$$L_{a\lambda}(\xi) = m_a E_{bn\lambda} [(\tau_{R\lambda} + \tau_{mR\lambda}) F_R(\xi) + \tau_{mg\lambda} F_R(0^\circ) + \varpi_0 \tau_{a\lambda} F_{a\lambda}(\xi)] \tag{6.4a}$$

where m_a is calculated in eqn (4.2), $\tau_{R\lambda}$ in eqn (4.4), and $\tau_{a\lambda}$ in eqn (4.21). $F_R(\xi)$ is the phase function for Rayleigh scattering (normalized here to 1), which, according to Lenoble (1993), may be obtained from

$$F_R(\xi) = [3 / (4 + 2\delta)] [1 + \delta + (1 - \delta) \cos^2\xi] / 4\pi \tag{6.4b}$$

where δ is the depolarization factor that appeared in eqn (4.3). $F_{a\lambda}(\xi)$ is the aerosol phase function, also normalized to 1, which describes the forward-peaked scattering pattern of the aerosol particles. This function is specific to each aerosol's size distribution and refractive index and is normally calculated from Mie theory. To simplify calculations in SMARTS2, a library of call-up functions of ξ, obtained by fitting published discrete data of $F_{a\lambda}(\xi)$ for $\xi \leq 10°$, is used. The spectral phase functions for the different Shettle and Fenn aerosol models have been fitted from the tabulated data in MODTRAN2. The phase function for Braslau and Dave's aerosol models C and C1 (based on Deirmendjian's *Haze L*) has been fitted from data in Lenoble (1985). Finally, the spectral phase functions for the three SRA aerosols have also been fitted from discrete calculations obtained by Putsay (1995a, 1995b). Examples of such phase functions are shown in Figs. 6.1 and 6.2 for rural and maritime aerosol models, respectively.

The only terms that remain to be evaluated in eqn (6.4a) are ϖ_0, $\tau_{mR\lambda}$, and $\tau_{mg\lambda}$. The first term is the aerosol single-scattering albedo, which has been discussed in Section 5.1. The second term corresponds to a fictitious optical thickness due to molecular multiple scattering. A fit of the data tabulated by Box and Deepak (1979) gives:

$$\tau_{mR\lambda} = 1.38 (\tau_{R\lambda} + \varpi_0 \tau_{a\lambda})^2. \tag{6.4c}$$

The third term corresponds to augmentation of the radiance by backscattering processes between the ground and the atmosphere. It is simply obtained as (Box and Deepak, 1979):

$$\tau_{mg\lambda} = \rho_{g\lambda} (\tau_{R\lambda} + \tau_{mR\lambda}) \tag{6.4d}$$

where $\rho_{g\lambda}$ is the zonal ground albedo, discussed in Section 5.4.

The integral in eqn (6.3) cannot be evaluated analytically, so it is approximated numerically using angular intervals of 0.1° and Simpson's rule. The circumsolar correction factors obtained with the method proposed here compare well to existing test cases of the literature (Putsay, 1995b; Tomasi, 1989) for different wavelengths and air masses .

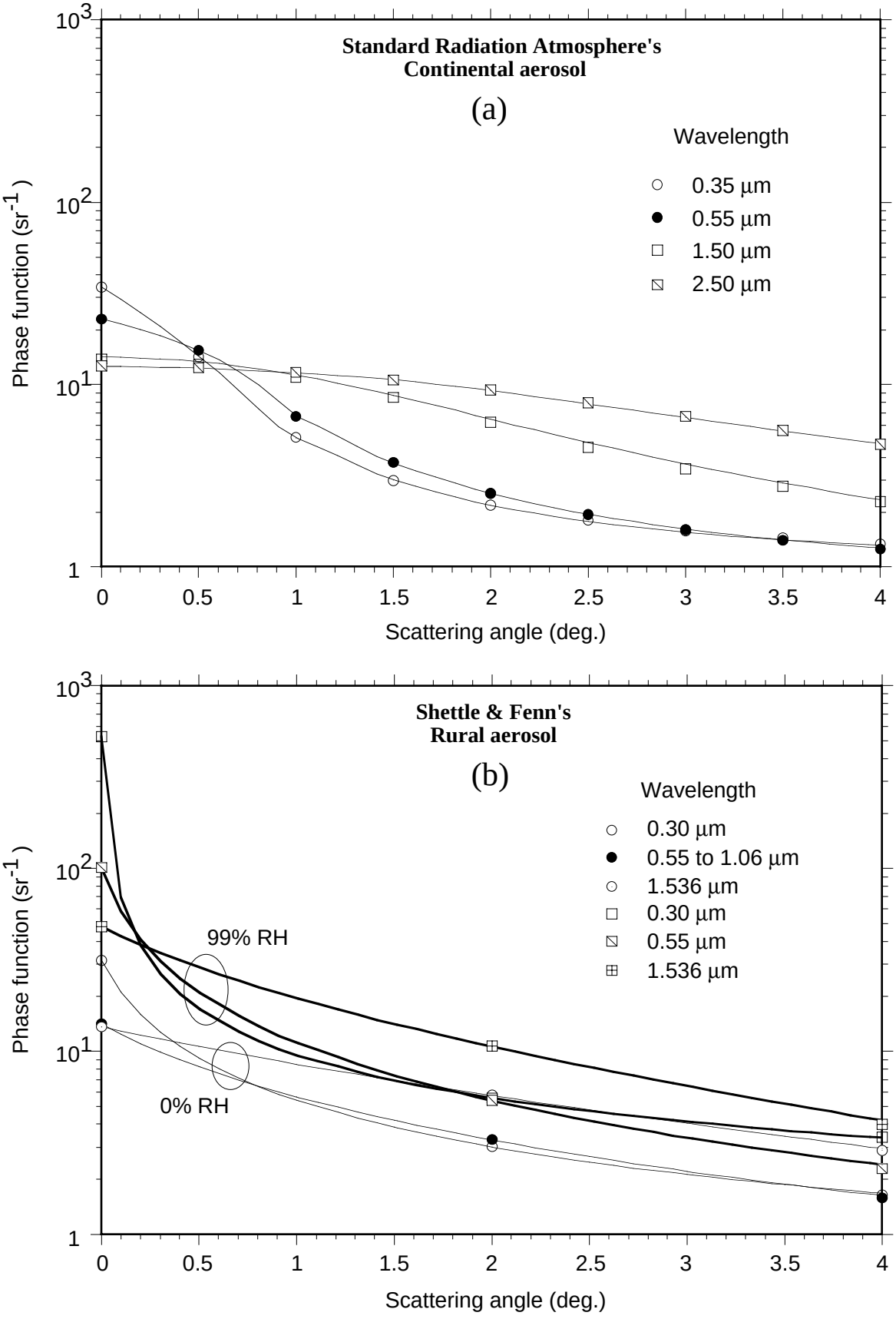

Fig. 6.1. Phase functions for different aerosol models. (a) SRA continental aerosol; (b) Shettle & Fenn's rural aerosol. Symbols indicate original data and continuous lines their least squares fits.

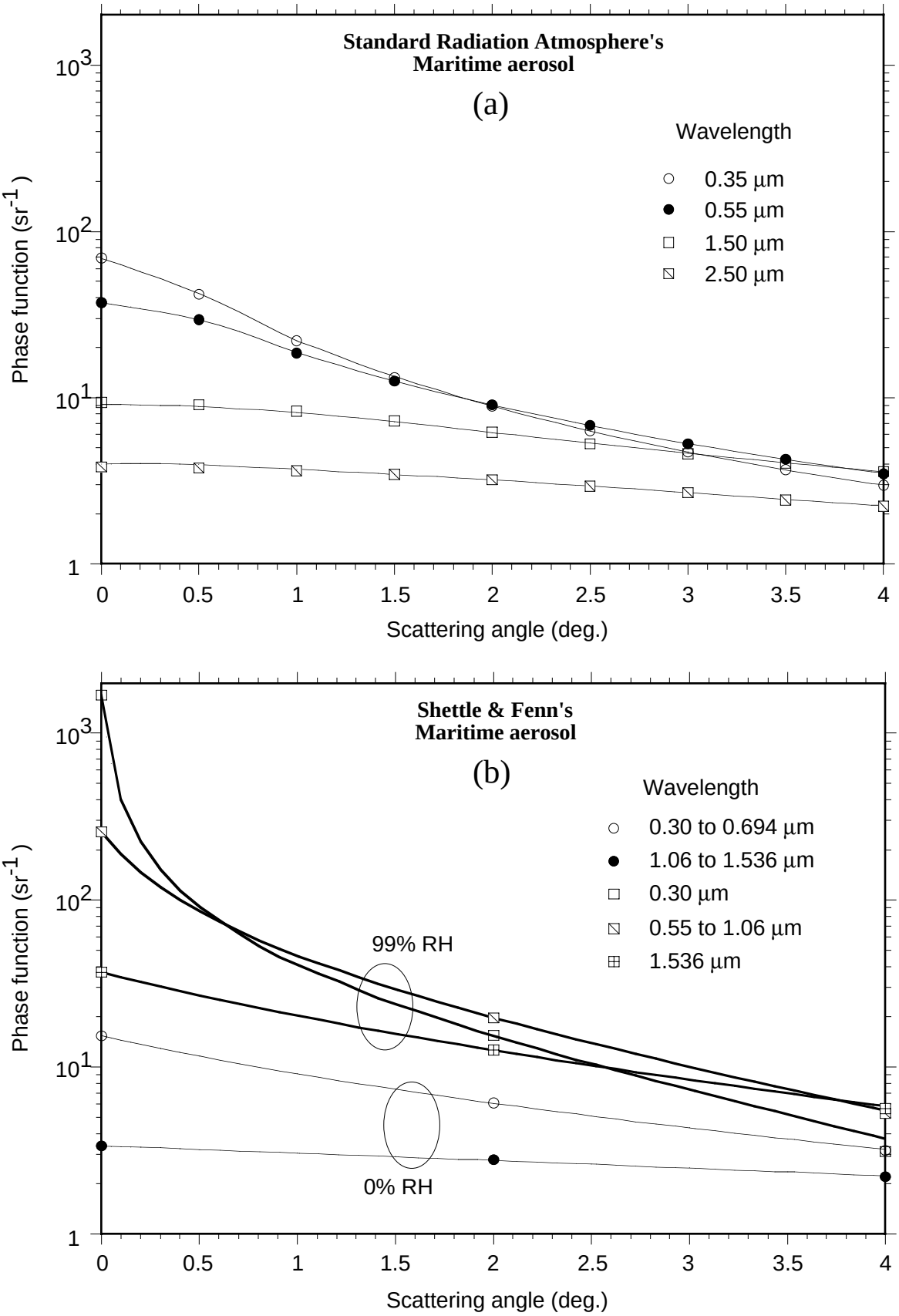

Fig. 6.2. Phase functions for different maritime aerosols.

As demonstrated by Fig. 6.3, the ratio of circumsolar radiation to beam radiation is highly variable, depending on solar zenith angle, wavelength, humidity, and aerosol optical characteristics. Obviously, the circumsolar contribution also increases with the radiometer's aperture angle. The increased circumsolar contribution from maritime aerosols compared to rural aerosols may be attributed to their steeper forward-peaking phase function (compare Figs. 6.1 and 6.2).

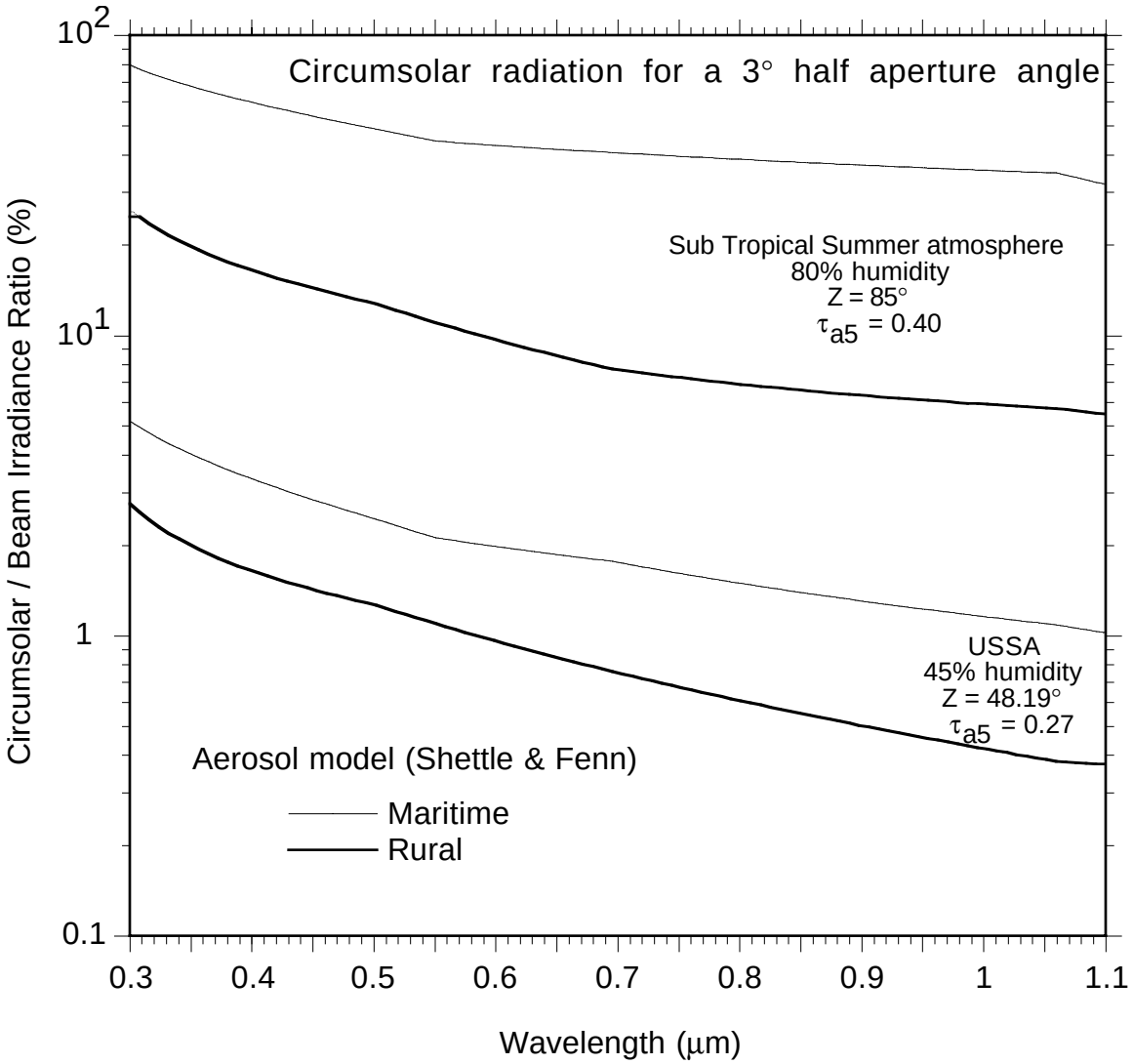

Fig. 6.3. Spectral circumsolar contribution for different atmospheric conditions.

7. OUTPUT DATA SMOOTHING

Spectroradiometric instruments are characterized by having different spectral bandpass shapes and widths. The Gaussian and triangular shapes are chosen here as representative (Fig. 7.1). A useful feature of SMARTS2 is a post-processor that scans the raw outputs (transmittances or irradiances) and smooths them to derive new outputs at optional relaxed bandwidths, approximating instrumental transmittance characteristics by a Gaussian or triangular function with a given bandwidth, characterized by its *full width at half maximum* (FWHM). This is similar to the optional postprocessor in MODTRAN2, except that the latter is limited to a triangular function. It is essential to perform such a data smoothing prior to comparing modelled and measured data, as will be shown in Section 8. In the case of Gaussian filtering for example, the weight applied to the irradiance or transmittance at wavelength λ is obtained with an equation form identical to that of a normal distribution with a mean λ_c and standard deviation σ, except for the normalizing coefficient (1 instead of $[2\pi]^{-0.5}$):

$$W(\lambda) = \exp\left[-\frac{(\lambda - \lambda_c)^2}{2\sigma^2}\right] \qquad (7.1)$$

where λ_C is the wavelength corresponding to the peak transmittance, and σ = FWHM $(8 \ln 2)^{-0.5}$ is such that $W(\lambda) = 0.5$ if $\lambda = \lambda_C + \text{FWHM}/2$. It is stressed that this exercise of simulating a radiometer supposes that it is ideal; in particular, it means that its transmittance is assumed perfectly symmetric around λ_C. For a non ideal instrument, eqn (7.1) would have to be replaced by a more specific function.

The broadened, or smoothed, value of a spectral variable $X(\lambda)$, irradiance or transmittance, is finally obtained numerically as:

$$\overline{X} = \sum_{\lambda_n}^{\lambda_x} W(\lambda) X(\lambda) \Big/ \sum_{\lambda_n}^{\lambda_x} W(\lambda) \qquad (7.2)$$

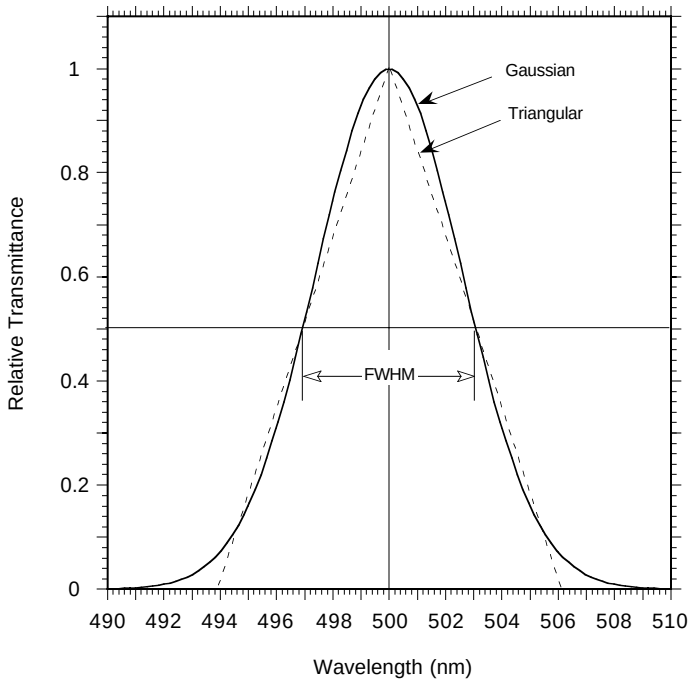

Fig. 7.1. Examples of smoothing functions for the simulation of spectroradiometers

where $\lambda_n = \lambda_c - \Delta\lambda$ and $\lambda_x = \lambda_c + \Delta\lambda$, $\Delta\lambda$ being the greatest integer smaller than (or equal to) FWHM/dλ + 3, where dλ is the wavelength interval of the original spectrum (1 nm below 1700 nm and 5 nm above, with the present extraterrestrial spectrum). For example, for λ_c = 500 nm, FWHM = 6.15 nm, dλ = 1 nm, the numerical integration in eqn (7.2) would be carried out between λ_n = 491 and λ_x = 509 nm.

8. PERFORMANCE ASSESSMENT

As SMARTS2 is intended to be used in a variety of applications, its accuracy is a critical factor and needs to be assessed under different atmospheric conditions. Incidentally, it must be pointed out that a numerical model cannot be "validated" or "verified"—despite the frequent usage of these terms in this field—because of fundamental reasons critically reviewed by Oreskes et al. (1994). This is why the term "performance assessment" is used extensively here.

The two possible ways to assess the performance of this type of numerical model—by comparison with more rigorous calculations, or with measured data of good quality—now will be successively examined.

8.1 Comparison with rigorous codes

Comparisons of SMARTS2 predictions with those of MODTRAN already appeared in Figs. 4.3–4.5 in the case of gaseous absorption, but they do not constitute independent tests as the corresponding SMARTS2 transmittance functions are primarily parameterizations of MODTRAN results. Published spectra obtained from rigorous codes are not common, therefore the possible comparisons will be essentially limited to a few data sets.

A comparison between SMARTS2 and the B&D model (Dave et al., 1975) can be made for a 60° zenith angle, an MLS atmosphere, and B&D's aerosol model Haze L, case C1. The beam normal

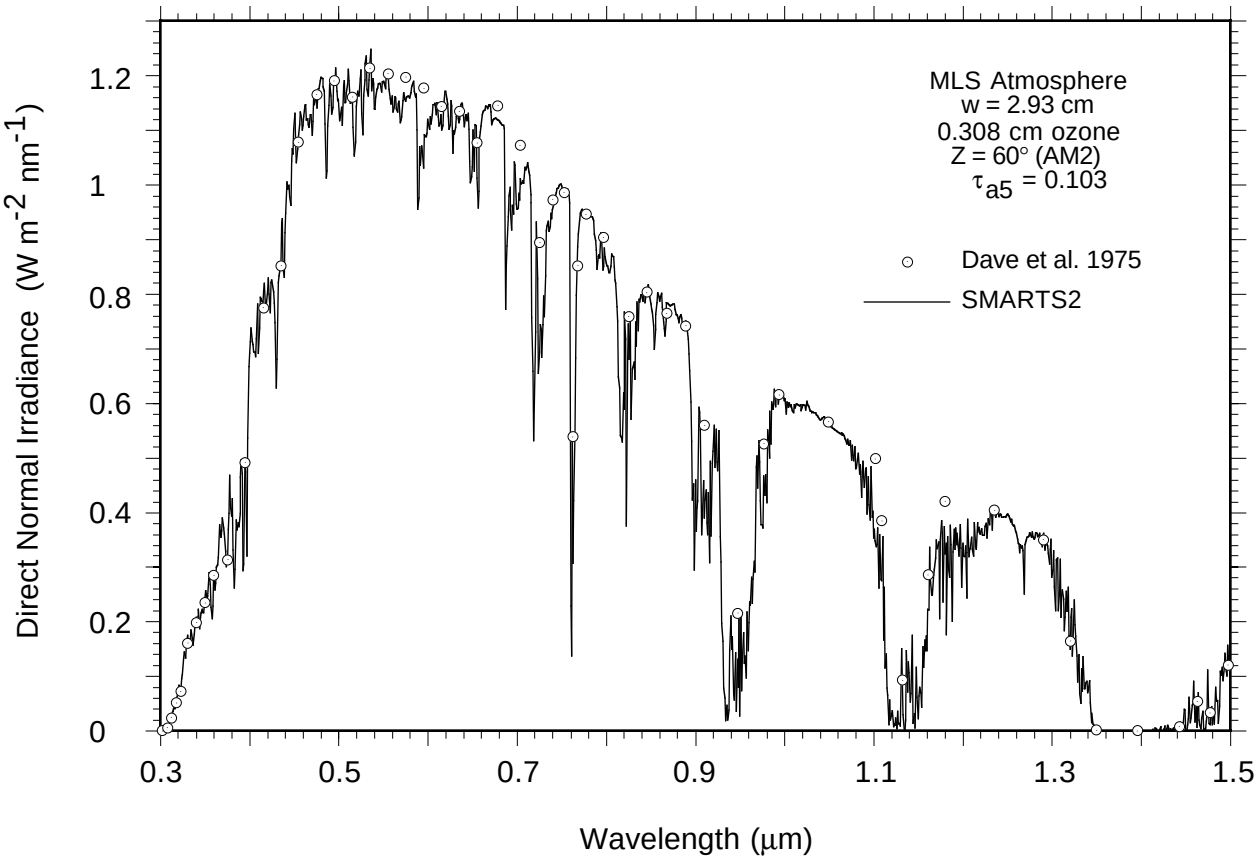

Fig. 8.1. Direct normal irradiance predicted by SMARTS2 and Dave et al. (1975) for a MidLatitude Summer reference atmosphere.

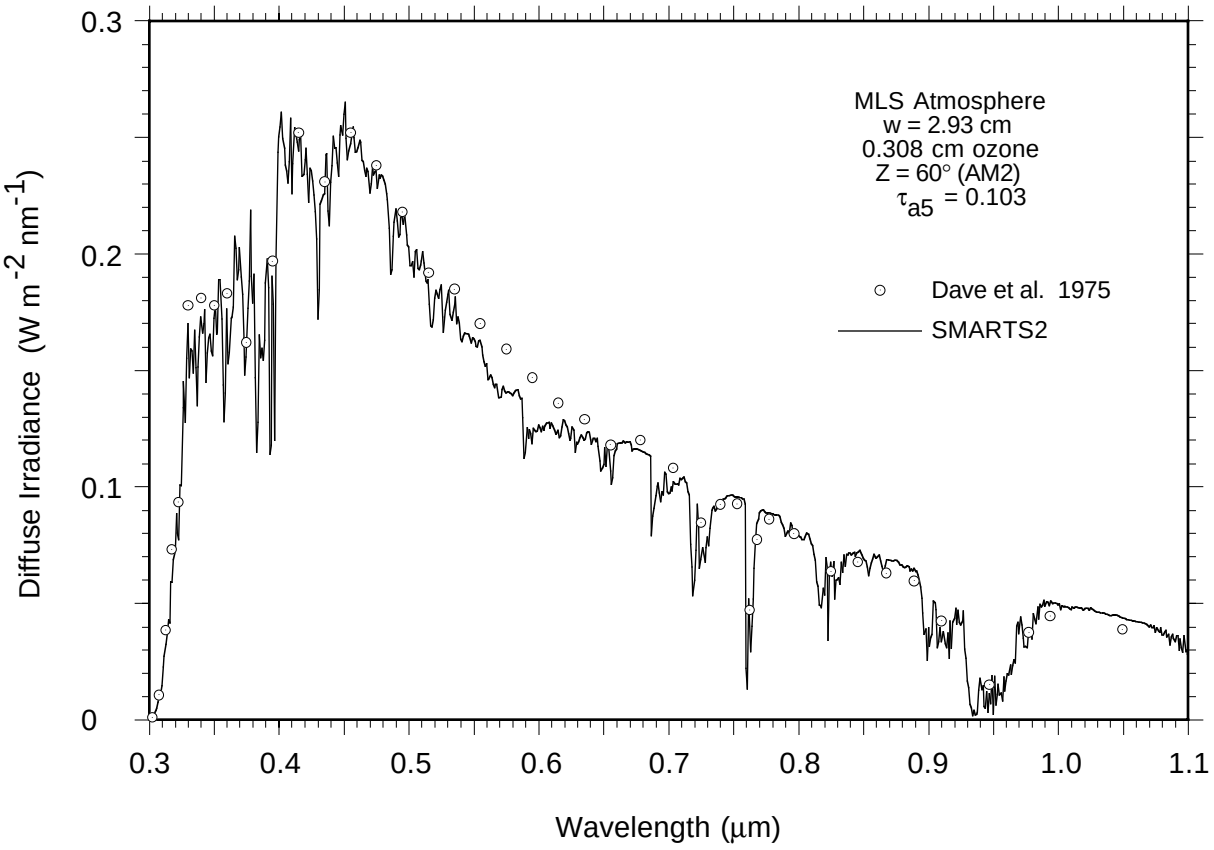

Fig. 8.2. Same as Fig. 8.1, but for diffuse irradiance.

irradiances are compared in Fig. 8.1, and show generally good agreement[11], although some differences are apparent in limited spectral ranges. In the near IR, these differences are most probably caused by the less detailed or accurate water vapor and mixed gases absorption data that were available in the early '70s when the B&D model was devised. In the visible, the differences in predicted irradiances between about 500 and 700 nm may be caused by differences in handling the aerosol optical characteristics. As mentioned earlier in Section 4.2.6, the aerosol optical thickness of the B&D aerosol model shows significant departure from the Angström equation. This translates into a slight but spectrally broad discrepancy between the transmittance predictions. Whereas inaccuracies in the aerosol transmittance translate into measurable but small (on a relative basis) inaccuracies of the direct normal irradiance, they simultaneously translate into relatively larger inaccuracies on the diffuse irradiance. This is probably the cause of the localized (around 340 and 550 nm) disagreement between the diffuse irradiances predicted by SMARTS2 and B&D for the same atmospheric conditions as above, as apparent in Fig. 8.2. Outside of these problematic bands, the agreement is excellent.

Further comparisons between SMARTS2 and B&D have been carried out in the UV because of the growing importance of this spectral region, and also because simplified models perform generally poorly there, especially with regard to diffuse radiation. The B&D spectral results were extracted from the tabulations provided by Dave and Halpern (1976) for different zenith angles, ozone thicknesses, and ground reflectances. In the present case, global radiation is considered,

[11] All the rigorous codes discussed in this section used older tabulations of the extraterrestrial spectrum. Their results have been corrected to match the SMARTS2 extraterrestrial spectrum, so that the remaining variance between the respective terrestrial spectra are only due to differences in modeling the atmospheric processes.

representing the maximum possible UV radiation (direct plus diffuse) for simulated cloudless atmospheric conditions. In the UV-B region of the spectrum, global radiation is predominantly diffuse radiation and is controlled by two essential parameters: zenith angle and total ozone thickness. (Surface reflectance may also have a significant effect in certain circumstances, as demonstrated in Section 5.4; it is fixed at a constant 0.3 for this comparison.) Three pairs of (Z, u_o) input data are considered, to encompass a wide range of atmospheric conditions: (0°, 0.2 cm), (60°, 0.3 cm), and (80°, 0.45 cm). The comparison between the predictions of SMARTS2 and B&D is illustrated in Fig. 8.3. It is found that SMARTS2 outputs are almost identical to the rigorous predictions, even under the most absorbtive conditions represented by the (80°, 0.45 cm) pair.

The predictions of SMARTS2 and BRITE (a Monte-Carlo code described by Bird and Hulstrom, 1982) were also analyzed. Their predicted direct normal, diffuse, and tilted global irradiances are compared in Figs. 8.4, 8.5, and 8.6, respectively, based on the tabulations of Bird et al. (1983), Hulstrom et al. (1985), and ASTM (1987a, 1987b). The conditions are: U.S. Standard Atmosphere, τ_{a5} = 0.27 using the SRA continental aerosol model in SMARTS2 to approximate the preliminary version of S&F rural model internal to BRITE, a constant ground reflectance of 0.2, circumsolar radiation admitted within a 3° opening angle, and Z = 48.19° (air mass 1.5). The ASTM /ISO standard spectra (ASTM, 1987a, 1987b; ISO, 1992) are for direct beam irradiance at normal incidence and global irradiance on a 37° tilted surface, as shown in Figs. 8.4 and 8.6.

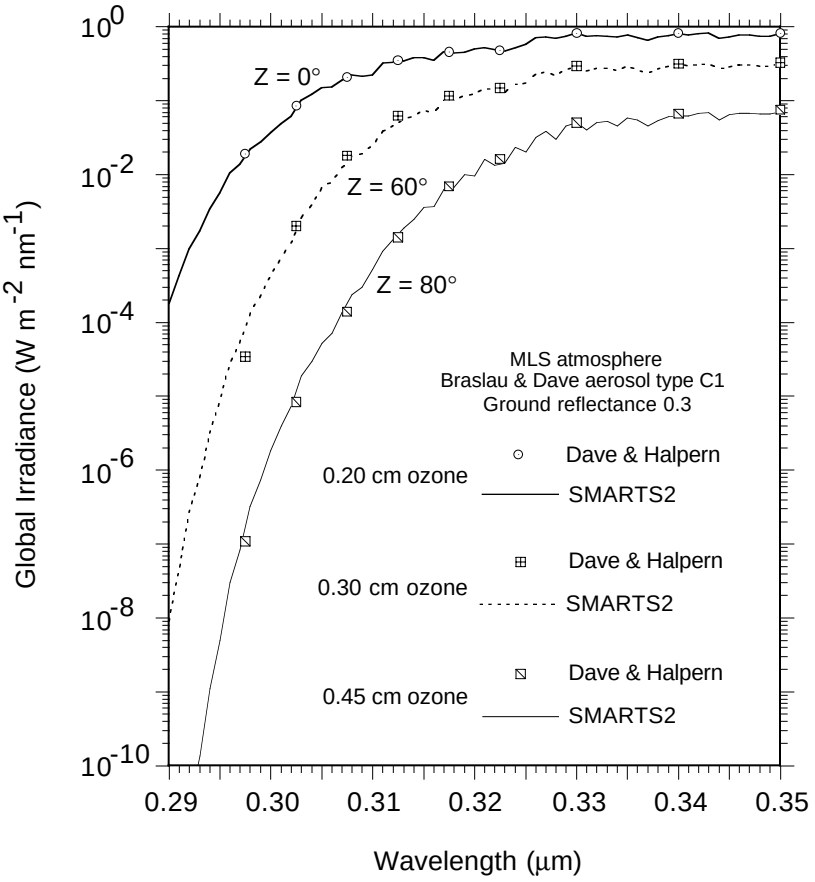

Fig. 8.3. Global UV irradiance predicted by SMARTS2 and Dave and Halpern (1976).

(There is no standard spectrum for diffuse irradiance.) It is clear from Figs. 8.4–8.6 that the predictions of SMARTS2 and BRITE are in close agreement, which suggests that SMARTS2 can be used to interpolate within the irradiance standards, to extrapolate these standards to lower wavelengths (they start at 305 nm), or to generate spectra for other "typical" conditions. (BRITE, the basic code behind these standards, is no longer available; therefore, new runs cannot be performed.)

Because the tabulations of Hulstrom et al. (1985) and the ASTM/ISO standards are for an "experimental" direct normal irradiance (with circumsolar radiation), whereas those of Bird et al.

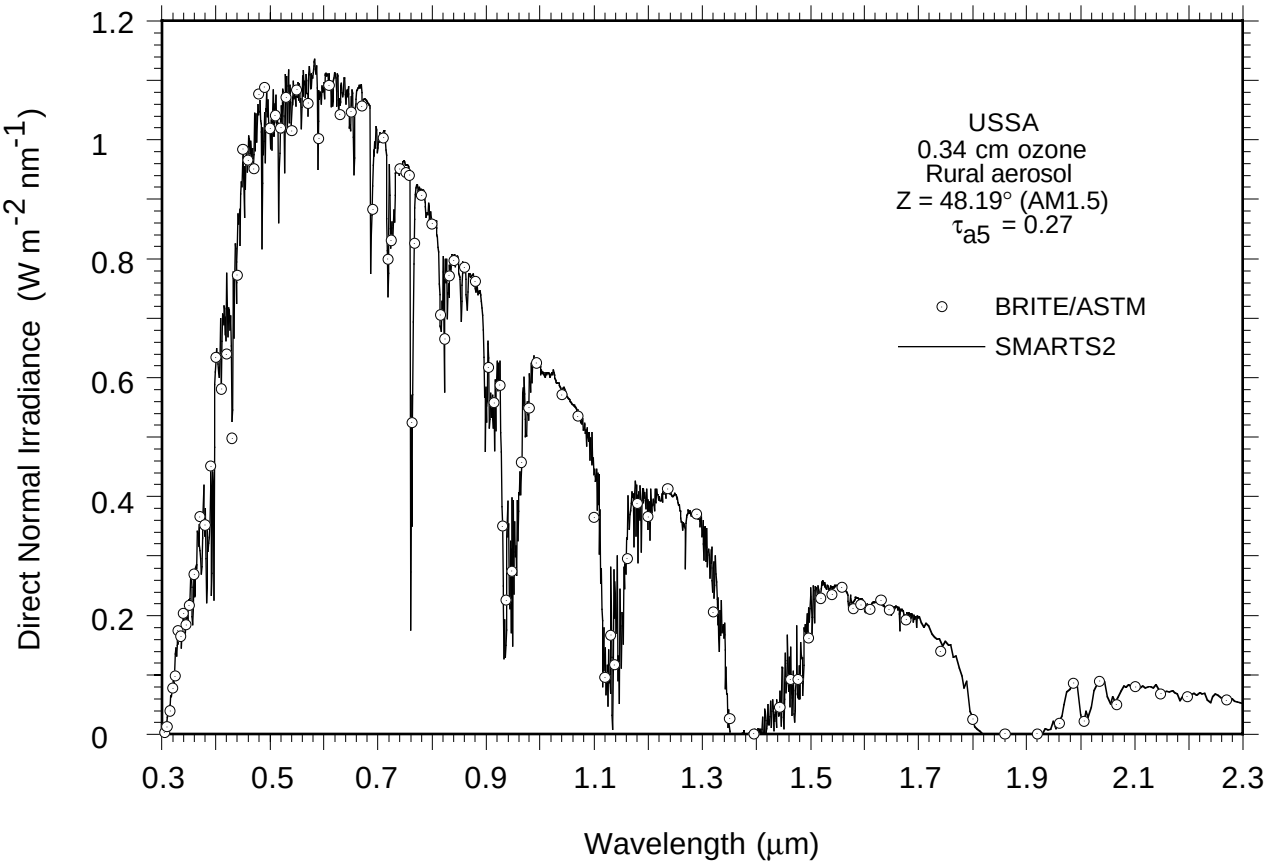

Fig. 8.4. Beam normal irradiance predicted by SMARTS2 and BRITE for the U.S. Standard Atmosphere.

(1983) are for ideal irradiance without the circumsolar contribution, it is possible to obtain the circumsolar contribution alone by simple subtraction, wavelength by wavelength. This provides a way of assessing the performance of the circumsolar algorithm descibed in Section 6. SMARTS2 was run both with the SRA continental aerosol and the S&F rural aerosol, which produced similar results. BRITE's results were obtained for a preliminary rural model of Shettle and Fenn (1975) which did not consider humidity effects. As shown in Fig. 8.7, the agreement between the SMARTS2 and BRITE predictions is close, although the aerosol models used in the two codes are not exactly identical. In this particular case, the circumsolar effect adds about 2.5 % to the beam irradiance at 300 nm, decreasing to 1.2 % at 500 nm, and to about 0.5 % at 1100 nm.

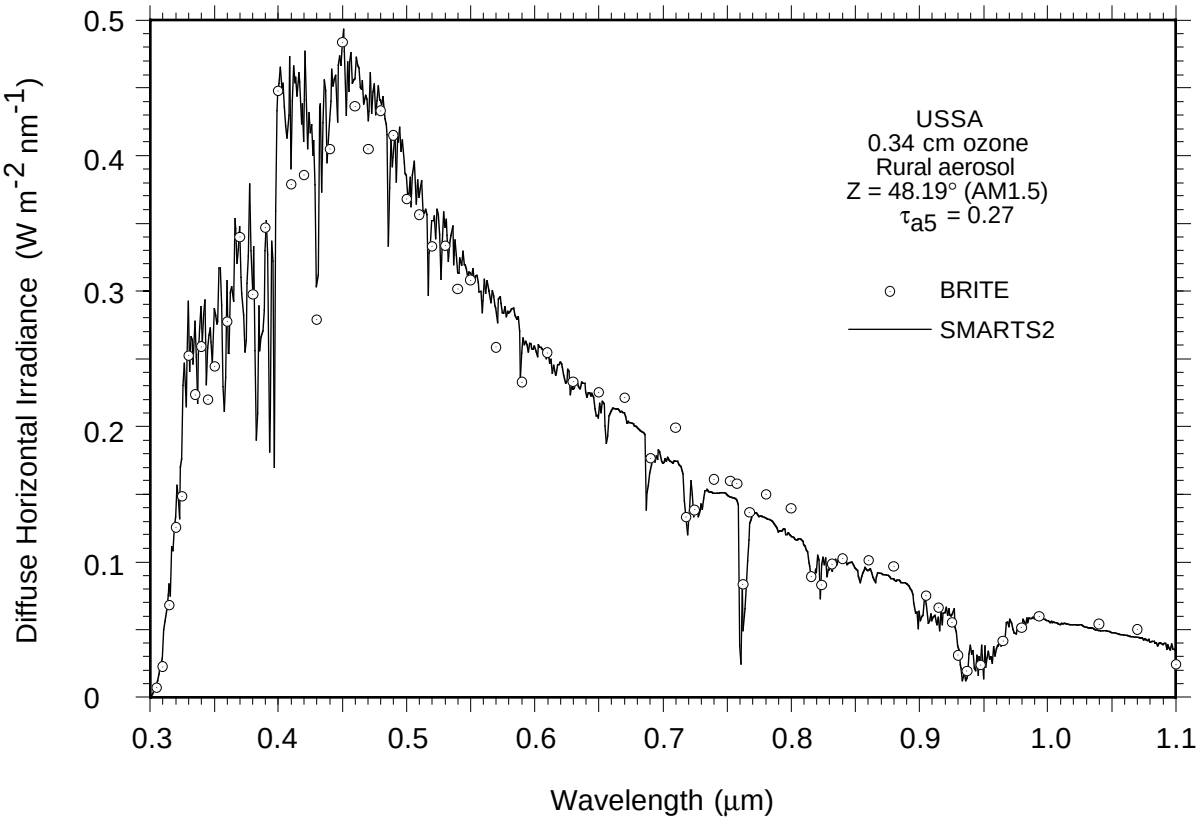

Fig. 8.5. Same as Fig. 8.4, but for diffuse irradiance on a horizontal surface.

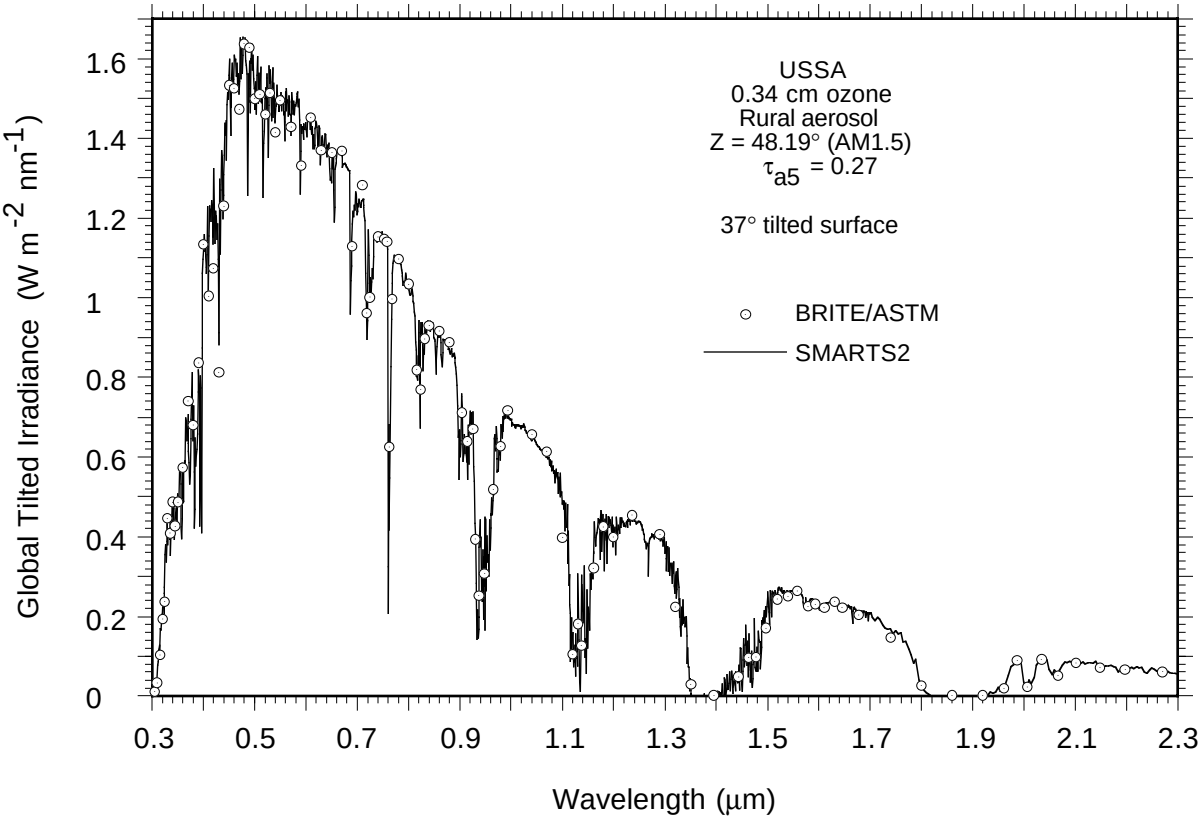

Fig. 8.6. Same as Fig. 8.4, but for global irradiance on a tilted surface.

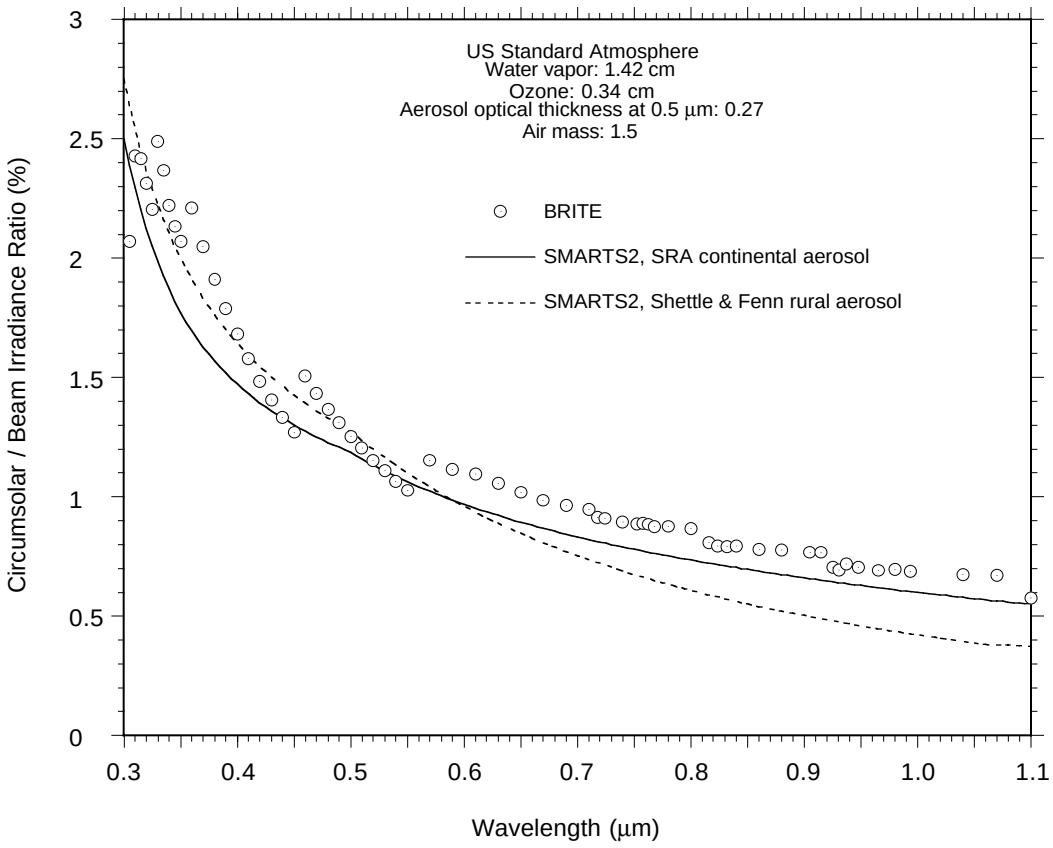

Fig. 8.7. Relative contribution of circumsolar radiation as predicted by SMARTS2 and BRITE for the conditions of the ASTM/ISO standards.

8.2 Comparison with measurements

Detailed comparison against carefully measured data is the classic way to assess the performance of a model. Some examples of such comparison will be provided here, using cloudless sky measurements in all cases.

First, measurements in the UV band are now routinely carried out at a number of sites worldwide because of their crucial importance in monitoring the variation of ozone in the atmosphere and its effect on the biologically active radiation at ground level. However, measurements in this spectral band are extremely delicate, so that regular calibrations and intercomparisons are necessary to maintain good data quality. Some of these studies (Booth et al., 1993; Gardiner et al., 1993; Koskela, 1994; McKenzie et al., 1993; Seckmeyer et al., 1994; Wang and Lenoble, 1994) show that some instruments may have practical problems that limit their intended operational spectral range, and that simultaneous measurements from different instruments at the same location may differ substantially.

The UV spectra that Bener measured in Switzerland about 25 years ago have been used by some authors to develop empirical UV irradiance models or to test them (e.g., Diffey, 1977; Green et al., 1974; Shettle and Green, 1974). One of Bener's datasets (as reproduced by Diffey, 1977) is compared to SMARTS2 predictions in Fig. 8.8. Considering the uncertainties of these relatively old measurements, and of the corresponding atmospheric and ground reflectance conditions, the agreement appears reasonably good.

Improved control over these conditions can be gained from more recent measurements. Of particular interest here are those that use reliable and well-characterized instruments, such as the Brewer and the Biospherical spectroradiometers. The former is now internationally accepted as a reference instrument for ozone and SO_2 measurements in the UV, as described by Brewer (1973). It has also undergone extensive tests and intercomparisons with other instruments (Koskela, 1994b). The Biospherical instrument is used throughout the National Science Foundation (NSF) network, now covering six sites in Alaska, Antartica, Argentina, and California. It scans both the UV and the visible spectrum and undergoes very frequent calibrations and a variety of post-measurement data processing, as detailed by Booth et al. (1993, 1995).

Figure 8.9 shows a comparison of measured UV data with SMARTS2 predictions for Sodankyla, Finland, during the Spring season when ozone is relatively high. The data were measured with a Brewer Mk II instrument (0.6 nm FWHM, PMT detector), and were obtained from the Finnish Meteorological Institute (Koskela, 1994a). The agreement is excellent from about 300 nm to 325 nm, the upper wavelength limit of this instrument. Below 300 nm, at an irradiance of about 50 $\mu W/m^2$ nm, the measured data tend to spread. This corresponds to the limit of sensitivity of this single-grating instrument, as the stray light level is reportedly on the order of 100 $\mu W/m^2$ nm (Koskela, 1994a). Another comparison for the same site—but for the Summer season, with a

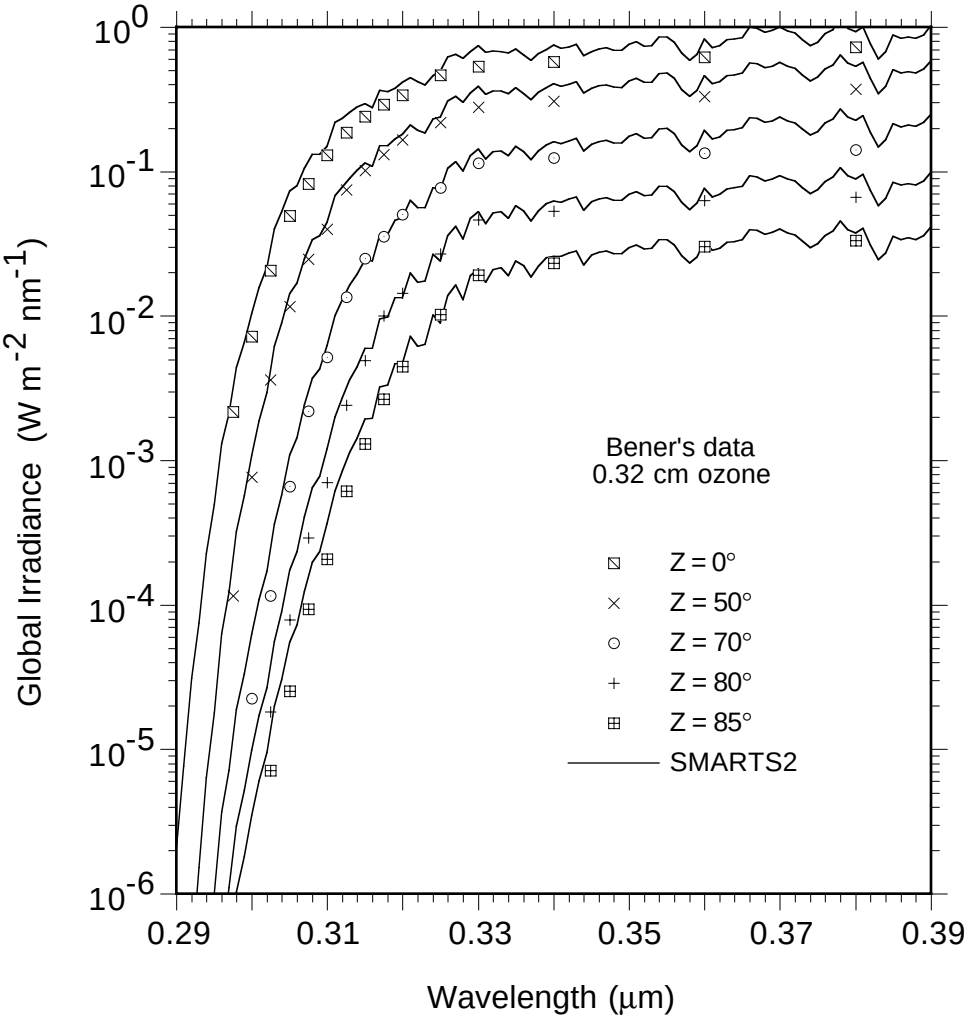

Fig. 8.8. Comparison of global UV irradiance predicted by SMARTS2 (continuous lines) to Bener's measurements in Switzerland (symbols).

lesser amount of ozone and a broader range of zenith angles—appears in Fig. 8.10. It is found that SMARTS2 is able to simulate spectroradiometric scans very accurately in the UV-B even at large zenith angles. (More structure is apparent in the measured data because the wavelength step of the instrument is 0.5 nm, or half the SMARTS2 step.)

A similar simulation, but for a Fall day at Norrköpping, Sweden, appears in Fig. 8.11. The measured data, obtained with an identical Brewer Mk II instrument (Josefsson, 1986), encompass a wide range of zenith angles, up to an extremely large value (Z = 89.4°) corresponding to the rising sun. As in Figs. 8.8–8.9, the agreement is consistently good at all zenith angles.

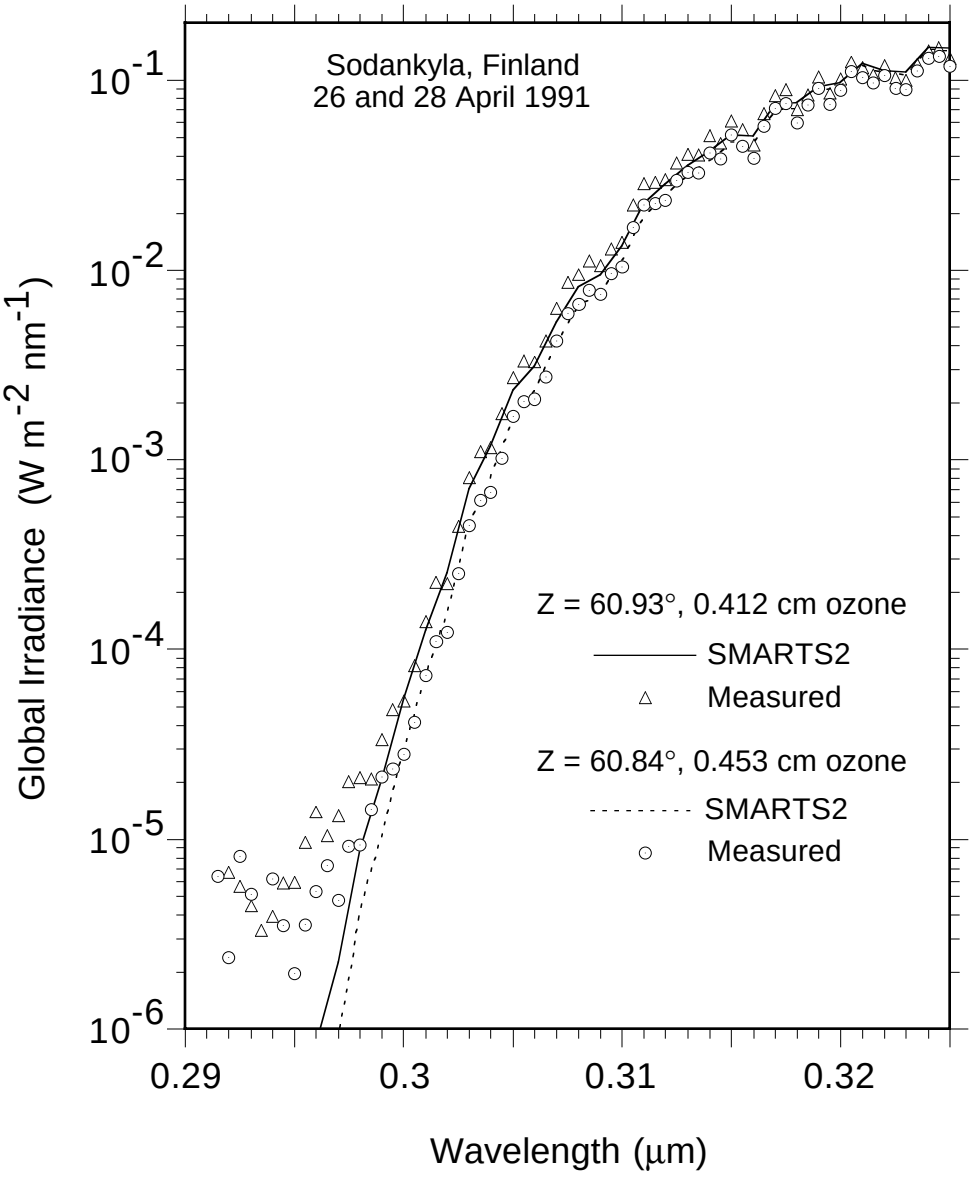

Fig. 8.9. Global irradiance predicted by SMARTS2 compared to actual UV measurements during a cloudless Spring day at Sodankyla, Finland (lat. 67.4°N, long. 26.6°E, alt. 179 m amsl).

Figure 8.12 exemplifies the use of the NSF polar UV data (Booth et al., 1995, and acompanying CD-ROM data discs) for assessing the performance of SMARTS2. Cloudless conditions are rare at Palmer, Antartica, but a few such events could be selected during episodes of very low ozone also called the “ozone hole”. Measurements of the total ozone column are provided by satellites (TOMS data). Precipitable water has been estimated from temperature and relative humidity using an empirical function (Gueymard, 1994). The experimental global irradiance was measured with a double-grating Biospherical SUV-100 spectroradiometer, which has a nominal spectral range of 280–700 nm, a FWHM of 0.7 nm, and uses a PMT detector (Booth et al., 1993). The modelled and measured data comparison in the UV-B that appears in Fig. 8.12a shows a good match down to about 300 nm, or an irradiance of about 100 $\mu W/m^2$ nm. The stray light contamination seems to be of the order of 50 $\mu W/m^2$ nm in this case. This stray light level is comparable to what has been found on another double-grating instrument (Gardiner et al., 1993).

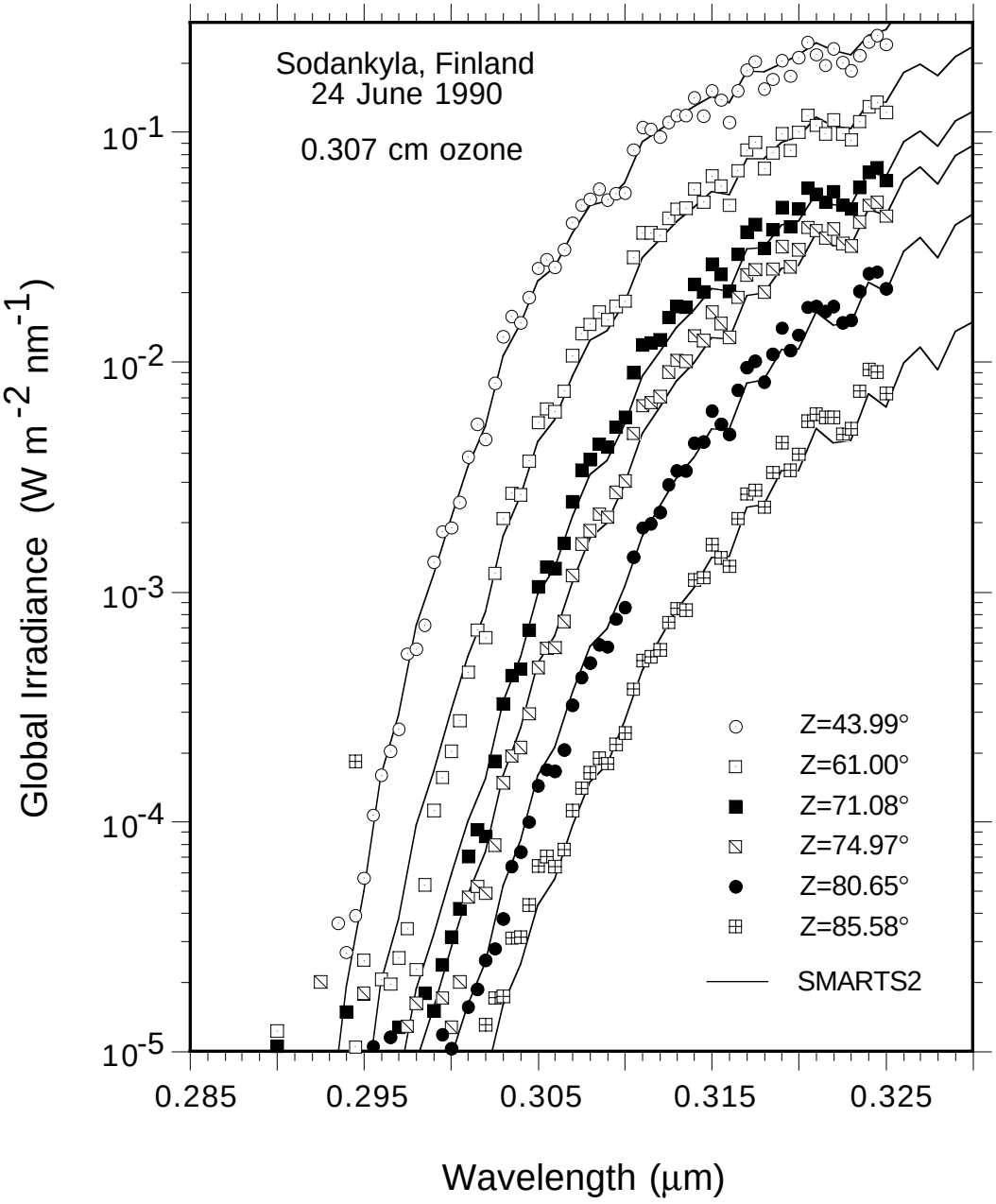

Fig. 8.10. Same as Fig. 8.9, but for a Summer day.

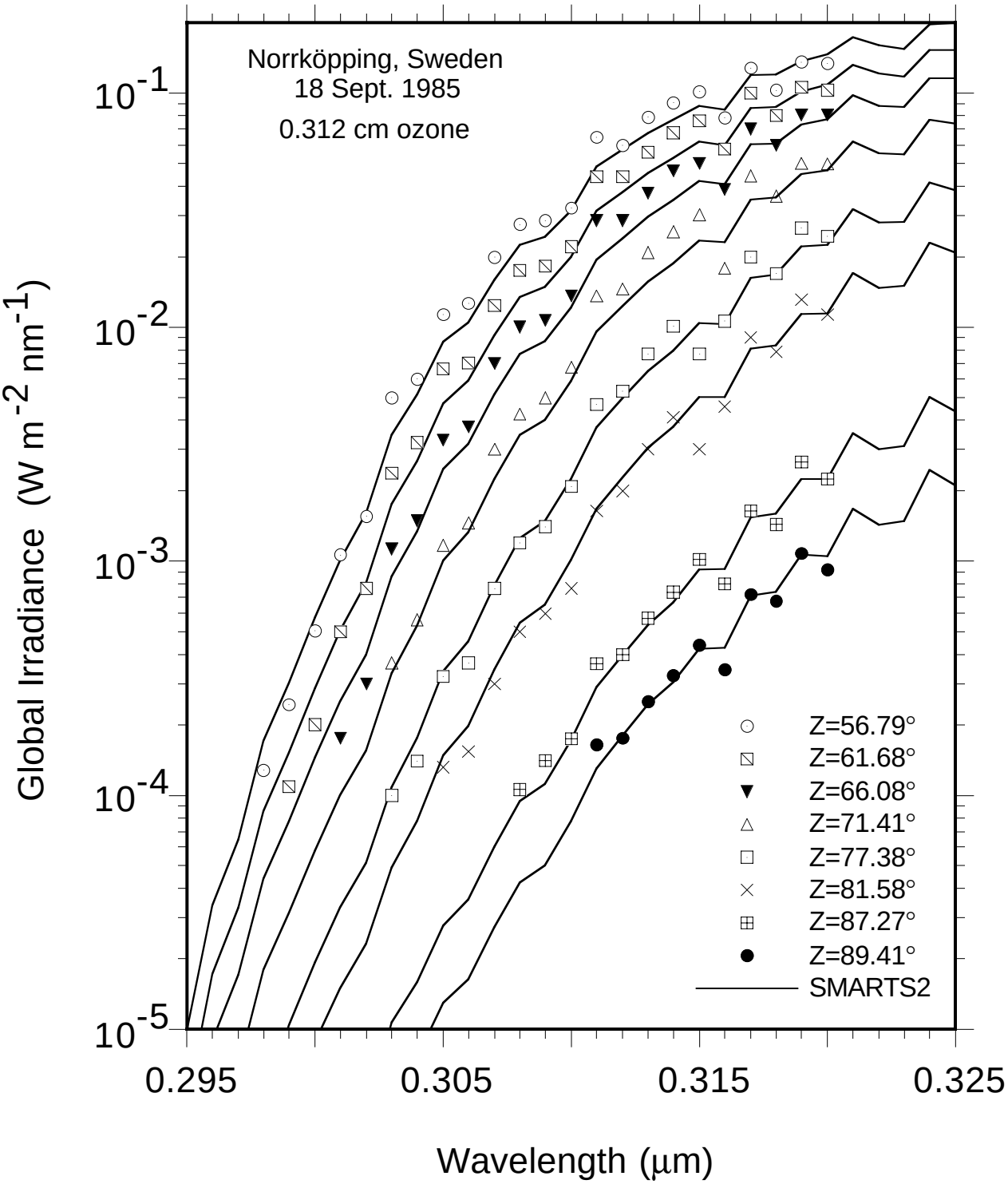

Fig. 8.11. Global irradiance predicted by SMARTS2 compared to actual UV measurements during a cloudless Fall day at Norrköpping, Sweden (lat. 58.58°N, long. 16.15°E, alt. 43 m amsl).

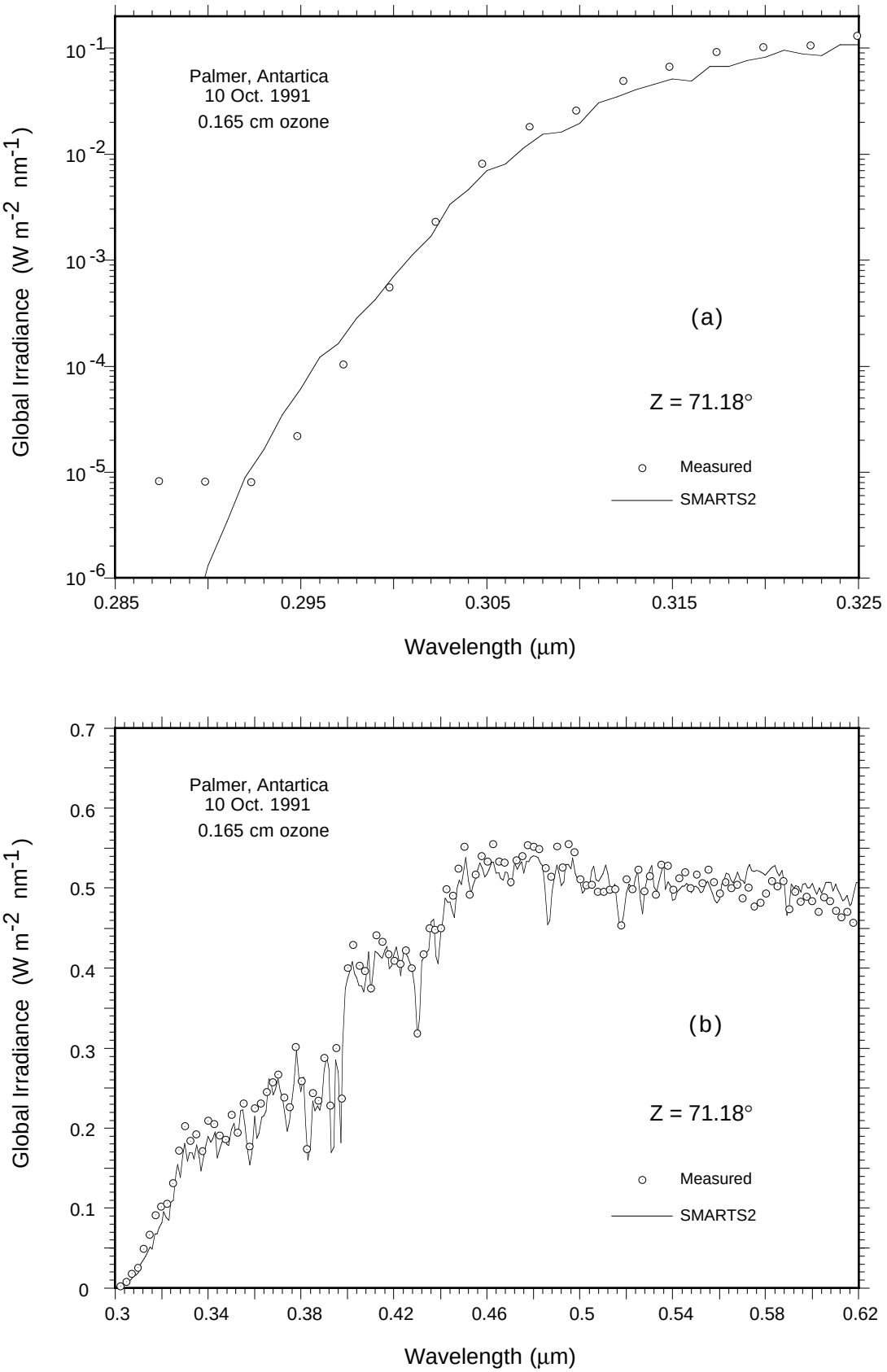

Fig. 8.12. Global irradiance predicted by SMARTS2 compared to actual UV measurements during a cloudless Spring day at Palmer, Antartica (lat. 64.77°S, long. 64.05°W, alt. 13 m amsl). (a) UV-B data; (b) UV and visible data.

Some of the discrepancy between the modelled and measured values may be caused by variations in the spectral ground reflectance from the model value (a constant value of 0.5 was assumed here) or in the spectral optical thickness of the aerosol (assumed here to follow Shettle & Fenn's maritime model with $\tau_{a5} = 0.02$). Figure 8.12b shows close overall agreement between modelled values and measured data, with some structure in the difference between them, alternating from match-up to slight over- or under-prediction.

A similar comparison for a different day at Palmer appears in Fig. 8.13, using a different instrument of the same type. The overall agreement between modelled values and measured data is as good as that in Fig. 12, except above about 520 nm where a downward trend of the measured data is very appparent. No particular or exceptional atmospheric condition is likely to explain the magnitude of this difference, if it were to be attributed to a model overprediction. This apparent experimental artifact may be related to the reduced sensitivity of the detector in that band. This problem has been discovered by the manufacturer, leading to a rating decrease from 700 to 620 nm, and to the advice that data beyond 600 nm should be ignored (Booth et al., 1993). It is more than likely that this instrument loses sensitivity at an even lower wavelength than anticipated, because of environmental conditions or other factors. This may significantly restrict the applicability of this instrument, as, by design, it was supposed to provide accurate scans in the Chappuis absorption band (ranging between about 500 and 700 nm with a peak around 600 nm) for supplemental ozone determinations.

Data similar to that in Figs 8.12–8.13, but from a temperate environment, appear in Fig. 8.14. The instrument is similar and is believed to be better maintained and more accurate, because it is the reference Biospherical instrument located at this manufacturer's headquarters in San Diego, approximately 5 km from the Pacific coast. Data from a clear day (August 26, 1993) were selected for this comparison because one of the scans was made for an air mass of exactly 1.2. It happens to be the air mass value chosen for the forthcoming ASTM standard UV spectrum (Zerlaut, 1995). This scan was simulated with SMARTS2, using a MidLatitude Summer atmosphere, a rural aerosol with 25 km visibility, a constant ground albedo of 0.12, and 0.284 atm-cm of ozone (from TOMS data for that day). This comparison in Fig. 8.14 shows excellent agreement over the whole scan. As discussed before, stray light contamination limits the sensitivity of the instrument below about 300 nm, where the noise floor (about 50 $\mu W/m^2$ nm) is reached. By comparison among Figs. 8.12 to 8.14, it appears that, beyond the apparent better total fit in the last figure, no sensitivity bias appears beyond 550 nm. Furthermore, the peaks and valleys of the spectrum appear to be correctly modelled in SMARTS2.

A broader spectral coverage at lower resolution is available from the data set measured at the Florida Solar Energy Center (FSEC) under the auspices of the National Renewable Energy Laboratory. A temperature-controlled LiCor LI-1800 spectroradiometer sampled the spectrum between 300 and 1100 nm at 2 nm intervals. This instrument uses a silicon detector, with a constant bandwidth (FWHM) of 6.15 nm. Its total uncertainty is better than ±5% between about 420 and 1100 nm, according to Myers (1989). The other experimental conditions are detailed by Riordan et al. (1989) and Riordan et al. (1990).

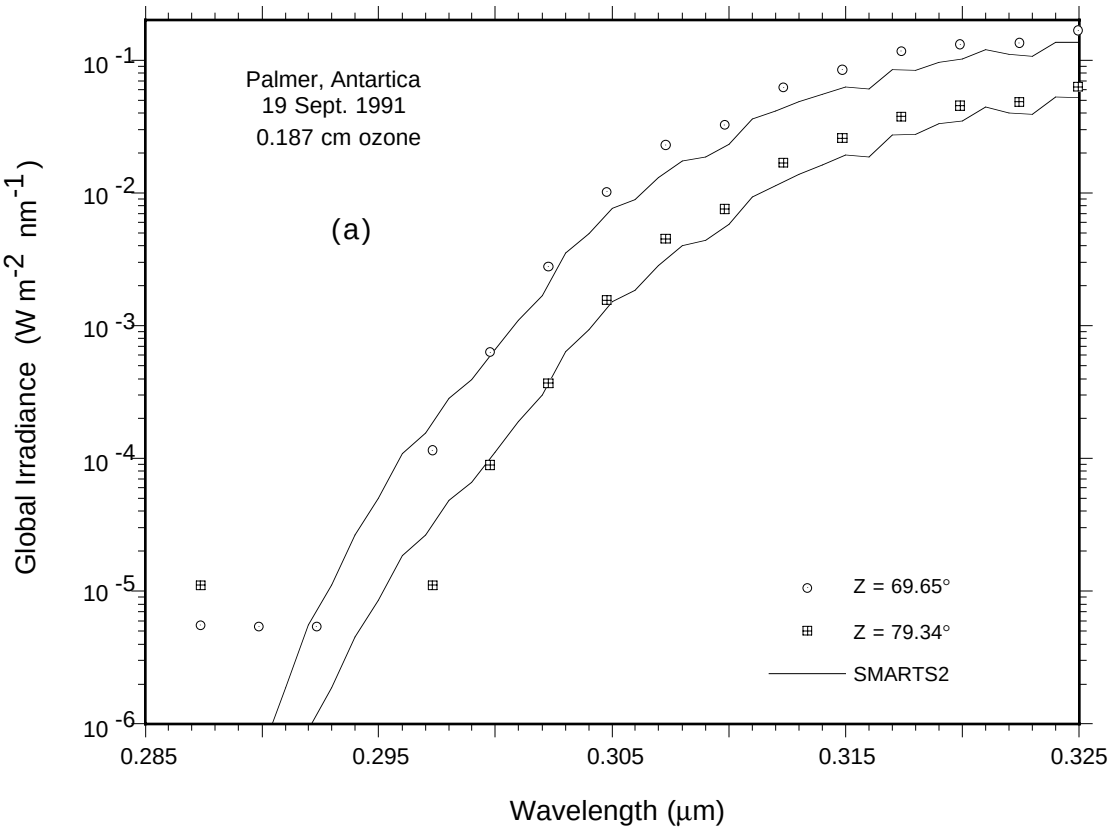

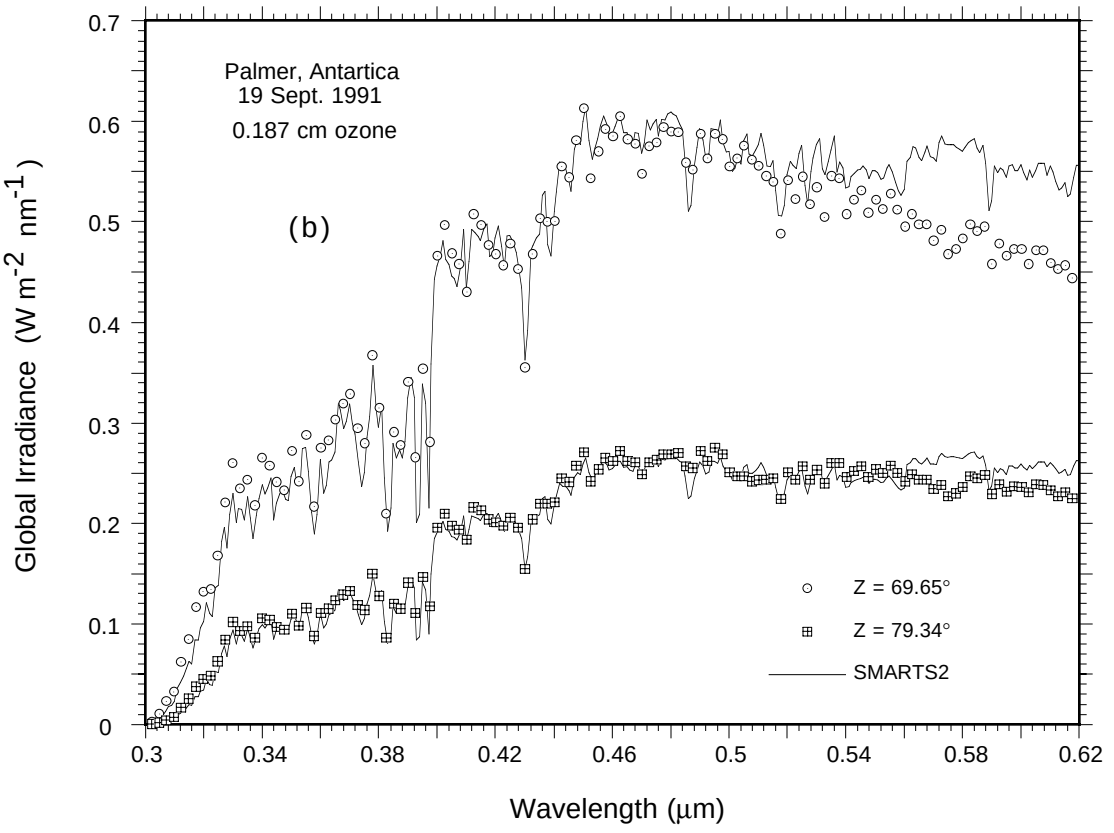

Fig. 8.13. Same as Fig. 8.12, but for a different day.
(a) UV-B data; (b) UV and visible data.

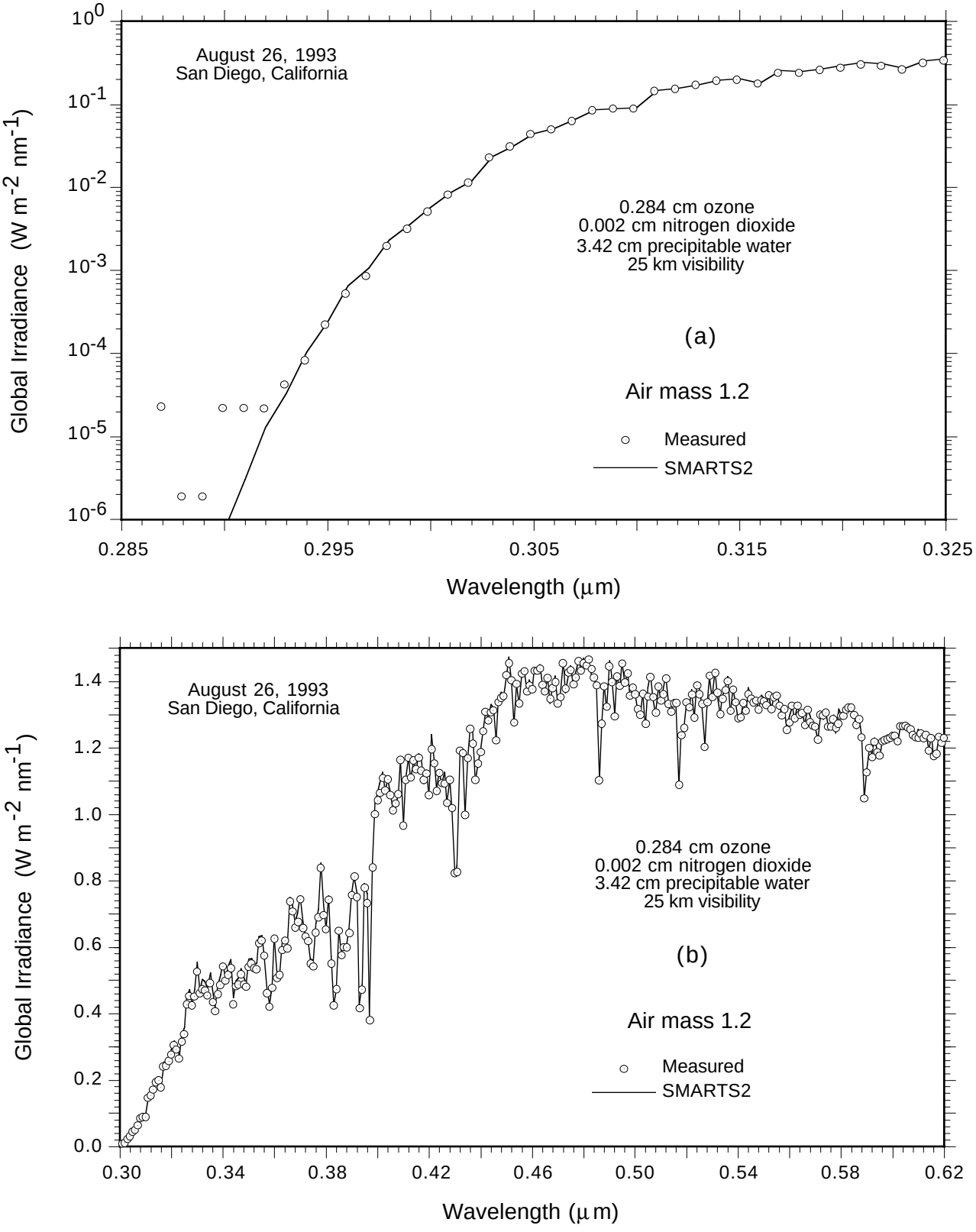

Fig. 8.14. Global irradiance predicted by SMARTS2 compared to actual UV measurements during a cloudless Summer day at San Diego, California (lat. 32.45°N, long. 117.11°W, alt. 9 m amsl). (a) UV-B data; (b) UV and visible data.

Figure 8.15 presents a comparison, in high and low spectral ranges, between measured data and calculated values of beam normal irradiance for summer conditions at an air mass of 1.46. Frequent radiosonde soundings from the nearby Kennedy Space Center provided the needed precipitable water input value, w = 4.5 cm, which is normal for that time of the year and was stable during the whole day (July 9, 1987). Whereas pressure was recorded, all the other atmospheric variables had to be assumed: u_n = 0.001 atm-cm, u_o = 0.3 atm-cm (seasonal average), and $ß$ = 0.087 (see further discussion below). Two different sets of modelled values were plotted: the first set at every other integer wavelength (to approximate the 2 nm step of the measured data), and a second set corrected for the circumsolar contribution and smoothed using the methodologies of Sections 6 and 7 to approximate the instrumental field of view and bandpass. It is clear from Fig. 8.15 that this smoothing proces is essential to make qualitatively and quantitatively correct comparisons. (The circumsolar correction is well within the instrumental error, as it decreases from 3 % at 300 nm, to 1.5 % at 550 nm, and to 1 % at 1100 nm; its importance may thus be considered marginal in this particular case.) It also appears that SMARTS2 closely follows the intricacies of the water vapor absorption features (among others). Some differences are apparent below 430 nm, in the 550–650 nm range, around 900 and 940 nm, and beyond 970 nm, but they may be caused at least in part by instrumental problems, as will be shown below.

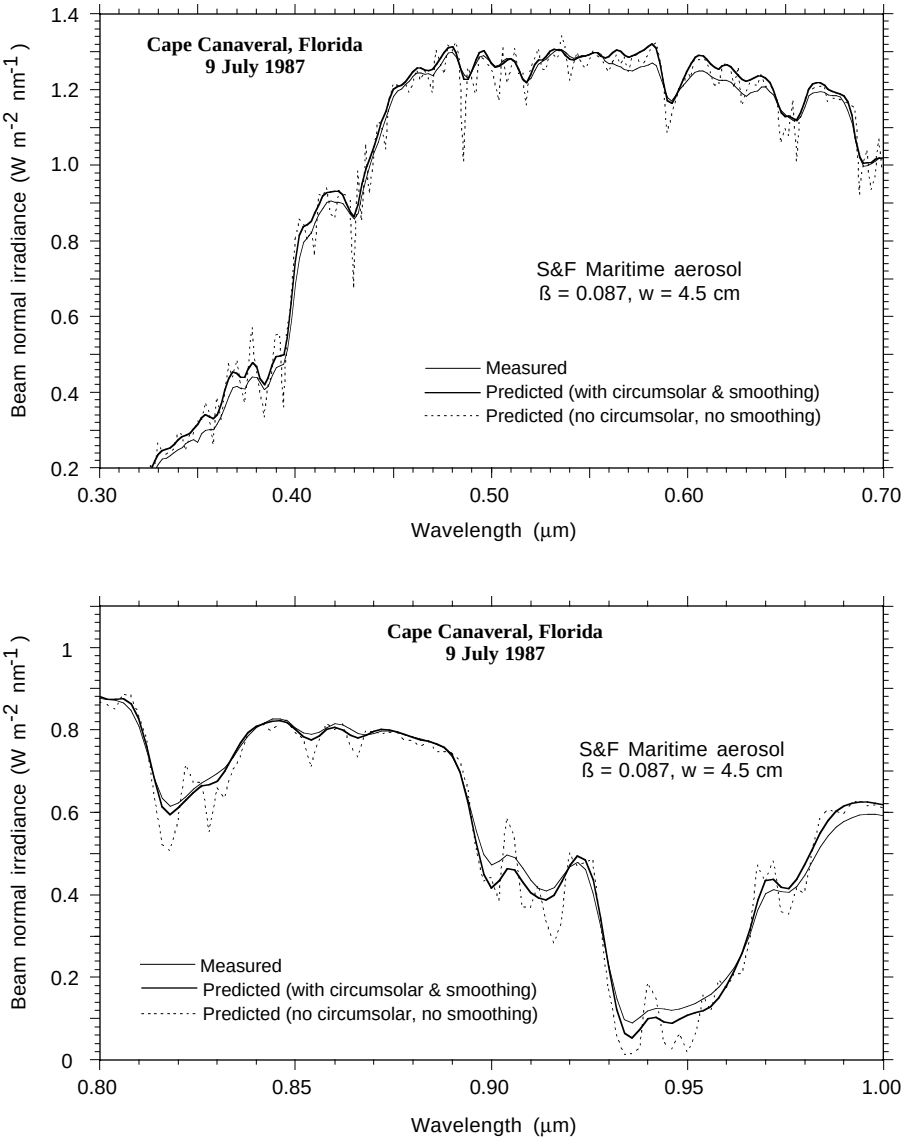

Fig. 8.15. Predicted *vs* measured beam normal irradiance at Cape Canaveral, Florida (lat. 28.42°N, long. 80.61°W, alt. 7 m amsl).

Figure 8.16 presents an illustration of the relative difference (in percent of the measured value) between the predictions of the model (including circumsolar correction and output smoothing) and the spectroradiometric data, along the whole spectral range of the instrument. The measurement is from the same summer day as for Fig. 8.15, using the same atmospheric conditions in the model predictions. Lacking discrimination from further atmospheric or meteorological input for this coastal location, the aerosol type is considered to be composed of maritime and rural contributions. Using Shettle & Fenn's maritime and rural models separately, a turbidity value was obtained after a preliminary analysis of the beam normal irradiance at 550 nm, as though ideal visibility observations were available. Turbidity values of $ß = 0.087$ for the maritime aerosol, or $ß = 0.043$ for the rural aerosol, produced a perfect match at that wavelength. (Note that no "fine tuning" of the input data was attempted besides this manipulation). The same approach was used for a winter day (January 28, 1988), as shown in Fig. 8.17. There is no way to totally isolate the performance of the model itself. However, if the experimental data were perfectly accurate, if there were no "hidden variables" missing from the model, and if perfect atmospheric input data were available, the curves in Fig. 8.16a and 8.17a would represent the actual performance of the model for the prediction of beam normal irradiance. Although the relative differences appear large in the 940 nm band, especially in summer (Fig. 8.16a), they correspond to only slight absolute differences because of the strong absorption there (Fig. 8.15).

The spikes in the O_2 band around 760 nm and in the H_2O band around 940 nm presumably correspond to a slight spectral calibration shift of the instrument. This is supported by the fact that the same spikes are also apparent in the instrumental uncertainty curves provided by Myers (1989) for this instrument and in the instrument-to-instrument precision curve of Riordan et al. (1989). Other common patterns are also apparent between the plots displayed in these two references and in Figs. 8.16 and 8.17: a large uncertainty in the UV[12], a decreasing uncertainty with increasing wavelength between 400 and 560 nm, two broad spikes at about 580 and 620 nm, and an increasing uncertainty above 970 nm. Most of these patterns are also apparent when considering the modelled *global normal* irradiance (Figs. 8.16b and 8.17b). Because of the similarity, consistency, and shape of these observed patterns in the experimental uncertainty on one hand, and in the differences between the modelled and measured irradiances on the other hand, it is argued that the latter cannot be explained by either reasonable modeling inconsistencies or estimation errors in the atmospheric conditions. For instance, the previously described patterns are still identifiable when switching from a moderate-ß maritime aerosol type to a low-ß rural aerosol type. (Incidentally, it seems that the former gives a better fit above 550 nm, and the latter a better fit below. It is also possible that the strong and opposite "errors" affecting the direct normal and global irradiances below 500 nm (Fig. 8.17a vs Fig. 8.17b) are caused by an underestimated aerosol optical thickness there, itself due to unusual aerosol conditions characterized by a very large α_1 and a low α_2.) It is concluded that, in this case, the model performance is within, or close to, the instrumental uncertainty limits.

These findings suggest that a detailed performance assessment of SMARTS2 requires very accurate and well-characterized experimental data, that would include a detailed set of simultaneous atmospheric and ground reflectance conditions. Obviously, the model can be run backwards to study atmospheric conditions (e.g., the aerosol spectral optical thickness) if accurately measured spectral data are available. It can also be used to detect some types of instrumental limitations or diagnose calibration deficiencies if appropriate inputs to the model can be measured or inferred with sufficient accuracy. (Such an application of models for the case of UV radiation has also been pointed out by Seckmeyer et al., 1994, and Wang and Lenoble, 1994.) This is achievable in part because of the relatively high resolution of the model, the sharp absorption bands that are now well-resolved and which can be modelled accurately, and the model's capability to approximate the behavior of spectroradiometers.

---

[12] Riordan et al. point out that "... the uncertainty in the absolute value of the outdoor measurements below 0.4 µm is high because of low spectral irradiance from the calibration lamps that results in a low signal-to-noise ratio for the spectroradiometer calibrations."

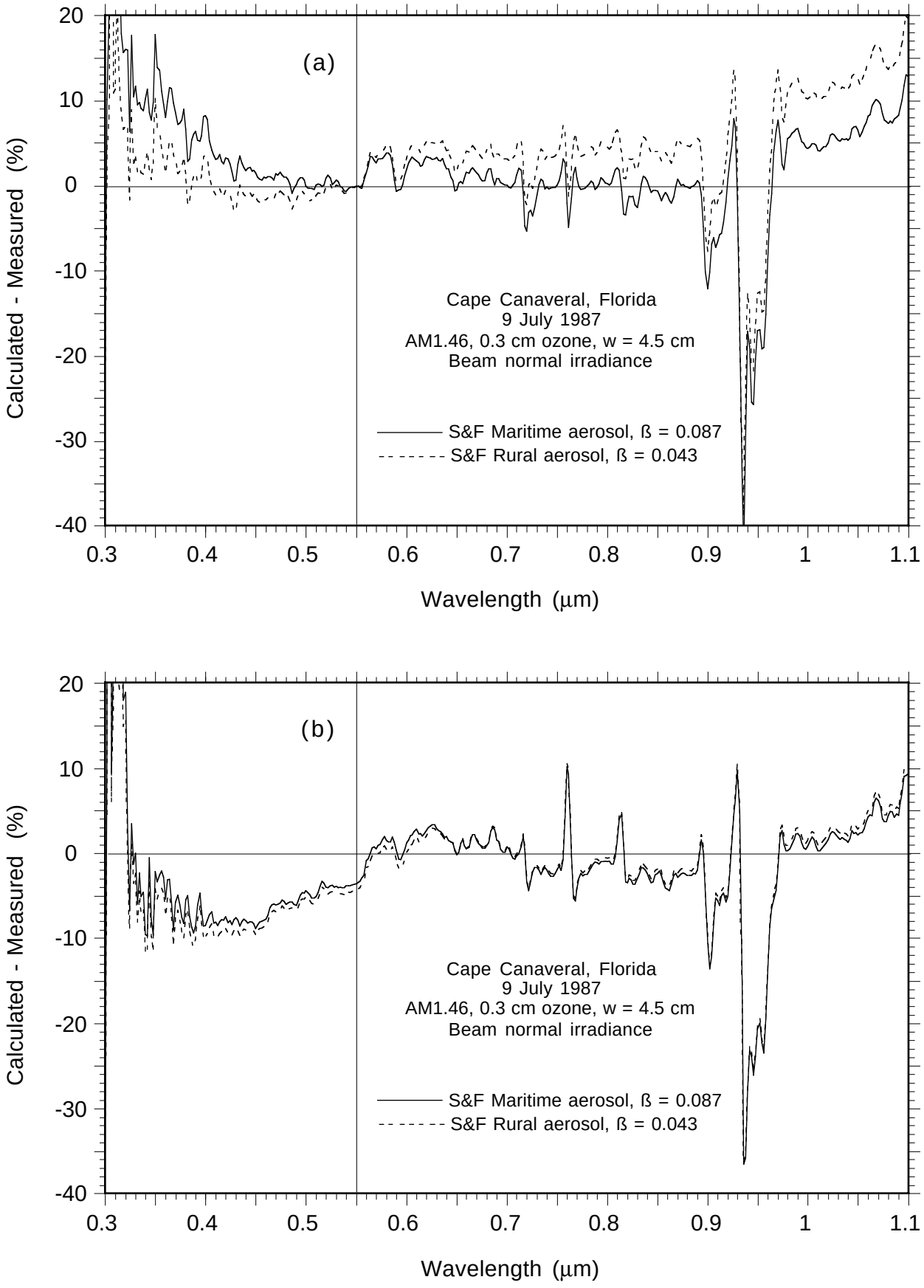

Fig. 8.16. Calculated *vs* measured irradiance (in percent of the measured value) at Cape Canaveral on July 9, 1987. (a) Beam normal irradiance; (b) Global normal irradiance.

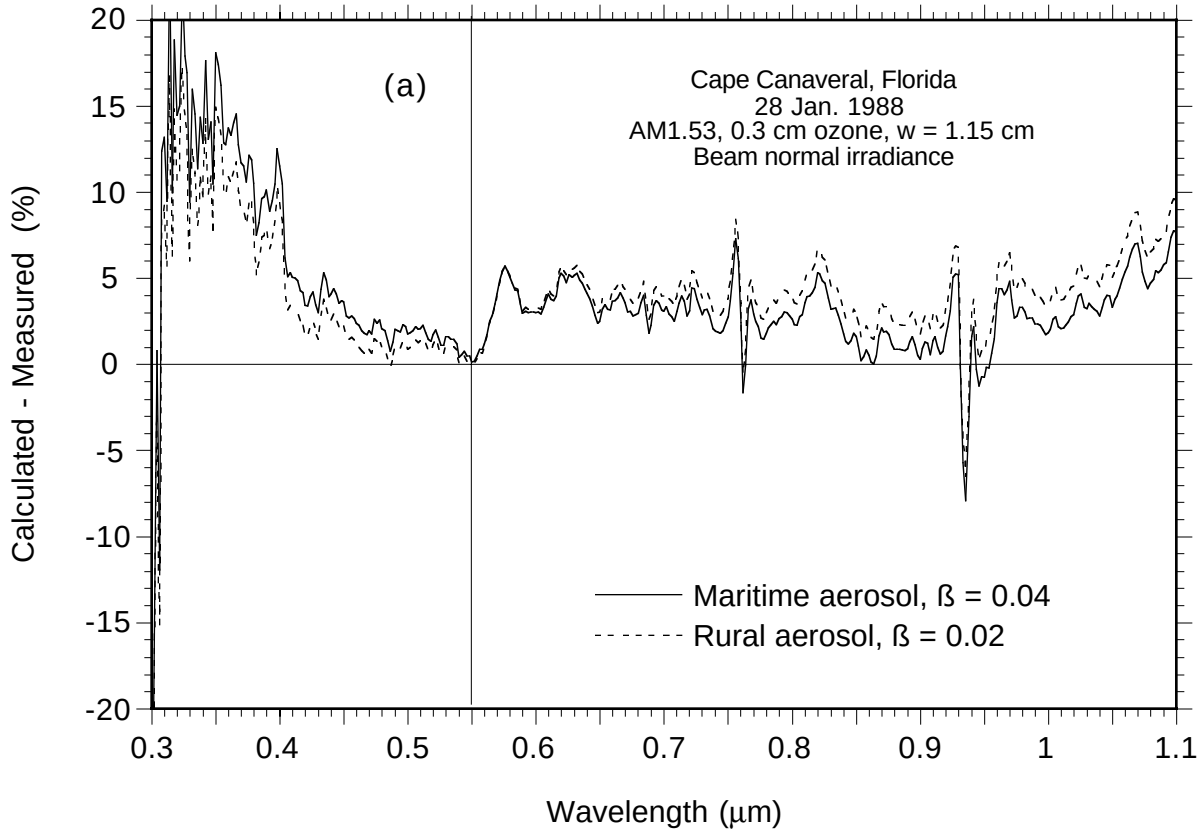

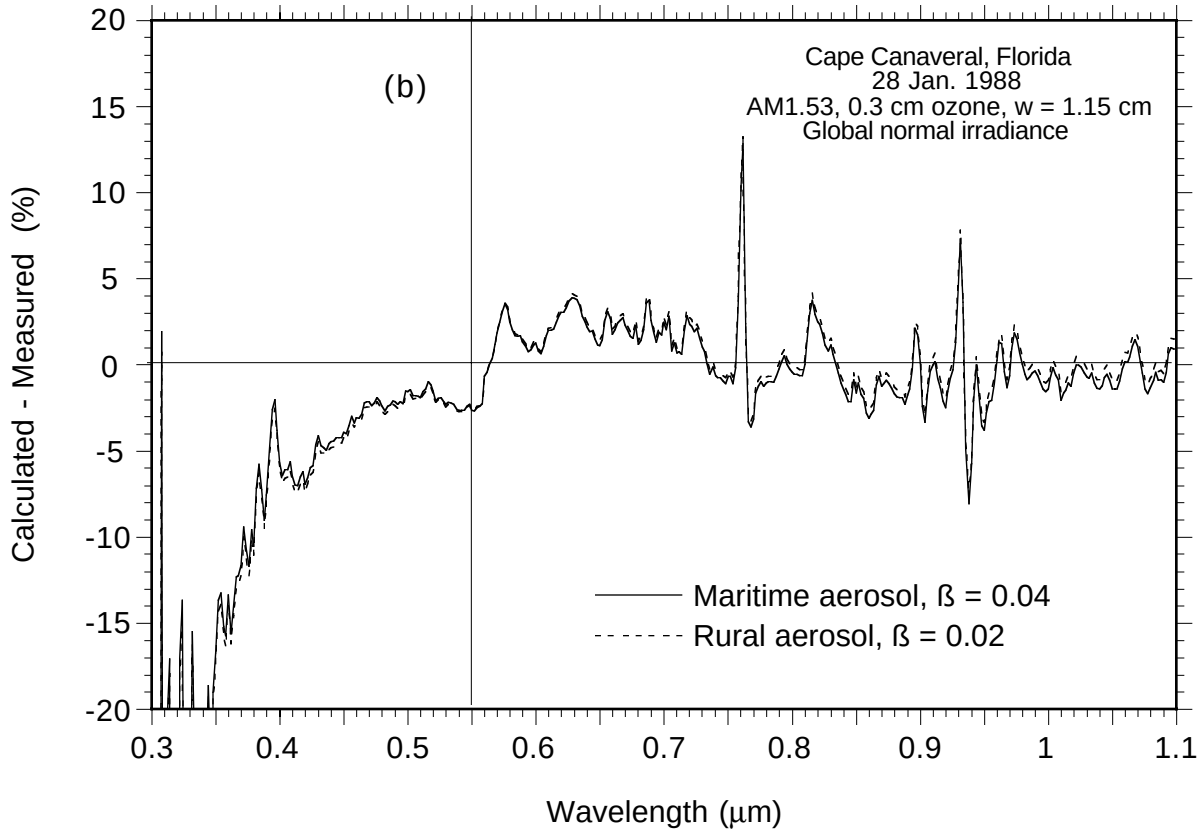

Fig. 8.17. Same as Fig. 8.16, but for Jan. 28, 1988.
(a) Beam normal irradiance; (b) Global normal irradiance.

9. CONCLUSION

The spectral model presented here closely fits the most recently available extinction data. It can be used to generate terrestrial spectra needed in various sensitivity analyses, to rapidly approximate the predictions of rigorous codes (e.g., MODTRAN2), or to simulate spectroradiometric data from atmospheric data. Its capabilities extend well into the UV region (to 280 nm), where it uses a recently measured extraterrestrial spectrum. An extensive performance assessment, using comparisons with both rigorous codes and measured data in a variety of atmospheric conditions and spectral bands, shows that SMARTS2 performs well and may even be used to detect some instrumental problems if sufficient auxiliary atmospheric variables are available. In the UV, it avoids the modeling flaws of existing simpler spectral models, and its results are shown to remain accurate even at large zenith angles.

Another application of SMARTS2 resides in its capability to generate reference spectra close to the existing standard ASTM/ISO terrestrial spectra, but with higher resolution and flexibility. Future work will be devoted to specific applications of this model, both spectral and broadband.

10. ACKNOWLEDGMENTS

The author is particularly thankful to all the individuals who contributed largely to this work by providing basic data or valuable discussions: Len Abreu, Gail P. Anderson, Rocky Booth, Chris A. Cantrell, James H. Chetwynd, Dominique Daumont, Jean-Jacques Delaunay, Bo-Cai Gao, L. A. Hall, Michael E. van Hoosier, Weine Josefsson, Tapani Koskela, Ross McCluney, Joe Michalsky, Benoit Molineaux, Marian Morys, Maria Putsay, Carol Riordan, Eric P. Shettle, and David E. Soule. The author also wishes to thank Paul Jindra for his help and thorough review of the successive versions of the manuscript.
This work was partially funded by grant DE-FG01-90CE21048 from the Office of Building Technologies, U.S. Department of Energy.

11. REFERENCES

D. Allard and I. Tombach, The effects of non-standard conditions on visibility measurements, *Atmos. Environ.* **15**, 1847-1857 (1981).

G. P. Anderson, J. H. Chetwynd, J. M. Theriault, P. Acharya, A. Berk, D. C. Robertson, F. X. Kneizys, M. L. Hoke, L. W. Abreu, and E. P. Shettle, MODTRAN2: Suitability for remote sensing, Proc. Conf. Atmospheric Propagation and Remote Sensing II, A. Kohnle and W.B. Miller eds., Orlando, SPIE, vol. 1968, p. 514-525 (1993).

G. P. Anderson, S. A. Clough, F. X. Kneizys, J. H. Chetwynd, and E. P. Shettle, *AFGL atmospheric constituent profiles (0–120 km),* Tech. rep. AFGL-TR-86-0110, Air Force Geophysics Lab., Hanscom AFB, MA (1986).

S. M. Anderson, Laser measurements of ozone absorption cross sections in the Chappuis band, *Geophys. Res. Lett.* **19**, 933-936 (1992).

S. M. Anderson, Ozone absorption cross section measurements in the Wulf bands, *Geophys. Res. Lett.* **20**, 1579-1582 (1993).

Anon., *U.S. Standard Atmosphere supplements, 1966,* ESSA/ NASA/ USAF, U.S. Gov. Printing Office, Washington, DC, (1966).

J. C. Arvesen, R. N. Griffin, and B. D. Pearson, Determination of extraterrestrial solar spectral irradiance from a research aircraft, *Appl. Opt.* **8**, 2215-2232 (1969).

S. Asano and A. Uchiyama, Application of an extended ESFT method to calculation of solar heating rates by water vapor absorption, *J. Quant. Spectrosc. Radiat.* **38**, 147-158 (1987).

ASTM, *Standard tables for terrestrial direct normal solar spectral irradiance for air mass 1.5,* Standard No. E891-87, American Society for Testing and Materials, Philadelphia, PA (1987a).

ASTM, *Standard tables for terrestrial solar spectral irradiance at air mass 1.5 for a 37° tilted surface,* Standard No. E892-87, American Society for Testing and Materials, Philadelphia, PA (1987b).

A. Berk, L. S. Bernstein, and D. C. Robertson, *MODTRAN: A moderate resolution model for LOWTRAN7,* Rep. GL-TR-89-0122, Air Force Geophysical Lab., Hanscom, MA (1989).

R. E. Bird, A simple, solar spectral model for direct-normal and diffuse horizontal irradiance, *Solar Energy* **32**, 461-471 (1984).

R. E. Bird and R. L. Hulstrom, *Extensive modeled solar spectral data sets with solar cell analysis,* Tech. rep. SERI/TR-215-1598, Solar Energy Research Institute, Golden, CO (1982).

R. E. Bird, R. L. Hulstrom, and L. J. Lewis, Terrestrial solar spectral data sets, *Solar Energy* **30**, 563-573 (1983).

R. E. Bird and C. Riordan, Simple solar spectral model for direct and diffuse irradiance on horizontal and tilted planes at the Earth's surface for cloudless atmospheres, *J. Clim. Appl. Meteorol.* **25**, 87-97 (1986).

M. Blumthaler and W. Ambach, Solar UVB-albedo of various surfaces, *Photochem. Photobiol.* **48**, 85-88 (1988).

C. R. Booth, T. B. Lucas, T. Mestechkina, J. R. Tusson, D. A. Neuschuler, and J. H. Morrow, *NSF polar programs UV spectroradiometer network 1991-1993 operations report,* Biospherical Instruments Inc., San Diego, CA (1993).

C. R. Booth, T. B. Lucas, T. Mestechkina, J. R. Tusson, D. A. Neuschuler, and J. H. Morrow, *NSF polar programs UV spectroradiometer network 1993-1994 operations report,* Biospherical Instruments Inc., San Diego, CA (1995).

D. E. Bowker, R. E. Davis, D. L. Myrick, K. Stacy, and W. T. Jones, *Spectral reflectances of natural targets for use in remote sensing studies,* Ref. Publ. 1139, NASA (1985).

M. A. Box and A. Deepak, Single and multiple scattering contributions to circumsolar radiation, *Appl. Opt.* **17**, 3794-3797 (1978).

M. A. Box and A. Deepak, Atmospheric scattering corrections to solar radiometry, *Appl. Opt.* **18**, 1941-1949 (1979).

N. Braslau and J. V. Dave, Effect of aerosols on the transfer of solar energy through realistic model atmospheres, *J. Appl. Meteorol.* **30**, 601-619 (1973).

A. W. Brewer, A replacement for the Dobson spectrophotometer?, *Pure Appl. Geophys.* **106**, 928-937 (1973).

A. W. Brewer, C. T. McElroy, and J. B. Kerr, Nitrogen dioxide concentrations in the atmosphere, *Nature* **246**, 129-133 (1973).

D. T. Brine and M. Iqbal, Diffuse and global solar spectral irradiance under cloudless skies, *Solar Energy* **30**, 447-453 (1983).

G. E. Brueckner, K. L. Edlow, L. E. Floyd, J. L. Lean, and M. E. VanHoosier, The Solar Ultraviolet Spectral Irradiance Monitor (SUSIM) experiment on board the Upper Atmosphere Research Satellite (UARS), *J. Geophys. Res.* **98D**, 10,695-10,711 (1993).

M. Cacciani, A. di Sarra, G. Fiocco, and A. Amoruso, Absolute determination of the cross sections of ozone in the wavelength region 339-355 nm at temperatures 220-293 K, *J. Geophys. Res.* **94D**, 8485-8490 (1989).

B. J. Choudhury and A. T. C. Chang, The solar reflectance of a snow field, *Cold Reg. Sci. Technol.* **1**, 121-128 (1979).

M. T. Coffey, On the temporal change of stratospheric NO_2, *Geophys. Res. Lett.* **15**, 331-334 (1988).

M. T. Coffey, W. G. Mankin, and A. Goldman, Simultaneous spectroscopic determination of the latitudinal, seasonal, and diurnal variability of stratospheric N_2O, NO, NO_2, and HNO_3, *J. Geophys. Res.* **86C**, 7331-7341 (1981).

K. L. Coulson and D. W. Reynolds, The spectral reflectance of natural surfaces, *J. Appl. Meteorol.* **10**, 1285-1295 (1971).

G. A. d'Almeida, P. Koepke, and E. P. Shettle, *Atmospheric aerosols: Global climatology and radiative characteristics*, A. Deepak Publ., Hampton, VA (1991).

D. Daumont, J. Brion, J. Charbonnier, and J. Malicet, Ozone UV spectroscopy I: Absorption cross-sections at room temperature, *J. Atmos. Chem.* **15**, 145-155 (1992).

J. V. Dave and P. M. Furukawa, Scattered radiation in the ozone absorption bands at selected levels of a terrestrial, Rayleigh atmosphere, *Meteorol. Monogr.* **7** (1966).

J. V. Dave and P. Halpern, Effects of changes in ozone amount on the ultraviolet radiation received at sea-level of a model atmosphere, *Atmos. Environ.* **10**, 547-555 (1976).

J. V. Dave, P. Halpern, and N. Braslau, *Spectral distribution of the direct and diffuse solar energy received at sea-level of a model atmosphere,* Tech. rep. G320-3332, IBM Palo Alto Scientific Center (1975).

J. A. Davidson, C. A. Cantrell, A. H. McDaniel, R. E. Shetter, S. Madronich, and J. G. Calvert, Visible-ultraviolet absorption cross sections for NO_2 as a function of temperature, *J. Geophys. Res.* **93D**, 7105-7112 (1988).

A. Deepak, M. A. Box, and G. P. Box, Retrieval of aerosol size distributions from scattering and extinction measurements in the presence of multiple scattering, in *Remote Sensing of Atmospheres and Oceans*, A. Deepak, ed., Academic Press, New York (1980).

B. L. Diffey, The calculation of the spectral distribution of natural ultraviolet under clear day conditions, *Phys. Med. Biol.* **22**, 309-316 (1977).

D. D. Doda and A. E. S. Green, Surface reflectance measurements in the ultraviolet from an airborne platform. Part 1, *Appl. Opt.* **19**, 2140-2145 (1980).

D. D. Doda and A. E. S. Green, Surface reflectance measurements in the ultraviolet from an airborne platform. Part 2, *Appl. Opt.* **20**, 636-642 (1981).

N. F. Elansky, A. Y. Arabov, A. S. Elokhov, and I. A. Senik, Spatial and temporal variability of the NO_2 total content based on annual observation data, in *Atmospheric Ozone* (Proc. Quadriennal Ozone Symp.), C.S. Zerefos and A. Ghazi eds., Halkidiki, Greece, D. Reidel Publ., p. 157-162 (1984).

N. F. Elansky, A. Y. Arabov, O. V. Makarov, V. V. Savastyuk, and I. A. Senik, Measurements of the total column amount of NO_2 at Kislovodsk observatory in 1979-1990, Proc. Conf. Ozone in the troposphere and stratosphere, R.D. Hudson ed., Charlottesville, VA, NASA Conf. Publ. 3266, vol. 2, p. 675-678 (1994).

A. S. Elokhov and A. N. Gruzdev, Total ozone and total NO_2 latitudinal distribution from measurements in the Atlantic ocean in May 1988, Proc. Conf. Ozone in the troposphere and stratosphere, R.D. Hudson ed., Charlottesville, VA, NASA Conf. Publ. 3266, vol. 2, p. 695-698 (1994).

B. W. Forgan, The effect of spectral albedos on diffuse irradiance, Proc. Solar World Congress, S. V. Szokolay, ed., Pergamon Press, p. 2235-2239 (1983).

C. Fröhlich and H. Quenzel, Influence of the sun's aureole on the determination of turbidity, in *Observation and measurement of atmospheric pollution*, Special Environmental rep. No. 3, WMO No. 368, World Meteorological Organization, Geneva (1974).

B. G. Gardiner, A. R. Webb, A. F. Bais, M. Blumthaler, I. Dirmhirn, P. Forster, D. Gillotay, K. Henriksen, M. Huber, P. J. Kirsch, P. C. Simon, T. Svenoe, P. Weihs, and C. S. Zerefos, European intercomparison of ultraviolet spectroradiometers, *Environ. Technol.* **14**, 25-43 (1993).

D. M. Gates and W. J. Harrop, Infrared transmission of the atmosphere to solar radiation, *Appl. Opt.* **2**, 887-898 (1963).

J. I. Gordon, *Daytime visibility, a conceptual review,* Rep. AFGL-TR-79-0257, Visibility Lab., UCSD, San Diego, CA (1979).

J. Gorraiz, H. Horvath, and G. Raimann, Influence of small color differences on the contrast threshold: its application to atmospheric visibility, *Appl. Opt.* **25**, 2537-2545 (1986).

H. Grassl, Calculated circumsolar radiation as a function of aerosol type, field of view, wavelength, and optical depth, *Appl. Opt.* **10**, 2542-2543 (1971).

A. E. S. Green, T. Sawada, and E. P. Shettle, The middle ultraviolet reaching the ground, *Photochem. Photobiol.* **19**, 251-259 (1974).

R. O. Green and B. C. Gao, A proposed update to the solar irradiance spectrum used in LOWTRAN and MODTRAN, Proc. AVIRIS Workshop, Summaries of the Fourth Annual JPL Airborne Geoscience Workshop, R. O. Green ed., NASA/JPL Publ. 93-26, vol. 1 (1993).

C. Gueymard, An anisotropic solar irradiance model for tilted surfaces and its comparison with selected engineering algorithms, *Solar Energy* **38**, 367-386 (1987). Erratum, *Solar Energy* **40**: 175 (1988).

C. Gueymard, Development and performance assessment of a clear sky spectral radiation model, Proc. 22nd ASES Conf., Solar '93, Washington, DC, American Solar Energy Society, p. 433-438 (1993a).

C. Gueymard, Mathematically integrable parameterization of clear-sky beam and global irradiances and its use in daily irradiation applications, *Solar Energy* **50**, 385-397 (1993b).

C. Gueymard, Analysis of monthly average atmospheric precipitable water and turbidity in Canada and Northern United States, *Solar Energy* **53**, 57-71 (1994).

H. Horvath, On the applicability of the Koschmieder visibility formula, *Atmos. Environ.* **5**, 177-184 (1971).

H. Horvath, Atmospheric visibility, *Atmos. Environ.* **15**, 1785-1796 (1981).

R. B. Husar and W. H. White, On the color of the Los Angeles smog, *Atmos. Environ.* **10**, 199-204 (1976).

IAMAP, *A preliminary cloudless standard atmosphere for radiation computation*, Rep. WCP-112, WMO/TD-No. 24, World Meteorological Organization, Geneva, Switzerland (1986).

M. Iqbal, *An introduction to solar radiation*, Academic Press, Toronto (1983).

ISO, *Solar energy—Reference solar spectral irradiance at the ground at different receiving conditions, pt. 1*, International Standard 9845-1, International Organization for Standardization, Geneva (1992).

P. V. Johnston, J. G. Keys, and R. L. McKenzie, NO_2 column changes induced by volcanic eruptions, Proc. Conf. Ozone in the troposphere and stratosphere, R.D. Hudson ed., Charlottesville, VA, NASA Conf. Publ. 3266, vol. 2, p. 615-618 (1994).

W. Josefsson, *Solar ultraviolet radiation in Sweden*, Rep. No. 53, Swedish Meteorological and Hydrological Institute, Norrköping, Sweden (1986).

C. G. Justus and M. V. Paris, A model for solar spectral irradiance and radiance at the bottom and top of a cloudless atmosphere, *J. Clim. Appl. Meteorol.* **24**, 193-205 (1985).

C. G. Justus and M. V. Paris, *Modeling solar spectral irradiance and radiance at the bottom and top of a cloudless atmosphere*, School of Geophysical Sciences Report, Georgia Institute of Technology, Atlanta (1987).

F. Kasten, A new table and approximation formula for the relative optical air mass, *Arch. Met. Geoph. Biokl.* **B14**, 206-223 (1965).

F. Kasten and A. T. Young, Revised optical air mass tables and approximation formula, *Appl. Opt.* **28**, 4735-4738 (1989).

G. M. Keating, M. C. Pitts, and D. F. Young, Ozone reference models for the middle atmosphere, *Adv. Space Res.* **10**, 317-355 (1990).

M. Kerker, *The scattering of light and other electromagnetic radiation*, Academic Press, New York (1969).

R. King and R. O. Buckius, Direct solar transmittance for a clear sky, *Solar Energy* **22**, 297-301 (1979).

F. X. Kneizys, E. P. Shettle, W. O. Gallery, J. H. Chetwynd Jr., L. W. Abreu, J. E. A. Selby, R. W. Fenn, and R. A. McClatchey, *Atmospheric transmittance/radiance: Computer code LOWTRAN 5*, Rep. AFGL TR-80-0067, Air Force Geophysics Lab., Hanscom AFB, MA (1980).

P. Koepke and H. Quenzel, Water vapor: spectral transmission at wavelengths between 0.7 μm and 1 μm, *Appl. Opt.* **17**, 2114-2118 (1978).

H. Koschmieder, Theorie der horizontalen Sichtweite, *Beitr. Phys. Atmos.* **12**, 33-53 (1924).

T. Koskela, Finnish Meteorological Institute, Helsinki, Finland, Personal communication (1994a).

T. Koskela, ed., *The Nordic intercomparison of ultraviolet and total ozone instruments at Izaña from 24 October to 5 November 1993*, Report No. 27, Finnish Meteorological Institute, Helsinki, Finland, (1994b).

K. Kreher, M. Fiedler, T. Gomer, J. Stutz, and U. Platt, The latitudianl distribution (50°N – 50°S) of NO_2 and O_3 in October/November 1990, *Geophys. Res. Lett.* **22**, 1217-1220 (1995).

K. T. Kriebel, *Reflection properties of vegetated surfaces: Tables of measured spectral biconical reflectance factors*, Mitteilung Nr. 29, Meteorologisches Institut, Universität München, Germany (1977).

E. L. Krinov, *Spectral reflectance properties of natural formations*, Rep. TT-439, translated from russian, National Research Council of Canada, Ottawa (1953).

B. Leckner, The spectral distribution of solar radiation at the Earth's surface—Elements of a model, *Solar Energy* **20**, 143-150 (1978).

J. Lenoble, *Radiative transfer in scattering and absorbing atmospheres: Standard computational procedures*, A. Deepak Publ., Hampton, VA (1985).

J. Lenoble, *Atmospheric radiative transfer*, A. Deepak Publ., Hampton, VA (1993).

J. London, *Distribution of atmospheric ozone and how it is measured*, in *Air quality meteorology and atmospheric ozone*, J.B. Wheeler et al., eds., ASTM Special Publ. 653, American Society for Testing and Materials, Philadelphia, PA, (1977).

G. Major, *Circumsolar correction for pyrheliometers and diffusometers*, Rep. WMO/TD-No. 635, World Meteorological Organization, Geneva (1994).

L. K. Matthews, G. P. Mulholland, and M. Stevens, Measurement and analysis of solar spectral irradiance, Proc. ASME/JSME/JSES Solar Engineering Conf., Honolulu, HI, p. 307-313 (1987).

E. J. McCartney, *Optics in the atmosphere*, Wiley, New York (1976).

R. McCluney and C. Gueymard, *SUNSPEC 1.0*, Rep. FSEC-SW-3-93, Florida Solar Energy Center (1993).

R. L. McKenzie and P. V. Johnston, Southern hemisphere nitrogen dioxide, in *Atmospheric Ozone*, Proc. Quadriennal Ozone Symp., C.S. Zerefos and A. Ghazi, eds., Halkidiki, Greece, D. Reidel Publ., p. 163-167 (1984).

R. L. McKenzie, M. Kotkamp, G. Seckmeyer, R. Erb, C. R. Roy, H. P. Gies, and S. J. Toomey, First Southern hemisphere intercomparison of measured solar UV spectra, *Geophys. Res. Lett.* **20**, 2223-2226 (1993).

J. J. Michalsky, The Astronomical Almanac's algorithm for approximate solar position (1950-2050), *Solar Energy* **40**, 227-235 (1988). Erratum, *Solar Energy* **41**, 113 (1988).

F. M. Miskolczi, et al., High resolution atmospheric radiance-transmittance code (HARTCODE), in *Meteorology and Environmental Sciences*, World Scientific, Singapore, p. 770 (1990).

L. T. Molina and M. J. Molina, Absolute absorption cross sections of ozone in the 185- to 350-nm wavelength range, *J Geophys. Res.* **91D**, 14,501-14,508 (1986).

G. H. Mount, D. W. Rusch, J. F. Noxon, J. M. Zawodny, and C. A. Barth, Measurements of stratospheric NO_2 from the solar mesosphere explorer satellite— 1. An overview of the results, *J. Geophys. Res.* **89D**, 1327-1340 (1984).

D. R. Myers, Estimates of uncertainty for measured spectra in the SERI spectral solar radiation data base, *Solar Energy* **43**, 347-353 (1989).

S. Nann and A. Bakenfelder, eds., *Narrow-band spectral radiation data acquisition, analysis and modelling*, Report No. IEA-SHCP-17C-1, Zentrum für Sonnenenergie- und Wasserstoff-Forschung, Stuttgart, Germany (1993).

S. Nann and C. Riordan, Solar spectral irradiance under clear and cloudy skies: Measurements and a semiempirical model, *J. Appl. Meteorol.* **30**, 447-462 (1991).

Nautical Almanac Office, *The astronomical almanac*, Washington & London (1992).

M. Nicolet, Solar spectral irradiances with their diversity between 120 and 900 nm, *Planet. Space Sci.* **37**, 1249-1289 (1989).

J. F. Noxon, Tropospheric NO_2, *J. Geophys. Res.* **83C**, 3051-3057 (1978).

J. F. Noxon, Stratospheric NO_2—2. Global behavior, *J. Geophys. Res.* **84C**, 5067-5076 (1979). Correction, *J. Geophys. Res.*, **85C**: 4560-4561 (1980).

N. Oreskes, K. Shrader-Frechette, and K. Belitz, Verification, validation, and confirmation of numerical models in the Earth sciences, *Science* **263**, 641-646 (1994).

R. Pastiels, *Contribution à l'étude du problème des méthodes actinométriques*, Publ. A11, Institut Royal Météorologique de Belgique, Uccle, Belgium (1959).

E. R. Peck and K. Reeder, Dispersion of air, *J. Opt. Soc. Am.* **62**, 958-962 (1972).

J. H. Pierluissi, C. E. Maragoudakis, and R. Tehrani-Movahed, New LOWTRAN band model for water vapor, *Appl. Opt.* **28**, 3792-3795 (1989).

J. H. Pierluissi and K. Tomiyama, Numerical methods for the generation of empirical and analytical transmittance functions with applications to atmospheric trace gases, *Appl. Opt.* **19**, 2298-2309 (1980).

J. H. Pierluissi and C. M. Tsai, Molecular transmittance band model for oxygen in the visible, *Appl. Opt.* **25**, 2458-2460 (1986).

J. H. Pierluissi and C. M. Tsai, New LOWTRAN models for the uniformly mixed gases, *Appl. Opt.* **26**, 616-618 (1987).

J. P. Pommereau and F. Goutail, O_3 and NO_2 ground-based measurements by visible spectrometry during Arctic winter and spring 1988, *Geophys. Res. Lett.* **15**, 891-894 (1988).

M. Putsay, The effect of circumsolar radiation on accuracy of turbidity measurements, *Idójárás* **84**, 261-267 (1980).

M. Putsay, Circumsolar radiation calculated for various aerosol models, *Idójárás* **99**, 67-76 (1995a).

M. Putsay, Spectral tabulations of aerosol phase functions, atmospheric radiance, and circumsolar irradiance, Personal communication (1995b).

N. M. Reiss and R. A. Eversole, Rectification of prevailing visibility statistics, *Atmos. Environ.* **12**, 945-950 (1978).

W. L. Ridgway and A. Arking, Parameterization of near infrared absorption by atmospheric gases, Preprint 6th Conf. Atmos. Radiation, Williamsburg, VA, American Meteorological Society, p. 190-193 (1986).

C. Riordan, SPCTRAL2, Fortran computer program printout, Personal communication (1990).

C. Riordan, D. Myers, M. Rymes, R. Hulstrom, W. Marion, C. Jennings, and C. Whitaker, Spectral solar radiation data base at SERI, *Solar Energy* **42**, 67-79 (1989).

C. J. Riordan, D. R. Myers, and R. L. Hulstrom, *Spectral data base documentation*, Tech. rep. SERI/TR-215-3513, 2 vols., Solar Energy Research Institute, Golden, CO (1990).

L. S. Rothman et al., The HITRAN molecular database: Editions of 1991 and 1992, *J. Quant. Spectrosc. Radiat.* **48**, 469-507 (1992).

A. Sarkissian, Values of air-mass factors predicted with eight radiative transfer models. Personal communication (1995).

A. Sarkissian, H. K. Roscoe, D. Fish, M. Van Roozendael, M. Gil, H. B. Chen, P. Wang, J. P. Pommereau, and J. Lenoble, Ozone and NO_2 air-mass factors for zenith-sky spectrometers: Intercomparison of calculations with different radiative transfer models, *Geophys. Res. Lett.* **22**, 1113-1116 (1995).

G. Schauberger, Anisotropic model for the diffuse biologicallly-effective irradiance of solar UV-radiation on inclined surfaces, *Theor. Appl. Climatol.* **46**, 45-51 (1992).

W. Schneider, G. K. Moortgat, G. S. Tyndall, and J. P. Burrows, Absorption cross-sections of NO_2 in the UV and visible region (200-700 nm) at 298 K, *J. Photochem. Photobiol.* **40**, 195-217 (1987).

R. Schroeder and J. A. Davies, Significance of nitrogen dioxide in estimating aerosol optical depth and size distributions, *Atmos. Ocean* **25**, 107-114 (1987).

G. Seckmeyer, S. Thiel, M. Blumthaler, P. Fabian, S. Gerber, A. Gugg-Helminger, D.-P. Häder, M. Huber, C. Kettner, U. Köhler, P. Köpke, H. Maier, J. Schäfer, P. Suppan, E. Tamm, and E. Thomalla, Intercomparison of spectral-UV-radiation measurement systems, *Appl. Opt.* **33**, 7805-7812 (1994).

G. M. Shah, Aperture effects on atmospheric turbidity measurements, *Solar Energy* **21**, 527-530 (1978).

E. P. Shettle, Models of aerosols, clouds and precipitation for atmospheric propagation studies, Proc. Conf. Atmospheric Propagation in the UV, Visible, IR and mm-Wave Region and Related Systems Aspects, Copenhagen, Denmark, AGARD, vol. 454, p. 15.1-15.13 (1989).

E. P. Shettle and R. W. Fenn, *Models for the aerosols of the lower atmosphere and the effects of humidity variations on their optical properties,* Rep. AFGL-TR-79-0214, Air Force Geophysics Lab., Hanscom, MA (1979).

E. P. Shettle and A. E. S. Green, Multiple scattering calculation of the middle ultraviolet reaching the ground, *Appl. Opt.* **13**, 1567-1581 (1974).

A. Skartveit and J. A. Olseth, Some simple formulas for multiple Rayleigh scattered irradiance, *Solar Energy* **41**, 19-20 (1988).

E. V. P. Smith and D. M. Gottlieb, Solar flux and its variations, *Space Science Rev.* **16**, 771-802 (1974).

R. C. Smith, Z. Wan, and K. S. Baker, Ozone depletion in Antartica: Modeling its effect on solar UV irradiance under clear-sky conditions, *J. Geophys. Res.* **97C**, 7383-7397 (1992).

S. Solomon and R. R. Garcia, On the distribution of nitrogen dioxide in the high-latitude stratosphere, *J. Geophys. Res.* **88C**, 5229-5239 (1983).

G. Song, Z. Xiuji, and Z. Xisochun, O_3, SO_2, NO_2 and UVB measurements in Beijing and baseline station of northwestern part of China, Proc. Conf. Ozone in the troposphere and stratosphere, R.D. Hudson ed., Charlottesville, VA, NASA Conf. Publ. 3266, vol. 2, p. 746-748 (1994).

P. M. Teillet, Rayleigh optical depth comparisons from various sources, *Appl. Opt.* **29**, 1897-1900 (1990).

C. Tomasi, Non-selective absorption by atmospheric water vapour at visible and near infrared wavelengths, *Quart. J. Roy. Meteorol. Soc.* **105**, 1027-1040 (1979).

F. E. Volz, Measurements of the skylight scattering function, *Appl. Opt.* **26**, 4098-4105 (1987).

P. Wang and J. Lenoble, Comparison between measurements and modeling of UV-B irradiance for clear sky: a case study, *Appl. Opt.* **33**, 3964-3971 (1994).

C. Wehrli, *Extraterrestrial solar spectrum,* Pub. No. 615, World Radiation Center, Davos, Switzerland (1985).

M. Weller and U. Leiterer, Experimental data on spectral aerosol optical thickness and its global distribution. *Beitr. Phys. Atmosph.* **61**, 1-9 (1988).

W. J. Wiscombe and S. G. Warren, A model for the spectral albedo of snow. I: Pure snow, *J. Atmos. Sci.* **37**, 2712-2733 (1980).

S. C. Wofsy, Temporal and latitudinal variations of stratospheric trace gases: A critical comparison between theory and experiment, *J. Geophys. Res.* **83C**, 364-378 (1978).

T. Yamanouchi and M. Tanaka, Absorption properties of the near-infrared water vapor bands, *J. Quant. Spectrosc. Radiat.* **34**, 463-472 (1985).

A. T. Young, *Observational technique and data reduction,* in *Astrophysics, pt. A: Optical and Infrared,* N. Carleton, ed., vol. 12, Academic Press, New York, (1974).

A. T. Young, On the Rayleigh-scattering optical depth of the atmosphere, *J. Appl. Meteorol.* **20**, 328-330 (1981).

G. Zerlaut, Chairman of ASTM Subcommittee G3.09 on Solar and Ultraviolet Radiation Measurements Standard, Personal communication (1995).

APPENDIX

Extraterrestrial spectrum and absorption coefficients at their reference temperature

λ	$E_{0n\lambda}$	$A_{w\lambda}$	$A_{g\lambda}$	$A_{o\lambda}$	$A_{n\lambda}$
280	0.0906	0.00E+00	0.00E+00	1.05E+02	1.46
281	0.1585	0.00E+00	0.00E+00	9.44E+01	1.52
282	0.2692	0.00E+00	0.00E+00	8.47E+01	1.55
283	0.3222	0.00E+00	0.00E+00	7.92E+01	1.68
284	0.3025	0.00E+00	0.00E+00	7.12E+01	1.78
285	0.1865	0.00E+00	0.00E+00	6.35E+01	1.91
286	0.2546	0.00E+00	0.00E+00	5.77E+01	1.94
287	0.3578	0.00E+00	0.00E+00	5.21E+01	1.99
288	0.3225	0.00E+00	0.00E+00	4.52E+01	2.08
289	0.4028	0.00E+00	0.00E+00	4.05E+01	2.21
290	0.5596	0.00E+00	0.00E+00	3.61E+01	2.33
291	0.6110	0.00E+00	0.00E+00	3.23E+01	2.52
292	0.5675	0.00E+00	0.00E+00	2.78E+01	2.58
293	0.5500	0.00E+00	0.00E+00	2.50E+01	2.60
294	0.5428	0.00E+00	0.00E+00	2.16E+01	2.71
295	0.5453	0.00E+00	0.00E+00	1.92E+01	2.83
296	0.5731	0.00E+00	0.00E+00	1.64E+01	3.05
297	0.5064	0.00E+00	0.00E+00	1.46E+01	3.30
298	0.5286	0.00E+00	0.00E+00	1.25E+01	3.31
299	0.5024	0.00E+00	0.00E+00	1.11E+01	3.38
300	0.4700	0.00E+00	0.00E+00	9.52E+00	3.42
301	0.4693	0.00E+00	0.00E+00	8.29E+00	3.62
302	0.4466	0.00E+00	0.00E+00	7.29E+00	3.90
303	0.6041	0.00E+00	0.00E+00	6.22E+00	4.08
304	0.6278	0.00E+00	0.00E+00	5.58E+00	4.16
305	0.6373	0.00E+00	0.00E+00	4.69E+00	4.24
306	0.6000	0.00E+00	0.00E+00	4.20E+00	4.38
307	0.6143	0.00E+00	0.00E+00	3.59E+00	4.51
308	0.6660	0.00E+00	0.00E+00	3.12E+00	4.70
309	0.6097	0.00E+00	0.00E+00	2.82E+00	4.96
310	0.5055	0.00E+00	0.00E+00	2.31E+00	5.09
311	0.7623	0.00E+00	0.00E+00	2.11E+00	5.30
312	0.7005	0.00E+00	0.00E+00	1.78E+00	5.47
313	0.6974	0.00E+00	0.00E+00	1.53E+00	5.49
314	0.7428	0.00E+00	0.00E+00	1.39E+00	5.71
315	0.6868	0.00E+00	0.00E+00	1.12E+00	5.88
316	0.5852	0.00E+00	0.00E+00	1.05E+00	6.06
317	0.7612	0.00E+00	0.00E+00	8.52E-01	6.40
318	0.7193	0.00E+00	0.00E+00	8.11E-01	6.51
319	0.7069	0.00E+00	0.00E+00	5.82E-01	6.65
320	0.7952	0.00E+00	0.00E+00	6.59E-01	6.86
321	0.7724	0.00E+00	0.00E+00	4.01E-01	6.94
322	0.7576	0.00E+00	0.00E+00	4.59E-01	7.22
323	0.6528	0.00E+00	0.00E+00	4.06E-01	7.33
324	0.7345	0.00E+00	0.00E+00	2.22E-01	7.55
325	0.8291	0.00E+00	0.00E+00	3.41E-01	7.80
326	0.9792	0.00E+00	0.00E+00	2.14E-01	7.98
327	0.9993	0.00E+00	0.00E+00	1.55E-01	8.11
328	0.9315	0.00E+00	0.00E+00	2.41E-01	8.28
329	0.9684	0.00E+00	0.00E+00	1.03E-01	8.49
330	1.1286	0.00E+00	0.00E+00	1.01E-01	8.55
331	0.9718	0.00E+00	0.00E+00	1.54E-01	8.75
332	1.0013	0.00E+00	0.00E+00	7.16E-02	9.30
333	0.9760	0.00E+00	0.00E+00	5.39E-02	9.25
334	0.9487	0.00E+00	0.00E+00	9.91E-02	9.23
335	1.0110	0.00E+00	0.00E+00	3.67E-02	9.43
336	0.9065	0.00E+00	0.00E+00	2.85E-02	9.57
337	0.8107	0.00E+00	0.00E+00	6.23E-02	9.61
338	0.9240	0.00E+00	0.00E+00	3.92E-02	10.30
339	0.9737	0.00E+00	0.00E+00	1.66E-02	10.43
340	1.0457	0.00E+00	0.00E+00	3.07E-02	10.61
341	0.9405	0.00E+00	0.00E+00	1.77E-02	10.72
342	1.0010	0.00E+00	0.00E+00	7.60E-03	10.28
343	1.0420	0.00E+00	0.00E+00	9.41E-03	10.49
344	0.8328	0.00E+00	0.00E+00	2.39E-02	10.81
345	0.9194	0.00E+00	0.00E+00	1.20E-02	11.19
346	0.9292	0.00E+00	0.00E+00	5.62E-03	11.59
347	0.9804	0.00E+00	0.00E+00	6.98E-03	11.85
348	0.9314	0.00E+00	0.00E+00	5.06E-03	12.15
349	0.8842	0.00E+00	0.00E+00	2.43E-03	11.49
350	1.0183	0.00E+00	0.00E+00	2.04E-03	11.7
351	1.0191	0.00E+00	0.00E+00	3.42E-03	11.85
352	0.9827	0.00E+00	0.00E+00	5.02E-03	11.68
353	0.9887	0.00E+00	0.00E+00	2.31E-03	12.35
354	1.1280	0.00E+00	0.00E+00	1.10E-03	13.07
355	1.1298	0.00E+00	0.00E+00	1.31E-03	12.71
356	1.0317	0.00E+00	0.00E+00	1.22E-03	13.17
357	0.8369	0.00E+00	0.00E+00	1.36E-03	13.48
358	0.7555	0.00E+00	0.00E+00	1.26E-03	12.85
359	0.8474	0.00E+00	0.00E+00	1.02E-03	12.72
360	1.1151	0.00E+00	0.00E+00	9.62E-04	13.23
361	0.8927	0.00E+00	0.00E+00	7.66E-04	13.51
362	0.9129	0.00E+00	0.00E+00	5.74E-04	13.5
363	1.0740	0.00E+00	0.00E+00	3.37E-04	13.55
364	1.0922	0.00E+00	0.00E+00	3.38E-04	14.19
365	1.0560	0.00E+00	0.00E+00	3.13E-04	14.5
366	1.2973	0.00E+00	0.00E+00	0.00E+00	13.98
367	1.2525	0.00E+00	0.00E+00	0.00E+00	14.21
368	1.1615	0.00E+00	0.00E+00	0.00E+00	14.13
369	1.2021	0.00E+00	0.00E+00	0.00E+00	14.15
370	1.2907	0.00E+00	0.00E+00	0.00E+00	14.09
371	1.1480	0.00E+00	0.00E+00	0.00E+00	14.75
372	1.0890	0.00E+00	0.00E+00	0.00E+00	14.95
373	1.0449	0.00E+00	0.00E+00	0.00E+00	14.55
374	0.9539	0.00E+00	0.00E+00	0.00E+00	14.39
375	0.9484	0.00E+00	0.00E+00	0.00E+00	15.3
376	1.1345	0.00E+00	0.00E+00	0.00E+00	15.4
377	1.2004	0.00E+00	0.00E+00	0.00E+00	14.54
378	1.4325	0.00E+00	0.00E+00	0.00E+00	14.55
379	1.2202	0.00E+00	0.00E+00	0.00E+00	15.55
380	1.0939	0.00E+00	0.00E+00	0.00E+00	15.6
381	1.2592	0.00E+00	0.00E+00	0.00E+00	15.23
382	0.9514	0.00E+00	0.00E+00	0.00E+00	14.93
383	0.7072	0.00E+00	0.00E+00	0.00E+00	15.3
384	0.7826	0.00E+00	0.00E+00	0.00E+00	15.7
385	1.0801	0.00E+00	0.00E+00	0.00E+00	15.44
386	0.9598	0.00E+00	0.00E+00	0.00E+00	15.35
387	0.9969	0.00E+00	0.00E+00	0.00E+00	15.7
388	0.9929	0.00E+00	0.00E+00	0.00E+00	15.86
389	1.0789	0.00E+00	0.00E+00	0.00E+00	15.97
390	1.2447	0.00E+00	0.00E+00	0.00E+00	15.97
391	1.3312	0.00E+00	0.00E+00	0.00E+00	16.25
392	1.2405	0.00E+00	0.00E+00	0.00E+00	15.82
393	0.6884	0.00E+00	0.00E+00	0.00E+00	15.25
394	0.7939	0.00E+00	0.00E+00	0.00E+00	15.5
395	1.2850	0.00E+00	0.00E+00	0.00E+00	16.11
396	1.2319	0.00E+00	0.00E+00	0.00E+00	15.68
397	0.6265	0.00E+00	0.00E+00	0.00E+00	16.1
398	1.3783	0.00E+00	0.00E+00	0.00E+00	16.4
399	1.6672	0.00E+00	0.00E+00	0.00E+00	16.43
400	1.7163	0.00E+00	0.00E+00	0.00E+00	16.88
401	1.7519	0.00E+00	0.00E+00	0.00E+00	16.1
402	1.8012	0.00E+00	0.00E+00	0.00E+00	15.25
403	1.7126	0.00E+00	0.00E+00	0.00E+00	15.55
404	1.7622	0.00E+00	0.00E+00	0.00E+00	16.2
405	1.6983	0.00E+00	0.00E+00	0.00E+00	15.7
406	1.6068	0.00E+00	0.00E+00	0.00E+00	14.75
407	1.6164	0.00E+00	0.00E+00	5.57E-05	15.5
408	1.6861	0.00E+00	0.00E+00	1.30E-04	16.64
409	1.8466	0.00E+00	0.00E+00	1.86E-04	16.45
410	1.5299	0.00E+00	0.00E+00	2.26E-04	16.22
411	1.7390	0.00E+00	0.00E+00	2.46E-04	15.33
412	1.8454	0.00E+00	0.00E+00	2.28E-04	16.2
413	1.7370	0.00E+00	0.00E+00	2.02E-04	16.5

414	1.8192	0.00E+00	0.00E+00	2.12E-04	15.39
415	1.7688	0.00E+00	0.00E+00	2.68E-04	14.3
416	1.8414	0.00E+00	0.00E+00	3.39E-04	14.3
417	1.8174	0.00E+00	0.00E+00	3.96E-04	14.92
418	1.6966	0.00E+00	0.00E+00	4.26E-04	15.21
419	1.7613	0.00E+00	0.00E+00	4.32E-04	15.7
420	1.6368	0.00E+00	0.00E+00	4.32E-04	15.82
421	1.9260	0.00E+00	0.00E+00	4.60E-04	15.8
422	1.7856	0.00E+00	0.00E+00	5.41E-04	15.72
423	1.6634	0.00E+00	0.00E+00	6.79E-04	15.97
424	1.7371	0.00E+00	0.00E+00	8.62E-04	15.5
425	1.6739	0.00E+00	0.00E+00	1.04E-03	13.9
426	1.7277	0.00E+00	0.00E+00	1.15E-03	13.7
427	1.5874	0.00E+00	0.00E+00	1.15E-03	14.9
428	1.6876	0.00E+00	0.00E+00	1.08E-03	14.15
429	1.5558	0.00E+00	0.00E+00	1.02E-03	13.4
430	1.2480	0.00E+00	0.00E+00	1.02E-03	14.65
431	1.2880	0.00E+00	0.00E+00	1.10E-03	14.1
432	1.8042	0.00E+00	0.00E+00	1.28E-03	13.4
433	1.8187	0.00E+00	0.00E+00	1.44E-03	14.45
434	1.5185	0.00E+00	0.00E+00	1.50E-03	15.46
435	1.7717	0.00E+00	0.00E+00	1.50E-03	15.08
436	1.9054	0.00E+00	0.00E+00	1.51E-03	13.4
437	1.8774	0.00E+00	0.00E+00	1.60E-03	12.16
438	1.6579	0.00E+00	0.00E+00	1.81E-03	14.05
439	1.7325	0.00E+00	0.00E+00	2.16E-03	14.5
440	1.8014	0.00E+00	0.00E+00	2.60E-03	12.3
441	1.8649	3.10E-06	0.00E+00	3.01E-03	11.15
442	1.9707	2.48E-05	0.00E+00	3.31E-03	11.5
443	1.9266	1.59E-04	0.00E+00	3.51E-03	12.4
444	1.9971	4.46E-05	0.00E+00	3.52E-03	13.95
445	1.9760	5.90E-05	0.00E+00	3.36E-03	13.1
446	1.8228	5.84E-05	0.00E+00	3.16E-03	12.3
447	2.0043	1.19E-05	0.00E+00	3.06E-03	13.9
448	2.0397	2.79E-06	0.00E+00	3.14E-03	13.45
449	2.0130	0.00E+00	0.00E+00	3.43E-03	11.79
450	2.0902	0.00E+00	0.00E+00	3.77E-03	11.7
451	2.1812	0.00E+00	0.00E+00	4.01E-03	11.71
452	2.0721	0.00E+00	0.00E+00	4.10E-03	11.9
453	1.8733	0.00E+00	0.00E+00	4.08E-03	11.21
454	2.0484	0.00E+00	0.00E+00	4.10E-03	11.2
455	1.9586	0.00E+00	0.00E+00	4.29E-03	10.91
456	2.1017	0.00E+00	0.00E+00	4.73E-03	10.51
457	2.1161	0.00E+00	0.00E+00	5.43E-03	11.77
458	2.0026	0.00E+00	0.00E+00	6.30E-03	11.49
459	2.0615	0.00E+00	0.00E+00	7.20E-03	11.3
460	2.0216	0.00E+00	0.00E+00	8.07E-03	11.47
461	2.1087	0.00E+00	0.00E+00	8.71E-03	10.72
462	2.0854	0.00E+00	0.00E+00	9.00E-03	11.5
463	2.1247	0.00E+00	0.00E+00	8.93E-03	11.75
464	2.0229	0.00E+00	0.00E+00	8.49E-03	10.3
465	1.9781	0.00E+00	0.00E+00	7.96E-03	9.1
466	2.0527	0.00E+00	0.00E+00	7.72E-03	9.86
467	1.9384	2.12E-06	0.00E+00	7.97E-03	10.15
468	2.0119	2.09E-06	0.00E+00	8.46E-03	9.21
469	2.0479	9.03E-06	0.00E+00	8.94E-03	8.65
470	1.9206	3.34E-05	0.00E+00	9.39E-03	8.62
471	1.9660	1.30E-05	0.00E+00	9.63E-03	8.78
472	2.1111	1.28E-05	0.00E+00	9.74E-03	9.15
473	1.9776	1.27E-05	0.00E+00	9.76E-03	10.6
474	2.0550	1.92E-06	0.00E+00	1.01E-02	10.95
475	2.0880	0.00E+00	0.00E+00	1.08E-02	9.78
476	1.9900	0.00E+00	0.00E+00	1.20E-02	8.82
477	2.0469	0.00E+00	0.00E+00	1.35E-02	8.42
478	2.1053	0.00E+00	0.00E+00	1.52E-02	8.59
479	2.0673	0.00E+00	0.00E+00	1.69E-02	9.21
480	2.1149	0.00E+00	0.00E+00	1.86E-02	8.85
481	2.0670	0.00E+00	0.00E+00	1.99E-02	8.21
482	2.0998	0.00E+00	0.00E+00	2.08E-02	7.11
483	2.0276	0.00E+00	0.00E+00	2.09E-02	6.64
484	2.0091	0.00E+00	0.00E+00	2.04E-02	6.89
485	1.9786	1.49E-05	0.00E+00	1.96E-02	7.04
486	1.5715	1.09E-05	0.00E+00	1.90E-02	6.9
487	1.7982	7.25E-06	0.00E+00	1.87E-02	7.35
488	1.9913	4.10E-06	0.00E+00	1.88E-02	8.92
489	1.8816	7.08E-06	0.00E+00	1.95E-02	8.5
490	2.0807	1.54E-06	0.00E+00	2.04E-02	7.07
491	2.0092	1.52E-06	0.00E+00	2.11E-02	6.45
492	1.8427	0.00E+00	0.00E+00	2.14E-02	6.55
493	2.0118	0.00E+00	0.00E+00	2.17E-02	7.21
494	1.9566	0.00E+00	0.00E+00	2.21E-02	7.69
495	2.0698	0.00E+00	0.00E+00	2.26E-02	7.57
496	1.9730	0.00E+00	0.00E+00	2.36E-02	7
497	2.0205	0.00E+00	0.00E+00	2.50E-02	5.8
498	1.9077	0.00E+00	0.00E+00	2.68E-02	4.95
499	1.9531	0.00E+00	0.00E+00	2.90E-02	4.5
500	1.9189	3.54E-06	0.00E+00	3.15E-02	4.62
501	1.8556	9.17E-06	0.00E+00	3.42E-02	5.16
502	1.8362	7.39E-05	0.00E+00	3.68E-02	5.89
503	1.9477	1.78E-04	0.00E+00	3.91E-02	6
504	1.8371	1.16E-03	0.00E+00	4.08E-02	6.58
505	1.9688	1.75E-04	0.00E+00	4.19E-02	6.1
506	2.0302	3.07E-04	0.00E+00	4.22E-02	5.5
507	1.9238	3.92E-04	0.00E+00	4.19E-02	5.17
508	1.8567	2.86E-04	0.00E+00	4.13E-02	5.5
509	1.9665	1.63E-04	0.00E+00	4.04E-02	5.98
510	1.9029	9.72E-05	0.00E+00	3.99E-02	5.85
511	1.9373	2.98E-05	0.00E+00	3.96E-02	5.61
512	1.9960	8.12E-06	0.00E+00	4.01E-02	5.3
513	1.8645	5.35E-06	0.00E+00	4.10E-02	4.61
514	1.8237	0.00E+00	0.00E+00	4.20E-02	4.12
515	1.8804	0.00E+00	0.00E+00	4.29E-02	3.8
516	1.8695	0.00E+00	0.00E+00	4.38E-02	3.59
517	1.5183	0.00E+00	0.00E+00	4.47E-02	3.7
518	1.7289	0.00E+00	0.00E+00	4.55E-02	4.2
519	1.7665	0.00E+00	0.00E+00	4.64E-02	4.28
520	1.8684	0.00E+00	0.00E+00	4.74E-02	4.05
521	1.8384	0.00E+00	0.00E+00	4.89E-02	3.73
522	1.9206	0.00E+00	0.00E+00	5.05E-02	3.68
523	1.7997	0.00E+00	0.00E+00	5.25E-02	3.75
524	1.9088	9.81E-06	0.00E+00	5.49E-02	4.3
525	1.9470	1.26E-05	0.00E+00	5.75E-02	4.77
526	1.8630	9.63E-07	0.00E+00	6.01E-02	4.52
527	1.6928	9.51E-06	0.00E+00	6.28E-02	4.17
528	1.8548	9.39E-07	0.00E+00	6.54E-02	3.89
529	1.9819	4.48E-06	0.00E+00	6.79E-02	3.62
530	1.8887	2.48E-06	0.00E+00	7.01E-02	3.6
531	2.0090	2.45E-06	0.00E+00	7.20E-02	3.53
532	1.9100	0.00E+00	0.00E+00	7.34E-02	3.45
533	1.8172	0.00E+00	0.00E+00	7.43E-02	3.06
534	1.8898	0.00E+00	0.00E+00	7.48E-02	2.6
535	1.9271	0.00E+00	0.00E+00	7.49E-02	2.29
536	1.9720	0.00E+00	0.00E+00	7.47E-02	2.21
537	1.8126	0.00E+00	0.00E+00	7.47E-02	2.35
538	1.9208	2.26E-06	0.00E+00	7.51E-02	2.7
539	1.8649	6.10E-06	0.00E+00	7.58E-02	2.59
540	1.7989	4.50E-05	0.00E+00	7.69E-02	2.3
541	1.8084	2.00E-04	0.00E+00	7.82E-02	2.65
542	1.8804	2.12E-04	0.00E+00	7.98E-02	3.09
543	1.8233	5.20E-05	0.00E+00	8.14E-02	3.1
544	1.9406	1.53E-04	0.00E+00	8.29E-02	3.03
545	1.9016	9.74E-05	0.00E+00	8.42E-02	3
546	1.8810	2.25E-04	0.00E+00	8.52E-02	2.74
547	1.8872	9.10E-05	0.00E+00	8.63E-02	2.88
548	1.8342	3.83E-05	0.00E+00	8.72E-02	2.88
549	1.8952	1.80E-05	0.00E+00	8.79E-02	2.7
550	1.8806	1.78E-05	0.00E+00	8.86E-02	2.34
551	1.8495	7.48E-06	0.00E+00	8.95E-02	2.15
552	1.8885	1.94E-06	0.00E+00	9.05E-02	2.29
553	1.8338	1.92E-06	0.00E+00	9.15E-02	2.27
554	1.8868	0.00E+00	0.00E+00	9.28E-02	1.95
555	1.8961	0.00E+00	0.00E+00	9.42E-02	1.6
556	1.8525	0.00E+00	0.00E+00	9.59E-02	1.48
557	1.7988	0.00E+00	0.00E+00	9.79E-02	1.47
558	1.8301	0.00E+00	0.00E+00	1.00E-01	1.41
559	1.7430	0.00E+00	0.00E+00	1.03E-01	1.33
560	1.8020	0.00E+00	0.00E+00	1.05E-01	1.4
561	1.8708	0.00E+00	0.00E+00	1.08E-01	1.53
562	1.8133	0.00E+00	0.00E+00	1.10E-01	1.7
563	1.8822	6.18E-07	0.00E+00	1.13E-01	2.12

564	1.8421	6.11E-07	0.00E+00	1.15E-01	2.29
565	1.8486	6.04E-07	0.00E+00	1.17E-01	1.98
566	1.8005	1.67E-06	0.00E+00	1.18E-01	1.54
567	1.8636	8.42E-06	0.00E+00	1.20E-01	1.6
568	1.8500	1.30E-04	0.00E+00	1.21E-01	1.69
569	1.8270	7.06E-04	0.00E+00	1.23E-01	1.68
570	1.8170	3.95E-04	0.00E+00	1.25E-01	1.9
571	1.7441	6.40E-05	0.00E+00	1.26E-01	1.94
572	1.8649	3.01E-04	0.00E+00	1.27E-01	1.75
573	1.8449	2.24E-04	0.00E+00	1.28E-01	1.42
574	1.8773	1.82E-04	0.00E+00	1.28E-01	1.15
575	1.8130	1.98E-04	0.00E+00	1.28E-01	0.95
576	1.7948	1.38E-04	0.00E+00	1.27E-01	0.8
577	1.8453	1.03E-04	0.00E+00	1.26E-01	0.8
578	1.7619	3.63E-05	0.00E+00	1.25E-01	0.99
579	1.8634	1.39E-05	0.00E+00	1.24E-01	1.1
580	1.8369	9.45E-06	0.00E+00	1.23E-01	1.02
581	1.8292	5.66E-06	0.00E+00	1.22E-01	0.85
582	1.8632	9.29E-06	0.00E+00	1.21E-01	0.78
583	1.8502	9.21E-06	0.00E+00	1.20E-01	0.82
584	1.8741	2.06E-05	0.00E+00	1.19E-01	1
585	1.8252	3.15E-05	0.00E+00	1.18E-01	1.15
586	1.7757	8.46E-05	0.00E+00	1.18E-01	1.13
587	1.8393	2.94E-04	0.00E+00	1.18E-01	1.01
588	1.8024	1.62E-03	0.00E+00	1.18E-01	0.93
589	1.6172	5.64E-03	0.00E+00	1.18E-01	1
590	1.7497	5.39E-03	0.00E+00	1.19E-01	1.04
591	1.8083	3.09E-03	0.00E+00	1.20E-01	1.28
592	1.8002	4.72E-03	0.00E+00	1.21E-01	1.38
593	1.8331	2.69E-03	0.00E+00	1.23E-01	1.21
594	1.7942	3.13E-03	0.00E+00	1.25E-01	0.92
595	1.7812	4.27E-03	0.00E+00	1.28E-01	0.72
596	1.7898	1.56E-03	0.00E+00	1.30E-01	0.67
597	1.7968	1.79E-03	0.00E+00	1.33E-01	0.66
598	1.8060	1.20E-03	0.00E+00	1.35E-01	0.68
599	1.7855	8.20E-04	0.00E+00	1.37E-01	0.79
600	1.7762	3.47E-04	0.00E+00	1.38E-01	0.83
601	1.7435	1.01E-04	0.00E+00	1.39E-01	0.8
602	1.7192	5.49E-05	0.00E+00	1.39E-01	0.68
603	1.7809	1.35E-05	0.00E+00	1.39E-01	0.49
604	1.7734	3.29E-06	0.00E+00	1.39E-01	0.39
605	1.7750	0.00E+00	0.00E+00	1.37E-01	0.378
606	1.7640	0.00E+00	0.00E+00	1.36E-01	0.375
607	1.7620	0.00E+00	0.00E+00	1.34E-01	0.395
608	1.7610	0.00E+00	0.00E+00	1.32E-01	0.413
609	1.7239	0.00E+00	0.00E+00	1.30E-01	0.419
610	1.7520	0.00E+00	0.00E+00	1.27E-01	0.47
611	1.7296	0.00E+00	0.00E+00	1.25E-01	0.67
612	1.7025	0.00E+00	0.00E+00	1.22E-01	0.835
613	1.7223	0.00E+00	0.00E+00	1.20E-01	0.75
614	1.6523	0.00E+00	0.00E+00	1.18E-01	0.66
615	1.7196	0.00E+00	0.00E+00	1.16E-01	0.66
616	1.6232	0.00E+00	0.00E+00	1.14E-01	0.741
617	1.6366	0.00E+00	0.00E+00	1.12E-01	0.68
618	1.7068	0.00E+00	0.00E+00	1.11E-01	0.54
619	1.6832	0.00E+00	0.00E+00	1.09E-01	0.56
620	1.7050	0.00E+00	0.00E+00	1.08E-01	0.589
621	1.7162	0.00E+00	0.00E+00	1.07E-01	0.52
622	1.7006	0.00E+00	0.00E+00	1.05E-01	0.495
623	1.6628	0.00E+00	0.00E+00	1.04E-01	0.472
624	1.6236	0.00E+00	0.00E+00	1.03E-01	0.45
625	1.6353	9.42E-07	0.00E+00	1.01E-01	0.432
626	1.7009	1.51E-05	0.00E+00	1.00E-01	0.42
627	1.6982	1.29E-04	0.00E+00	9.87E-02	0.416
628	1.6607	3.36E-04	4.53E-04	9.73E-02	0.395
629	1.6580	2.30E-04	6.06E-05	9.58E-02	0.387
630	1.6444	9.55E-05	1.08E-04	9.43E-02	0.379
631	1.6276	2.28E-05	2.27E-05	9.29E-02	0.371
632	1.6706	2.63E-04	6.17E-06	9.15E-02	0.362
633	1.6648	1.25E-04	8.78E-07	9.00E-02	0.355
634	1.6340	6.27E-05	7.51E-08	8.84E-02	0.35
635	1.6236	8.93E-05	1.07E-08	8.68E-02	0.347
636	1.6257	6.20E-05	0.00E+00	8.53E-02	0.344
637	1.6606	6.48E-05	0.00E+00	8.36E-02	0.341
638	1.6550	1.97E-05	0.00E+00	8.20E-02	0.338
639	1.6530	2.83E-05	0.00E+00	8.03E-02	0.335
640	1.6094	2.36E-05	0.00E+00	7.87E-02	0.332
641	1.5836	3.27E-05	0.00E+00	7.71E-02	0.331
642	1.6121	2.33E-05	0.00E+00	7.56E-02	0.33
643	1.6142	5.36E-05	0.00E+00	7.42E-02	0.329
644	1.5963	5.63E-05	0.00E+00	7.29E-02	0.328
645	1.6200	1.33E-04	0.00E+00	7.16E-02	0.327
646	1.6159	7.13E-04	0.00E+00	7.03E-02	0.326
647	1.5812	1.95E-03	0.00E+00	6.91E-02	0.325
648	1.5619	3.21E-03	0.00E+00	6.79E-02	0.324
649	1.5600	2.64E-03	0.00E+00	6.69E-02	0.323
650	1.5189	9.60E-04	0.00E+00	6.57E-02	0.322
651	1.5944	5.85E-04	0.00E+00	6.47E-02	0.317
652	1.595	3.52E-03	0.00E+00	6.36E-02	0.312
653	1.6077	6.57E-04	0.00E+00	6.25E-02	0.307
654	1.5962	5.71E-04	0.00E+00	6.14E-02	0.302
655	1.4982	1.48E-03	0.00E+00	6.03E-02	0.297
656	1.3960	9.80E-04	0.00E+00	5.92E-02	0.292
657	1.4362	9.52E-04	0.00E+00	5.81E-02	0.287
658	1.5382	4.90E-04	0.00E+00	5.70E-02	0.282
659	1.5509	2.81E-04	0.00E+00	5.60E-02	0.277
660	1.5576	2.16E-04	0.00E+00	5.50E-02	0.272
661	1.5702	5.96E-05	0.00E+00	5.40E-02	0.267
662	1.5664	1.35E-05	0.00E+00	5.31E-02	0.262
663	1.5700	2.45E-05	0.00E+00	5.21E-02	0.257
664	1.5661	1.33E-05	0.00E+00	5.11E-02	0.252
665	1.5728	8.72E-06	0.00E+00	5.00E-02	0.247
666	1.5674	4.91E-06	0.00E+00	4.89E-02	0.242
667	1.5591	3.81E-06	0.00E+00	4.77E-02	0.237
668	1.5642	0.00E+00	0.00E+00	4.66E-02	0.232
669	1.5589	2.16E-07	0.00E+00	4.55E-02	0.227
670	1.5610	0.00E+00	0.00E+00	4.45E-02	0.222
671	1.5394	0.00E+00	0.00E+00	4.34E-02	0.217
672	1.5061	0.00E+00	0.00E+00	4.24E-02	0.212
673	1.5157	0.00E+00	0.00E+00	4.13E-02	0.207
674	1.5150	0.00E+00	0.00E+00	4.04E-02	0.202
675	1.5150	0.00E+00	0.00E+00	3.96E-02	0.201
676	1.5140	0.00E+00	0.00E+00	3.87E-02	0.198
677	1.5110	0.00E+00	0.00E+00	3.78E-02	0.195
678	1.5070	0.00E+00	0.00E+00	3.70E-02	0.192
679	1.5040	0.00E+00	0.00E+00	3.62E-02	0.189
680	1.5010	1.97E-07	0.00E+00	3.56E-02	0.186
681	1.4980	1.81E-06	0.00E+00	3.50E-02	0.183
682	1.4940	4.42E-06	0.00E+00	3.44E-02	0.18
683	1.4910	5.44E-06	0.00E+00	3.39E-02	0.177
684	1.4880	1.33E-05	0.00E+00	3.34E-02	0.174
685	1.4850	7.70E-06	0.00E+00	3.28E-02	0.171
686	1.4783	1.32E-05	7.51E-08	3.21E-02	0.168
687	1.4414	3.55E-05	1.43E-02	3.14E-02	0.165
688	1.4220	7.56E-06	7.07E-03	3.05E-02	0.162
689	1.4430	1.45E-05	5.68E-03	2.97E-02	0.159
690	1.4740	3.07E-05	3.86E-03	2.88E-02	0.156
691	1.4719	1.20E-04	2.02E-03	2.80E-02	0.153
692	1.4612	7.34E-04	6.80E-04	2.72E-02	0.15
693	1.4610	3.79E-03	1.94E-04	2.65E-02	0.147
694	1.4600	7.05E-03	4.00E-05	2.58E-02	0.144
695	1.4590	4.75E-03	1.98E-06	2.50E-02	0.141
696	1.4500	5.54E-03	4.28E-07	2.43E-02	0.138
697	1.4410	8.79E-04	1.07E-08	2.36E-02	0.135
698	1.4320	9.06E-04	0.00E+00	2.30E-02	0.132
699	1.4230	3.60E-03	0.00E+00	2.24E-02	0.129
700	1.4140	3.87E-03	0.00E+00	2.18E-02	0.126
701	1.4300	4.32E-03	0.00E+00	2.13E-02	0
702	1.4375	3.21E-03	0.00E+00	2.09E-02	0
703	1.4369	3.91E-03	0.00E+00	2.05E-02	0
704	1.4348	2.00E-03	0.00E+00	2.01E-02	0
705	1.4258	2.16E-03	0.00E+00	1.97E-02	0
706	1.4139	1.77E-03	0.00E+00	1.94E-02	0
707	1.4035	1.41E-03	0.00E+00	1.91E-02	0
708	1.3987	1.42E-03	0.00E+00	1.89E-02	0
709	1.4051	6.94E-04	0.00E+00	1.86E-02	0
710	1.4129	1.02E-03	0.00E+00	1.84E-02	0
711	1.4109	7.85E-04	0.00E+00	1.82E-02	0
712	1.4034	4.94E-04	0.00E+00	1.80E-02	0
713	1.3944	8.01E-04	0.00E+00	1.79E-02	0

714	1.3855	7.57E-04	0.00E+00	1.78E-02	0
715	1.3780	1.80E-03	0.00E+00	1.77E-02	0
716	1.3706	2.20E-03	0.00E+00	1.75E-02	0
717	1.3645	2.03E-02	0.00E+00	1.71E-02	0
718	1.3571	3.55E-02	0.00E+00	1.67E-02	0
719	1.3455	6.52E-02	0.00E+00	1.61E-02	0
720	1.3395	4.68E-02	0.00E+00	1.56E-02	0
721	1.3473	2.29E-02	0.00E+00	1.50E-02	0
722	1.3592	3.76E-03	0.00E+00	1.45E-02	0
723	1.3655	1.23E-02	0.00E+00	1.41E-02	0
724	1.3678	3.78E-02	0.00E+00	1.37E-02	0
725	1.3645	3.03E-02	0.00E+00	1.33E-02	0
726	1.3558	2.19E-02	0.00E+00	1.30E-02	0
727	1.3444	2.29E-02	0.00E+00	1.27E-02	0
728	1.3357	2.99E-02	0.00E+00	1.23E-02	0
729	1.3325	2.02E-02	0.00E+00	1.19E-02	0
730	1.3320	1.39E-02	0.00E+00	1.16E-02	0
731	1.3302	1.84E-02	0.00E+00	1.14E-02	0
732	1.3270	1.00E-02	0.00E+00	1.12E-02	0
733	1.3252	3.66E-03	0.00E+00	1.10E-02	0
734	1.3248	3.22E-03	0.00E+00	1.09E-02	0
735	1.3270	2.86E-03	0.00E+00	1.08E-02	0
736	1.3252	3.81E-03	0.00E+00	1.08E-02	0
737	1.3140	2.94E-03	0.00E+00	1.07E-02	0
738	1.3001	1.46E-03	0.00E+00	1.06E-02	0
739	1.2903	1.52E-03	0.00E+00	1.07E-02	0
740	1.2832	8.61E-04	0.00E+00	1.07E-02	0
741	1.2761	4.72E-04	0.00E+00	1.08E-02	0
742	1.2717	2.11E-04	0.00E+00	1.09E-02	0
743	1.2713	1.55E-04	0.00E+00	1.11E-02	0
744	1.2723	5.79E-05	0.00E+00	1.12E-02	0
745	1.2732	1.21E-05	0.00E+00	1.14E-02	0
746	1.2755	1.08E-05	0.00E+00	1.15E-02	0
747	1.2778	4.62E-06	0.00E+00	1.15E-02	0
748	1.2787	2.34E-06	0.00E+00	1.13E-02	0
749	1.2783	1.19E-06	0.00E+00	1.11E-02	0
750	1.2740	7.33E-07	0.00E+00	1.06E-02	0
751	1.2683	1.18E-06	0.00E+00	1.01E-02	0
752	1.2653	3.69E-07	0.00E+00	9.54E-03	0
753	1.2650	1.16E-07	0.00E+00	8.99E-03	0
754	1.2646	3.65E-07	0.00E+00	8.47E-03	0
755	1.2629	1.57E-06	0.00E+00	8.03E-03	0
756	1.2613	9.31E-09	0.00E+00	7.63E-03	0
757	1.2570	0.00E+00	0.00E+00	7.31E-03	0
758	1.2501	0.00E+00	1.07E-08	7.05E-03	0
759	1.2432	0.00E+00	5.97E-05	6.85E-03	0
760	1.2389	0.00E+00	1.97E-01	6.67E-03	0
761	1.2386	0.00E+00	3.38E-01	6.54E-03	0
762	1.2370	0.00E+00	3.97E-02	6.69E-03	0
763	1.2315	0.00E+00	1.31E-01	7.02E-03	0
764	1.2246	0.00E+00	7.30E-02	6.94E-03	0
765	1.2205	0.00E+00	3.77E-02	6.86E-03	0
766	1.2176	0.00E+00	1.54E-02	6.78E-03	0
767	1.2121	0.00E+00	5.11E-03	6.70E-03	0
768	1.2053	0.00E+00	9.81E-04	6.73E-03	0
769	1.2020	0.00E+00	4.19E-04	6.75E-03	0
770	1.2040	0.00E+00	8.48E-05	6.77E-03	0
771	1.2050	0.00E+00	1.40E-05	6.90E-03	0
772	1.2070	0.00E+00	4.20E-06	7.06E-03	0
773	1.2090	5.29E-08	2.37E-06	7.25E-03	0
774	1.1990	8.53E-08	8.78E-07	7.52E-03	0
775	1.1890	8.49E-08	2.57E-07	7.85E-03	0
776	1.1930	8.44E-08	3.66E-08	8.13E-03	0
777	1.1970	5.18E-08	1.07E-08	8.31E-03	0
778	1.1920	3.56E-07	0.00E+00	8.43E-03	0
779	1.1900	4.62E-07	0.00E+00	8.47E-03	0
780	1.1906	2.37E-07	0.00E+00	8.38E-03	0
781	1.1891	2.31E-07	0.00E+00	8.15E-03	0
782	1.1863	4.55E-07	0.00E+00	7.88E-03	0
783	1.1861	4.53E-07	0.00E+00	7.50E-03	0
784	1.1858	4.51E-07	0.00E+00	7.09E-03	0
785	1.1843	1.40E-05	0.00E+00	6.67E-03	0
786	1.1815	3.14E-05	0.00E+00	6.34E-03	0
787	1.1780	3.48E-04	0.00E+00	6.09E-03	0
788	1.1760	6.03E-04	0.00E+00	5.83E-03	0
789	1.1750	1.09E-03	0.00E+00	5.57E-03	0
790	1.1670	2.34E-03	0.00E+00	5.37E-03	0
791	1.1590	1.17E-03	0.00E+00	5.16E-03	0
792	1.1580	1.04E-03	0.00E+00	4.93E-03	0
793	1.1570	1.21E-03	0.00E+00	4.74E-03	0
794	1.1560	8.13E-05	0.00E+00	4.55E-03	0
795	1.1550	2.69E-04	0.00E+00	4.39E-03	0
796	1.1540	2.03E-03	0.00E+00	4.29E-03	0
797	1.1530	1.74E-03	0.00E+00	4.22E-03	0
798	1.1440	4.10E-04	0.00E+00	4.17E-03	0
799	1.1360	6.68E-04	0.00E+00	4.09E-03	0
800	1.1390	1.16E-03	0.00E+00	4.00E-03	0
801	1.1430	1.43E-03	0.00E+00	3.97E-03	0
802	1.1360	1.25E-03	0.00E+00	3.96E-03	0
803	1.1300	1.57E-03	0.00E+00	3.95E-03	0
804	1.1230	1.32E-03	0.00E+00	3.96E-03	0
805	1.1160	7.69E-04	0.00E+00	4.02E-03	0
806	1.1180	2.75E-04	0.00E+00	4.10E-03	0
807	1.1210	3.92E-04	0.00E+00	4.22E-03	0
808	1.1160	3.15E-04	0.00E+00	4.40E-03	0
809	1.1100	7.23E-04	0.00E+00	4.61E-03	0
810	1.1050	1.36E-03	0.00E+00	4.82E-03	0
811	1.1030	1.59E-03	0.00E+00	5.01E-03	0
812	1.1010	3.76E-03	0.00E+00	5.21E-03	0
813	1.1100	6.09E-03	0.00E+00	5.40E-03	0
814	1.1200	1.88E-02	0.00E+00	5.56E-03	0
815	1.1050	2.07E-02	0.00E+00	5.68E-03	0
816	1.0900	3.63E-02	0.00E+00	5.73E-03	0
817	1.0880	3.71E-02	0.00E+00	5.71E-03	0
818	1.0860	3.91E-02	0.00E+00	5.61E-03	0
819	1.0820	2.01E-02	0.00E+00	5.45E-03	0
820	1.0790	2.52E-02	0.00E+00	5.23E-03	0
821	1.0710	3.12E-03	0.00E+00	4.94E-03	0
822	1.0630	6.34E-03	0.00E+00	4.61E-03	0
823	1.0720	9.27E-02	0.00E+00	4.28E-03	0
824	1.0820	1.17E-02	0.00E+00	3.95E-03	0
825	1.0800	5.09E-03	0.00E+00	3.65E-03	0
826	1.0780	1.15E-02	0.00E+00	3.37E-03	0
827	1.0740	4.50E-03	0.00E+00	3.10E-03	0
828	1.0700	2.80E-02	0.00E+00	2.88E-03	0
829	1.0565	1.22E-02	0.00E+00	2.69E-03	0
830	1.0430	1.06E-02	0.00E+00	2.53E-03	0
831	1.0500	9.80E-03	0.00E+00	2.38E-03	0
832	1.0570	1.46E-02	0.00E+00	2.28E-03	0
833	1.0475	3.37E-03	0.00E+00	2.19E-03	0
834	1.0380	6.28E-03	0.00E+00	2.11E-03	0
835	1.0335	1.07E-03	0.00E+00	2.07E-03	0
836	1.0290	3.58E-03	0.00E+00	2.04E-03	0
837	1.0385	1.02E-03	0.00E+00	2.02E-03	0
838	1.0480	1.51E-03	0.00E+00	2.00E-03	0
839	1.0375	7.70E-04	0.00E+00	2.00E-03	0
840	1.0270	5.08E-04	0.00E+00	2.01E-03	0
841	1.0285	8.81E-04	0.00E+00	2.03E-03	0
842	1.030	4.69E-04	0.00E+00	2.07E-03	0
843	1.015	1.44E-04	0.00E+00	2.12E-03	0
844	1.000	3.37E-04	0.00E+00	2.19E-03	0
845	1.005	9.55E-05	0.00E+00	2.29E-03	0
846	1.010	6.46E-05	0.00E+00	2.42E-03	0
847	1.011	8.30E-06	0.00E+00	2.57E-03	0
848	1.012	8.08E-05	0.00E+00	2.75E-03	0
849	0.994	8.10E-05	0.00E+00	2.97E-03	0
850	0.976	7.72E-05	0.00E+00	3.22E-03	0
851	0.971	1.52E-04	0.00E+00	3.46E-03	0
852	0.966	1.57E-04	0.00E+00	3.67E-03	0
853	0.921	3.11E-05	0.00E+00	3.79E-03	0
854	0.876	1.13E-04	0.00E+00	3.80E-03	0
855	0.912	1.81E-05	0.00E+00	3.73E-03	0
856	0.948	4.66E-05	0.00E+00	3.62E-03	0
857	0.971	1.20E-05	0.00E+00	3.49E-03	0
858	0.994	1.75E-05	0.00E+00	3.34E-03	0
859	0.981	7.29E-06	0.00E+00	3.16E-03	0
860	0.968	1.55E-07	0.00E+00	2.93E-03	0
861	0.9765	2.21E-06	0.00E+00	2.69E-03	0
862	0.985	3.54E-08	3.66E-08	2.47E-03	0
863	0.953	2.18E-07	7.51E-08	2.27E-03	0

864	0.921	3.49E-07	1.07E-08	2.08E-03	0
865	0.904	3.50E-08	1.07E-08	1.89E-03	0
866	0.887	3.49E-08	3.66E-08	1.73E-03	0
867	0.9245	3.47E-08	3.66E-08	1.60E-03	0
868	0.962	8.37E-08	1.07E-08	1.49E-03	0
869	0.961	3.45E-08	1.07E-08	1.40E-03	0
870	0.96	3.43E-08	0.00E+00	1.33E-03	0
871	0.9565	2.21E-07	0.00E+00	1.27E-03	0
872	0.953	5.61E-08	0.00E+00	1.20E-03	0
873	0.9545	5.59E-08	0.00E+00	1.14E-03	0
874	0.956	5.57E-08	0.00E+00	1.10E-03	0
875	0.957	4.70E-07	0.00E+00	1.07E-03	0
876	0.958	1.60E-06	0.00E+00	1.05E-03	0
877	0.946	4.51E-07	0.00E+00	1.04E-03	0
878	0.934	4.79E-06	0.00E+00	1.03E-03	0
879	0.9345	3.64E-06	0.00E+00	1.04E-03	0
880	0.935	2.74E-06	0.00E+00	1.06E-03	0
881	0.929	2.03E-05	0.00E+00	1.07E-03	0
882	0.923	3.38E-05	0.00E+00	1.10E-03	0
883	0.93	1.33E-05	0.00E+00	1.14E-03	0
884	0.937	2.18E-05	0.00E+00	1.18E-03	0
885	0.9295	1.52E-05	0.00E+00	1.23E-03	0
886	0.922	1.76E-04	0.00E+00	1.28E-03	0
887	0.923	5.11E-05	0.00E+00	1.31E-03	0
888	0.924	1.86E-04	0.00E+00	1.34E-03	0
889	0.922	1.14E-05	0.00E+00	1.35E-03	0
890	0.92	2.02E-04	0.00E+00	1.35E-03	0
891	0.9155	8.93E-05	0.00E+00	1.34E-03	0
892	0.911	4.38E-04	0.00E+00	1.34E-03	0
893	0.9125	1.48E-03	0.00E+00	1.37E-03	0
894	0.914	3.37E-03	0.00E+00	1.43E-03	0
895	0.9165	8.76E-03	0.00E+00	1.50E-03	0
896	0.919	2.06E-02	0.00E+00	1.58E-03	0
897	0.9065	4.68E-02	0.00E+00	1.64E-03	0
898	0.894	3.58E-02	0.00E+00	1.66E-03	0
899	0.8915	1.07E-01	0.00E+00	1.65E-03	0
900	0.889	3.29E-02	0.00E+00	1.60E-03	0
901	0.89	6.65E-02	0.00E+00	1.53E-03	0
902	0.891	4.97E-02	0.00E+00	1.45E-03	0
903	0.886	4.38E-02	0.00E+00	1.36E-03	0
904	0.881	7.32E-03	0.00E+00	1.28E-03	0
905	0.881	8.47E-03	0.00E+00	1.18E-03	0
906	0.881	1.32E-02	0.00E+00	1.08E-03	0
907	0.8675	6.50E-02	0.00E+00	9.87E-04	0
908	0.854	5.03E-02	0.00E+00	9.18E-04	0
909	0.8595	2.93E-02	0.00E+00	8.51E-04	0
910	0.865	5.23E-02	0.00E+00	7.85E-04	0
911	0.869	4.08E-02	0.00E+00	7.22E-04	0
912	0.873	3.60E-02	0.00E+00	6.69E-04	0
913	0.869	5.61E-02	0.00E+00	6.25E-04	0
914	0.865	6.49E-02	0.00E+00	5.77E-04	0
915	0.8625	3.59E-02	0.00E+00	5.42E-04	0
916	0.86	9.20E-02	0.00E+00	5.22E-04	0
917	0.8605	2.14E-02	0.00E+00	5.01E-04	0
918	0.861	6.60E-02	0.00E+00	4.82E-04	0
919	0.848	2.06E-02	0.00E+00	4.67E-04	0
920	0.835	1.51E-02	0.00E+00	4.53E-04	0
921	0.8315	7.47E-03	0.00E+00	4.46E-04	0
922	0.828	1.98E-02	0.00E+00	4.43E-04	0
923	0.831	8.24E-03	0.00E+00	4.39E-04	0
924	0.834	1.86E-02	0.00E+00	4.37E-04	0
925	0.8365	2.19E-02	0.00E+00	4.40E-04	0
926	0.839	1.78E-02	0.00E+00	4.42E-04	0
927	0.842	9.63E-03	0.00E+00	4.41E-04	0
928	0.845	6.34E-02	0.00E+00	4.38E-04	0
929	0.8425	8.74E-02	0.00E+00	4.41E-04	0
930	0.84	1.91E-01	0.00E+00	4.43E-04	0
931	0.844	2.44E-01	0.00E+00	4.48E-04	0
932	0.848	5.04E-01	0.00E+00	4.46E-04	0
933	0.8415	6.11E-01	0.00E+00	4.37E-04	0
934	0.835	1.21E+00	0.00E+00	4.40E-04	0
935	0.8275	7.26E-01	0.00E+00	4.59E-04	0
936	0.82	1.16E+00	0.00E+00	4.93E-04	0
937	0.824	1.00E+00	0.00E+00	5.45E-04	0
938	0.828	8.21E-01	0.00E+00	6.15E-04	0
939	0.8245	2.70E-01	0.00E+00	6.91E-04	0
940	0.821	1.67E-01	0.00E+00	7.80E-04	0
941	0.8135	2.59E-01	0.00E+00	8.79E-04	0
942	0.806	2.15E-01	0.00E+00	9.73E-04	0
943	0.814	5.55E-01	0.00E+00	1.05E-03	0
944	0.822	6.33E-01	0.00E+00	1.09E-03	0
945	0.8195	2.78E-01	0.00E+00	1.08E-03	0
946	0.817	8.44E-01	0.00E+00	1.03E-03	0
947	0.809	3.00E-01	0.00E+00	9.39E-04	0
948	0.801	4.73E-01	0.00E+00	8.41E-04	0
949	0.802	1.48E-01	0.00E+00	7.38E-04	0
950	0.803	9.85E-01	0.00E+00	6.53E-04	0
951	0.7995	1.52E-01	0.00E+00	5.76E-04	0
952	0.796	5.06E-01	0.00E+00	5.20E-04	0
953	0.7905	2.95E-01	0.00E+00	4.54E-04	0
954	0.785	1.97E-01	0.00E+00	4.11E-04	0
955	0.792	3.16E-01	0.00E+00	4.04E-04	0
956	0.799	2.83E-01	0.00E+00	3.86E-04	0
957	0.7975	4.03E-01	0.00E+00	3.67E-04	0
958	0.796	1.52E-01	0.00E+00	3.42E-04	0
959	0.794	2.59E-01	0.00E+00	3.12E-04	0
960	0.792	1.75E-01	0.00E+00	2.86E-04	0
961	0.7915	1.32E-01	0.00E+00	2.66E-04	0
962	0.791	1.37E-01	0.00E+00	2.51E-04	0
963	0.7895	9.46E-02	0.00E+00	2.39E-04	0
964	0.788	1.34E-01	0.00E+00	2.31E-04	0
965	0.784	9.60E-02	0.00E+00	2.23E-04	0
966	0.78	7.35E-02	0.00E+00	2.12E-04	0
967	0.789	8.71E-02	0.00E+00	1.92E-04	0
968	0.798	1.65E-02	0.00E+00	1.75E-04	0
969	0.7905	1.20E-02	0.00E+00	1.63E-04	0
970	0.783	2.27E-02	0.00E+00	1.47E-04	0
971	0.783	7.08E-03	0.00E+00	1.35E-04	0
972	0.783	1.32E-02	0.00E+00	1.25E-04	0
973	0.775	2.77E-02	0.00E+00	1.17E-04	0
974	0.767	4.03E-02	0.00E+00	1.13E-04	0
975	0.775	4.12E-02	0.00E+00	1.08E-04	0
976	0.783	4.57E-02	0.00E+00	1.06E-04	0
977	0.782	1.79E-02	0.00E+00	1.03E-04	0
978	0.781	2.61E-02	0.00E+00	1.02E-04	0
979	0.7765	1.68E-02	0.00E+00	1.00E-04	0
980	0.772	2.81E-02	0.00E+00	9.96E-05	0
981	0.773	4.36E-03	0.00E+00	1.03E-04	0
982	0.774	7.40E-03	0.00E+00	1.09E-04	0
983	0.775	1.11E-02	0.00E+00	1.18E-04	0
984	0.776	1.95E-03	0.00E+00	1.35E-04	0
985	0.767	6.71E-03	0.00E+00	1.60E-04	0
986	0.758	5.00E-04	0.00E+00	1.94E-04	0
987	0.7625	1.18E-03	0.00E+00	2.35E-04	0
988	0.767	8.84E-04	0.00E+00	2.81E-04	0
989	0.765	9.85E-05	0.00E+00	3.39E-04	0
990	0.763	9.78E-04	0.00E+00	4.98E-04	0
991	0.7585	1.42E-04	0.00E+00	7.88E-04	0
992	0.754	8.64E-05	0.00E+00	7.35E-04	0
993	0.755	5.26E-04	0.00E+00	5.99E-04	0
994	0.756	4.45E-05	0.00E+00	5.89E-04	0
995	0.7495	1.49E-05	0.00E+00	5.58E-04	0
996	0.743	5.82E-05	0.00E+00	4.59E-04	0
997	0.743	3.32E-05	0.00E+00	3.67E-04	0
998	0.743	4.32E-05	0.00E+00	3.06E-04	0
999	0.742	3.95E-05	0.00E+00	2.53E-04	0
1000	0.741	1.23E-04	0.00E+00	2.06E-04	0
1001	0.7378	2.53E-05	0.00E+00	1.93E-04	0
1002	0.7346	6.45E-04	0.00E+00	1.63E-04	0
1003	0.7314	4.00E-05	0.00E+00	1.49E-04	0
1004	0.7282	1.48E-04	0.00E+00	1.38E-04	0
1005	0.725	1.25E-05	0.00E+00	1.14E-04	0
1006	0.7246	7.62E-05	0.00E+00	1.17E-04	0
1007	0.7242	3.55E-05	0.00E+00	1.01E-04	0
1008	0.7238	1.08E-04	0.00E+00	9.07E-05	0
1009	0.7234	2.16E-04	0.00E+00	9.21E-05	0
1010	0.723	3.04E-04	0.00E+00	8.02E-05	0
1011	0.7228	2.73E-05	0.00E+00	7.31E-05	0
1012	0.7226	9.85E-05	0.00E+00	7.41E-05	0
1013	0.7224	1.51E-05	0.00E+00	6.86E-05	0

1014	0.7222	1.41E-05	0.00E+00	6.30E-05	0	1089	0.6124	2.19E-03	0.00E+00	1.72E-05	0
1015	0.722	2.24E-05	0.00E+00	6.02E-05	0	1090	0.612	4.00E-03	0.00E+00	1.28E-05	0
1016	0.7208	2.59E-05	0.00E+00	6.02E-05	0	1091	0.6094	1.06E-03	0.00E+00	1.01E-05	0
1017	0.7196	3.23E-05	0.00E+00	5.59E-05	0	1092	0.6068	9.01E-04	0.00E+00	0.00E+00	0
1018	0.7184	7.50E-06	0.00E+00	5.16E-05	0	1093	0.6042	1.06E-02	0.00E+00	0.00E+00	0
1019	0.7172	1.38E-04	0.00E+00	5.09E-05	0	1094	0.6016	1.61E-03	0.00E+00	0.00E+00	0
1020	0.716	1.79E-05	0.00E+00	4.91E-05	0	1095	0.599	7.02E-03	0.00E+00	0.00E+00	0
1021	0.7178	4.90E-06	0.00E+00	4.42E-05	0	1096	0.6008	1.25E-02	0.00E+00	0.00E+00	0
1022	0.7196	3.21E-05	0.00E+00	4.07E-05	0	1097	0.6026	6.31E-04	0.00E+00	0.00E+00	0
1023	0.7214	4.19E-05	0.00E+00	3.92E-05	0	1098	0.6044	1.20E-02	0.00E+00	0.00E+00	0
1024	0.7232	2.29E-04	0.00E+00	3.88E-05	0	1099	0.6062	1.01E-02	0.00E+00	0.00E+00	0
1025	0.725	7.42E-06	0.00E+00	3.71E-05	0	1100	0.608	2.23E-02	0.00E+00	0.00E+00	0
1026	0.72	2.21E-05	0.00E+00	3.59E-05	0	1101	0.6066	1.74E-02	0.00E+00	0.00E+00	0
1027	0.715	2.09E-05	0.00E+00	3.61E-05	0	1102	0.6052	2.32E-02	0.00E+00	0.00E+00	0
1028	0.71	2.43E-05	0.00E+00	3.77E-05	0	1103	0.6038	2.65E-02	0.00E+00	0.00E+00	0
1029	0.705	2.92E-05	0.00E+00	3.78E-05	0	1104	0.6024	2.48E-02	0.00E+00	0.00E+00	0
1030	0.7	2.34E-06	0.00E+00	3.81E-05	0	1105	0.601	1.62E-02	0.00E+00	0.00E+00	0
1031	0.699	9.56E-06	0.00E+00	3.81E-05	0	1106	0.6012	6.10E-02	0.00E+00	0.00E+00	0
1032	0.698	1.93E-06	0.00E+00	3.89E-05	0	1107	0.6014	1.90E-02	0.00E+00	0.00E+00	0
1033	0.697	2.33E-06	0.00E+00	4.01E-05	0	1108	0.6016	5.22E-02	0.00E+00	0.00E+00	0
1034	0.696	6.74E-07	0.00E+00	4.23E-05	0	1109	0.6018	5.34E-02	0.00E+00	0.00E+00	0
1035	0.695	1.31E-07	0.00E+00	4.52E-05	0	1110	0.602	2.07E-02	0.00E+00	0.00E+00	0
1036	0.6918	1.56E-06	0.00E+00	4.75E-05	0	1111	0.5992	1.55E-01	0.00E+00	0.00E+00	0
1037	0.6886	1.31E-07	2.19E-06	5.05E-05	0	1112	0.5964	5.91E-02	0.00E+00	0.00E+00	0
1038	0.6854	1.30E-07	3.09E-07	5.25E-05	0	1113	0.5936	2.55E-01	0.00E+00	0.00E+00	0
1039	0.6822	4.49E-07	8.23E-07	5.59E-05	0	1114	0.5908	1.96E-01	0.00E+00	0.00E+00	0
1040	0.679	1.30E-07	8.23E-07	6.13E-05	0	1115	0.588	3.85E-01	0.00E+00	0.00E+00	0
1041	0.6804	4.47E-07	3.09E-07	6.73E-05	0	1116	0.586	4.64E-01	0.00E+00	0.00E+00	0
1042	0.6818	1.29E-07	0.00E+00	7.39E-05	0	1117	0.584	1.45E+00	0.00E+00	0.00E+00	0
1043	0.6832	1.29E-07	0.00E+00	8.39E-05	0	1118	0.582	5.11E-01	0.00E+00	0.00E+00	0
1044	0.6846	1.29E-07	0.00E+00	1.02E-04	0	1119	0.58	1.06E+00	0.00E+00	0.00E+00	0
1045	0.686	1.29E-07	0.00E+00	1.44E-04	0	1120	0.578	7.94E-01	0.00E+00	0.00E+00	0
1046	0.6824	1.28E-07	0.00E+00	1.88E-04	0	1121	0.576	7.03E-01	0.00E+00	0.00E+00	0
1047	0.6788	1.28E-07	0.00E+00	1.56E-04	0	1122	0.574	1.70E+00	0.00E+00	0.00E+00	0
1048	0.6752	1.28E-07	0.00E+00	1.38E-04	0	1123	0.572	1.30E+00	0.00E+00	0.00E+00	0
1049	0.6716	1.28E-07	4.84E-06	1.39E-04	0	1124	0.57	1.47E+00	0.00E+00	0.00E+00	0
1050	0.668	1.27E-07	6.91E-06	1.34E-04	0	1125	0.568	9.31E-01	0.00E+00	0.00E+00	0
1051	0.6662	1.27E-07	8.23E-07	1.18E-04	0	1126	0.5674	2.25E+00	0.00E+00	0.00E+00	0
1052	0.6644	1.27E-07	3.01E-06	9.58E-05	0	1127	0.5668	7.11E-01	0.00E+00	0.00E+00	0
1053	0.6626	1.27E-07	2.19E-06	8.42E-05	0	1128	0.5662	1.30E+00	0.00E+00	0.00E+00	0
1054	0.6608	1.26E-07	8.23E-07	7.32E-05	0	1129	0.5656	1.23E+00	0.00E+00	0.00E+00	0
1055	0.659	4.36E-07	3.09E-07	7.02E-05	0	1130	0.565	1.64E+00	0.00E+00	0.00E+00	0
1056	0.6572	6.50E-07	0.00E+00	6.07E-05	0	1131	0.5644	1.66E-01	0.00E+00	0.00E+00	0
1057	0.6554	4.35E-07	0.00E+00	6.06E-05	0	1132	0.5638	3.15E-01	0.00E+00	0.00E+00	0
1058	0.6536	4.34E-07	0.00E+00	5.33E-05	0	1133	0.5632	8.06E-01	0.00E+00	0.00E+00	0
1059	0.6518	1.18E-06	3.09E-07	5.13E-05	0	1134	0.5626	2.93E+00	0.00E+00	0.00E+00	0
1060	0.65	4.33E-07	3.09E-07	4.98E-05	0	1135	0.562	5.83E+00	0.00E+00	0.00E+00	0
1061	0.6496	8.94E-07	3.09E-07	4.63E-05	0	1136	0.5608	1.03E+00	0.00E+00	0.00E+00	0
1062	0.6492	5.18E-06	3.09E-07	4.90E-05	0	1137	0.5596	1.71E-01	0.00E+00	0.00E+00	0
1063	0.6488	7.04E-06	2.19E-06	5.03E-05	0	1138	0.5584	4.05E-01	0.00E+00	0.00E+00	0
1064	0.6484	2.57E-07	5.85E-06	5.33E-05	0	1139	0.5572	2.13E-01	0.00E+00	0.00E+00	0
1065	0.648	2.67E-05	5.85E-06	6.20E-05	0	1140	0.556	2.64E-01	0.00E+00	0.00E+00	0
1066	0.6464	1.49E-06	6.91E-06	6.05E-05	0	1141	0.5556	5.22E-01	0.00E+00	0.00E+00	0
1067	0.6448	1.15E-05	2.19E-06	5.16E-05	0	1142	0.5552	4.18E-01	0.00E+00	0.00E+00	0
1068	0.6432	3.16E-05	2.14E-05	4.83E-05	0	1143	0.5548	1.26E-01	0.00E+00	0.00E+00	0
1069	0.6416	5.68E-05	3.89E-06	4.96E-05	0	1144	0.5544	1.23E+00	0.00E+00	0.00E+00	0
1070	0.64	1.89E-04	8.23E-07	4.54E-05	0	1145	0.554	7.73E-01	0.00E+00	0.00E+00	0
1071	0.6382	1.31E-05	8.23E-07	3.85E-05	0	1146	0.5518	7.76E-01	0.00E+00	0.00E+00	0
1072	0.6364	1.78E-04	1.46E-06	3.38E-05	0	1147	0.5496	2.03E+00	0.00E+00	0.00E+00	0
1073	0.6346	1.40E-04	8.23E-07	3.00E-05	0	1148	0.5474	2.31E-01	0.00E+00	0.00E+00	0
1074	0.6328	8.31E-06	3.09E-07	2.86E-05	0	1149	0.5452	4.60E-01	0.00E+00	0.00E+00	0
1075	0.631	1.08E-03	3.09E-07	2.85E-05	0	1150	0.543	9.44E-01	0.00E+00	0.00E+00	0
1076	0.629	6.50E-05	0.00E+00	2.57E-05	0	1151	0.5448	4.45E-01	0.00E+00	0.00E+00	0
1077	0.627	5.63E-04	0.00E+00	2.61E-05	0	1152	0.5466	3.55E-01	0.00E+00	0.00E+00	0
1078	0.625	8.58E-04	0.00E+00	2.34E-05	0	1153	0.5484	4.19E-01	0.00E+00	0.00E+00	0
1079	0.623	3.52E-05	0.00E+00	2.28E-05	0	1154	0.5502	6.20E-01	0.00E+00	0.00E+00	0
1080	0.621	1.59E-03	0.00E+00	2.05E-05	0	1155	0.552	1.56E-01	0.00E+00	0.00E+00	0
1081	0.6196	1.41E-03	0.00E+00	1.85E-05	0	1156	0.5492	2.33E-01	0.00E+00	0.00E+00	0
1082	0.6182	4.49E-04	0.00E+00	1.86E-05	0	1157	0.5464	1.34E-01	0.00E+00	0.00E+00	0
1083	0.6168	1.82E-04	0.00E+00	1.89E-05	0	1158	0.5436	1.66E-01	0.00E+00	0.00E+00	0
1084	0.6154	2.05E-03	0.00E+00	1.89E-05	0	1159	0.5408	1.23E-01	0.00E+00	0.00E+00	0
1085	0.614	8.82E-04	0.00E+00	1.87E-05	0	1160	0.538	1.64E-01	0.00E+00	0.00E+00	0
1086	0.6136	6.46E-03	0.00E+00	2.10E-05	0	1161	0.536	7.06E-02	0.00E+00	0.00E+00	0
1087	0.6132	1.59E-03	0.00E+00	2.00E-05	0	1162	0.534	7.16E-02	0.00E+00	0.00E+00	0
1088	0.6128	5.91E-04	0.00E+00	1.94E-05	0	1163	0.532	1.49E-02	0.00E+00	0.00E+00	0

1164	0.53	3.53E-02	0.00E+00	0.00E+00	0	1239	0.4664	2.03E-05	3.09E-07	0.00E+00	0
1165	0.528	4.92E-02	0.00E+00	0.00E+00	0	1240	0.466	4.91E-06	3.09E-07	0.00E+00	0
1166	0.5286	5.07E-02	0.00E+00	0.00E+00	0	1241	0.4634	1.09E-04	3.09E-07	0.00E+00	0
1167	0.5292	3.17E-02	0.00E+00	0.00E+00	0	1242	0.4608	7.21E-06	0.00E+00	0.00E+00	0
1168	0.5298	2.74E-02	0.00E+00	0.00E+00	0	1243	0.4582	3.01E-06	3.09E-07	0.00E+00	0
1169	0.5304	2.02E-02	0.00E+00	0.00E+00	0	1244	0.4556	2.02E-05	3.09E-07	0.00E+00	0
1170	0.531	1.15E-02	0.00E+00	0.00E+00	0	1245	0.453	3.44E-06	1.46E-06	0.00E+00	0
1171	0.5294	1.51E-02	0.00E+00	0.00E+00	0	1246	0.4546	3.00E-06	0.00E+00	0.00E+00	0
1172	0.5278	1.38E-02	0.00E+00	0.00E+00	0	1247	0.4562	7.19E-06	3.89E-06	0.00E+00	0
1173	0.5262	1.13E-02	0.00E+00	0.00E+00	0	1248	0.4578	3.12E-05	1.04E-05	0.00E+00	0
1174	0.5246	8.15E-02	0.00E+00	0.00E+00	0	1249	0.4594	3.89E-06	4.84E-06	0.00E+00	0
1175	0.523	1.03E-02	0.00E+00	0.00E+00	0	1250	0.461	5.42E-06	1.56E-05	0.00E+00	0
1176	0.5208	3.94E-03	0.00E+00	0.00E+00	0	1251	0.459	4.37E-06	5.92E-05	0.00E+00	0
1177	0.5186	6.91E-03	0.00E+00	0.00E+00	0	1252	0.457	9.14E-06	8.23E-07	0.00E+00	0
1178	0.5164	5.50E-02	0.00E+00	0.00E+00	0	1253	0.455	4.88E-06	1.09E-04	0.00E+00	0
1179	0.5142	4.72E-03	0.00E+00	0.00E+00	0	1254	0.453	3.87E-05	1.89E-04	0.00E+00	0
1180	0.512	1.46E-02	0.00E+00	0.00E+00	0	1255	0.451	1.63E-05	8.23E-07	0.00E+00	0
1181	0.5114	9.63E-03	0.00E+00	0.00E+00	0	1256	0.4472	9.12E-06	2.95E-04	0.00E+00	0
1182	0.5108	1.08E-01	0.00E+00	0.00E+00	0	1257	0.4434	5.96E-06	3.88E-04	0.00E+00	0
1183	0.5102	7.12E-03	0.00E+00	0.00E+00	0	1258	0.4396	2.64E-05	2.61E-05	0.00E+00	0
1184	0.5096	2.13E-02	0.00E+00	0.00E+00	0	1259	0.4358	6.53E-06	6.70E-04	0.00E+00	0
1185	0.509	2.92E-02	0.00E+00	0.00E+00	0	1260	0.432	2.53E-05	4.28E-04	0.00E+00	0
1186	0.5088	3.96E-03	0.00E+00	0.00E+00	0	1261	0.4308	2.52E-05	1.62E-03	0.00E+00	0
1187	0.5086	1.01E-02	0.00E+00	0.00E+00	0	1262	0.4296	7.76E-06	2.68E-03	0.00E+00	0
1188	0.5084	8.06E-02	0.00E+00	0.00E+00	0	1263	0.4284	3.72E-05	2.35E-03	0.00E+00	0
1189	0.5082	1.30E-02	0.00E+00	0.00E+00	0	1264	0.4272	3.59E-05	4.82E-03	0.00E+00	0
1190	0.508	4.82E-03	0.00E+00	0.00E+00	0	1265	0.426	1.20E-05	2.42E-03	0.00E+00	0
1191	0.506	1.16E-02	0.00E+00	0.00E+00	0	1266	0.4262	5.37E-06	3.68E-03	0.00E+00	0
1192	0.504	4.16E-03	0.00E+00	0.00E+00	0	1267	0.4264	5.12E-05	2.64E-03	0.00E+00	0
1193	0.502	8.74E-03	0.00E+00	0.00E+00	0	1268	0.4266	2.20E-05	4.23E-03	0.00E+00	0
1194	0.5	4.97E-03	0.00E+00	0.00E+00	0	1269	0.4268	1.80E-05	2.63E-02	0.00E+00	0
1195	0.498	9.11E-03	0.00E+00	0.00E+00	0	1270	0.427	1.28E-05	2.66E-03	0.00E+00	0
1196	0.4968	1.33E-02	0.00E+00	0.00E+00	0	1271	0.4298	9.11E-05	1.22E-03	0.00E+00	0
1197	0.4956	2.60E-03	0.00E+00	0.00E+00	0	1272	0.4326	5.42E-05	1.28E-03	0.00E+00	0
1198	0.4944	9.16E-03	0.00E+00	0.00E+00	0	1273	0.4354	4.11E-05	1.48E-03	0.00E+00	0
1199	0.4932	3.28E-02	0.00E+00	0.00E+00	0	1274	0.4382	9.89E-05	1.27E-03	0.00E+00	0
1200	0.492	7.12E-03	0.00E+00	0.00E+00	0	1275	0.441	1.71E-05	1.18E-03	0.00E+00	0
1201	0.4914	1.22E-02	0.00E+00	0.00E+00	0	1276	0.4376	6.37E-05	8.83E-04	0.00E+00	0
1202	0.4908	1.28E-02	0.00E+00	0.00E+00	0	1277	0.4342	3.63E-04	4.69E-04	0.00E+00	0
1203	0.4902	7.47E-03	6.12E-05	0.00E+00	0	1278	0.4308	1.20E-05	3.63E-04	0.00E+00	0
1204	0.4896	3.78E-02	9.30E-04	0.00E+00	0	1279	0.4274	2.12E-04	1.98E-04	0.00E+00	0
1205	0.489	8.89E-03	3.95E-04	0.00E+00	0	1280	0.424	2.57E-04	2.07E-04	0.00E+00	0
1206	0.488	1.09E-03	1.04E-04	0.00E+00	0	1281	0.4244	2.76E-04	6.75E-05	0.00E+00	0
1207	0.487	1.11E-02	2.56E-04	0.00E+00	0	1282	0.4248	3.19E-05	4.54E-05	0.00E+00	0
1208	0.486	7.38E-03	3.01E-04	0.00E+00	0	1283	0.4252	5.71E-05	6.96E-05	0.00E+00	0
1209	0.485	7.29E-03	1.58E-04	0.00E+00	0	1284	0.4256	2.86E-04	1.99E-05	0.00E+00	0
1210	0.484	4.18E-03	7.84E-05	0.00E+00	0	1285	0.426	1.81E-04	3.27E-05	0.00E+00	0
1211	0.486	8.19E-03	3.80E-05	0.00E+00	0	1286	0.427	1.20E-04	8.23E-07	0.00E+00	0
1212	0.488	1.19E-02	1.99E-05	0.00E+00	0	1287	0.428	4.80E-04	3.10E-05	0.00E+00	0
1213	0.49	1.86E-03	5.85E-06	0.00E+00	0	1288	0.429	5.76E-04	3.09E-07	0.00E+00	0
1214	0.492	8.35E-03	2.19E-06	0.00E+00	0	1289	0.43	1.91E-03	1.84E-05	0.00E+00	0
1215	0.494	9.73E-03	8.23E-07	0.00E+00	0	1290	0.431	4.63E-04	4.84E-06	0.00E+00	0
1216	0.4902	1.96E-03	3.09E-07	0.00E+00	0	1291	0.4302	2.11E-04	1.99E-05	0.00E+00	0
1217	0.4864	3.43E-03	0.00E+00	0.00E+00	0	1292	0.4294	2.55E-03	3.89E-06	0.00E+00	0
1218	0.4826	1.86E-03	1.45E-04	0.00E+00	0	1293	0.4286	1.01E-03	3.89E-06	0.00E+00	0
1219	0.4788	2.16E-03	5.31E-04	0.00E+00	0	1294	0.4278	1.39E-03	3.89E-06	0.00E+00	0
1220	0.475	2.41E-03	1.64E-04	0.00E+00	0	1295	0.427	1.62E-03	5.85E-06	0.00E+00	0
1221	0.4748	1.75E-03	5.71E-05	0.00E+00	0	1296	0.427	3.03E-03	3.89E-06	0.00E+00	0
1222	0.4746	2.56E-03	1.64E-04	0.00E+00	0	1297	0.427	6.18E-03	1.46E-06	0.00E+00	0
1223	0.4744	2.57E-03	1.69E-04	0.00E+00	0	1298	0.427	2.24E-03	8.23E-07	0.00E+00	0
1224	0.4742	2.89E-03	8.97E-05	0.00E+00	0	1299	0.427	6.45E-04	3.09E-07	0.00E+00	0
1225	0.474	1.44E-03	3.62E-05	0.00E+00	0	1300	0.427	1.21E-02	3.09E-07	0.00E+00	0
1226	0.4744	9.47E-04	2.45E-05	0.00E+00	0	1301	0.4252	8.44E-03	0.00E+00	0.00E+00	0
1227	0.4748	3.82E-03	1.84E-05	0.00E+00	0	1302	0.4234	2.22E-03	0.00E+00	0.00E+00	0
1228	0.4752	5.92E-04	9.18E-06	0.00E+00	0	1303	0.4216	1.65E-02	0.00E+00	0.00E+00	0
1229	0.4756	7.54E-04	2.19E-06	0.00E+00	0	1304	0.4198	3.67E-02	0.00E+00	0.00E+00	0
1230	0.476	1.28E-03	3.01E-06	0.00E+00	0	1305	0.418	3.88E-03	0.00E+00	0.00E+00	0
1231	0.4744	1.20E-04	3.01E-06	0.00E+00	0	1306	0.4162	3.33E-03	0.00E+00	0.00E+00	0
1232	0.4728	1.48E-04	2.19E-06	0.00E+00	0	1307	0.4144	3.53E-02	0.00E+00	0.00E+00	0
1233	0.4712	1.83E-03	1.46E-06	0.00E+00	0	1308	0.4126	1.67E-02	0.00E+00	0.00E+00	0
1234	0.4696	1.39E-05	3.01E-06	0.00E+00	0	1309	0.4108	3.00E-03	0.00E+00	0.00E+00	0
1235	0.468	9.84E-05	2.19E-06	0.00E+00	0	1310	0.409	4.03E-02	0.00E+00	0.00E+00	0
1236	0.4676	2.67E-05	3.09E-07	0.00E+00	0	1311	0.4084	1.95E-02	0.00E+00	0.00E+00	0
1237	0.4672	2.45E-04	8.23E-07	0.00E+00	0	1312	0.4078	1.59E-02	3.09E-07	0.00E+00	0
1238	0.4668	2.03E-05	8.23E-07	0.00E+00	0	1313	0.4072	2.26E-02	8.02E-06	0.00E+00	0

1314	0.4066	5.93E-02	3.98E-05	0.00E+00	0	1389	0.355	7.99E+00	0.00E+00	0.00E+00	0
1315	0.406	3.88E-02	5.31E-05	0.00E+00	0	1390	0.354	9.07E+00	0.00E+00	0.00E+00	0
1316	0.4062	1.61E-02	2.29E-05	0.00E+00	0	1391	0.3538	8.55E+00	0.00E+00	0.00E+00	0
1317	0.4064	3.32E-02	6.91E-06	0.00E+00	0	1392	0.3536	2.09E+01	0.00E+00	0.00E+00	0
1318	0.4066	1.38E-02	1.99E-05	0.00E+00	0	1393	0.3534	1.62E+01	0.00E+00	0.00E+00	0
1319	0.4068	6.69E-02	2.45E-05	0.00E+00	0	1394	0.3532	1.02E+01	0.00E+00	0.00E+00	0
1320	0.407	9.65E-02	2.14E-05	0.00E+00	0	1395	0.353	3.75E+01	0.00E+00	0.00E+00	0
1321	0.406	3.99E-02	1.42E-05	0.00E+00	0	1396	0.3522	5.20E+01	0.00E+00	0.00E+00	0
1322	0.405	3.05E-02	6.91E-06	0.00E+00	0	1397	0.3514	1.89E+01	0.00E+00	0.00E+00	0
1323	0.404	1.14E-01	2.19E-06	0.00E+00	0	1398	0.3506	5.14E+00	0.00E+00	0.00E+00	0
1324	0.403	7.62E-02	8.23E-07	0.00E+00	0	1399	0.3498	6.88E+00	0.00E+00	0.00E+00	0
1325	0.402	2.17E-02	3.09E-07	0.00E+00	0	1400	0.349	4.72E+01	0.00E+00	0.00E+00	0
1326	0.4008	4.76E-02	0.00E+00	0.00E+00	0	1401	0.3484	5.27E+01	0.00E+00	0.00E+00	0
1327	0.3996	6.52E-02	0.00E+00	0.00E+00	0	1402	0.3478	7.20E+00	0.00E+00	0.00E+00	0
1328	0.3984	1.11E-01	0.00E+00	0.00E+00	0	1403	0.3472	4.78E+00	0.00E+00	0.00E+00	0
1329	0.3972	2.24E-01	0.00E+00	0.00E+00	0	1404	0.3466	1.06E+01	0.00E+00	0.00E+00	0
1330	0.396	1.06E-01	0.00E+00	0.00E+00	0	1405	0.346	3.46E+01	0.00E+00	0.00E+00	0
1331	0.3952	3.08E-01	0.00E+00	0.00E+00	0	1406	0.3454	5.10E+00	0.00E+00	0.00E+00	0
1332	0.3944	4.19E-01	0.00E+00	0.00E+00	0	1407	0.3448	2.01E+01	0.00E+00	0.00E+00	0
1333	0.3936	1.51E-01	0.00E+00	0.00E+00	0	1408	0.3442	5.14E+00	0.00E+00	0.00E+00	0
1334	0.3928	2.83E-01	0.00E+00	0.00E+00	0	1409	0.3436	1.26E+01	0.00E+00	0.00E+00	0
1335	0.392	1.10E-01	3.09E-07	0.00E+00	0	1410	0.343	1.06E+01	0.00E+00	0.00E+00	0
1336	0.3916	2.63E-01	3.01E-06	0.00E+00	0	1411	0.3426	5.14E+00	0.00E+00	0.00E+00	0
1337	0.3912	2.63E-01	9.18E-06	0.00E+00	0	1412	0.3422	5.32E+00	0.00E+00	0.00E+00	0
1338	0.3908	2.25E-01	1.56E-05	0.00E+00	0	1413	0.3418	2.35E+00	0.00E+00	0.00E+00	0
1339	0.3904	2.10E-01	1.16E-05	0.00E+00	0	1414	0.3414	1.12E+01	0.00E+00	0.00E+00	0
1340	0.39	2.96E-01	2.19E-06	0.00E+00	0	1415	0.341	1.29E+01	0.00E+00	0.00E+00	0
1341	0.3894	2.72E-01	3.89E-06	0.00E+00	0	1416	0.3408	1.70E+00	0.00E+00	0.00E+00	0
1342	0.3888	2.05E-01	1.04E-05	0.00E+00	0	1417	0.3406	1.88E+00	0.00E+00	0.00E+00	0
1343	0.3882	3.95E-01	1.04E-05	0.00E+00	0	1418	0.3404	2.80E+00	0.00E+00	0.00E+00	0
1344	0.3876	1.02E+00	5.85E-06	0.00E+00	0	1419	0.3402	1.07E+01	0.00E+00	0.00E+00	0
1345	0.387	6.04E-01	3.89E-06	0.00E+00	0	1420	0.34	4.70E+00	0.00E+00	0.00E+00	0
1346	0.3856	1.18E+00	1.46E-06	0.00E+00	0	1421	0.341	3.21E+00	0.00E+00	0.00E+00	0
1347	0.3842	1.19E+00	8.23E-07	0.00E+00	0	1422	0.342	1.43E+00	0.00E+00	0.00E+00	0
1348	0.3828	4.46E+00	3.09E-07	0.00E+00	0	1423	0.343	3.51E+00	0.00E+00	0.00E+00	0
1349	0.3814	1.92E+00	0.00E+00	0.00E+00	0	1424	0.344	3.51E+00	0.00E+00	0.00E+00	0
1350	0.38	3.27E+00	0.00E+00	0.00E+00	0	1425	0.345	2.32E+00	0.00E+00	0.00E+00	0
1351	0.379	4.29E+00	3.09E-07	0.00E+00	0	1426	0.343	2.28E+00	0.00E+00	0.00E+00	0
1352	0.378	6.75E+00	0.00E+00	0.00E+00	0	1427	0.341	1.30E+00	0.00E+00	0.00E+00	0
1353	0.377	1.34E+01	3.09E-07	0.00E+00	0	1428	0.339	4.26E+00	0.00E+00	0.00E+00	0
1354	0.376	1.28E+01	0.00E+00	0.00E+00	0	1429	0.337	1.85E+00	3.09E-07	0.00E+00	0
1355	0.375	3.11E+01	0.00E+00	0.00E+00	0	1430	0.335	1.21E+00	5.85E-06	0.00E+00	0
1356	0.3744	1.66E+01	0.00E+00	0.00E+00	0	1431	0.3338	1.18E+00	2.54E-02	0.00E+00	0
1357	0.3738	1.57E+01	0.00E+00	0.00E+00	0	1432	0.3326	5.23E+00	3.50E-02	0.00E+00	0
1358	0.3732	2.98E+01	0.00E+00	0.00E+00	0	1433	0.3314	1.66E+00	1.72E-02	0.00E+00	0
1359	0.3726	3.65E+01	0.00E+00	0.00E+00	0	1434	0.3302	2.74E+00	3.65E-03	0.00E+00	0
1360	0.372	2.31E+01	0.00E+00	0.00E+00	0	1435	0.329	2.29E+00	6.83E-03	0.00E+00	0
1361	0.3704	6.07E+01	0.00E+00	0.00E+00	0	1436	0.3282	1.57E+00	1.02E-02	0.00E+00	0
1362	0.3688	1.49E+02	0.00E+00	0.00E+00	0	1437	0.3274	1.96E+00	8.68E-03	0.00E+00	0
1363	0.3672	2.55E+01	0.00E+00	0.00E+00	0	1438	0.3266	3.93E+00	6.57E-03	0.00E+00	0
1364	0.3656	2.67E+01	0.00E+00	0.00E+00	0	1439	0.3258	1.01E+00	8.52E-03	0.00E+00	0
1365	0.364	9.13E+01	0.00E+00	0.00E+00	0	1440	0.325	1.47E+00	6.55E-03	0.00E+00	0
1366	0.3638	1.66E+01	0.00E+00	0.00E+00	0	1441	0.3234	1.56E+00	3.88E-03	0.00E+00	0
1367	0.3636	2.48E+01	0.00E+00	0.00E+00	0	1442	0.3218	2.01E+00	2.36E-03	0.00E+00	0
1368	0.3634	9.50E+01	0.00E+00	0.00E+00	0	1443	0.3202	1.92E+00	1.17E-03	0.00E+00	0
1369	0.3632	2.89E+01	3.09E-07	0.00E+00	0	1444	0.3186	8.21E-01	1.59E-03	0.00E+00	0
1370	0.363	3.52E+01	3.09E-07	0.00E+00	0	1445	0.317	1.35E+00	7.39E-04	0.00E+00	0
1371	0.363	5.18E+01	3.09E-07	0.00E+00	0	1446	0.318	3.68E+00	6.62E-04	0.00E+00	0
1372	0.363	2.91E+01	3.09E-07	0.00E+00	0	1447	0.319	1.45E+00	3.56E-04	0.00E+00	0
1373	0.363	1.53E+01	0.00E+00	0.00E+00	0	1448	0.32	4.32E-01	2.40E-04	0.00E+00	0
1374	0.363	1.21E+01	3.09E-07	0.00E+00	0	1449	0.321	4.44E-01	1.19E-04	0.00E+00	0
1375	0.363	1.27E+01	3.09E-07	0.00E+00	0	1450	0.322	2.22E+00	6.96E-05	0.00E+00	0
1376	0.3622	1.20E+01	3.09E-07	0.00E+00	0	1451	0.3188	4.60E+00	4.54E-05	0.00E+00	0
1377	0.3614	1.26E+01	3.09E-07	0.00E+00	0	1452	0.3156	1.13E+00	2.45E-05	0.00E+00	0
1378	0.3606	6.50E+00	0.00E+00	0.00E+00	0	1453	0.3124	6.89E-01	1.42E-05	0.00E+00	0
1379	0.3598	1.83E+01	0.00E+00	0.00E+00	0	1454	0.3092	2.66E-01	8.02E-06	0.00E+00	0
1380	0.359	1.62E+01	0.00E+00	0.00E+00	0	1455	0.306	8.77E-01	4.84E-06	0.00E+00	0
1381	0.359	5.03E+01	0.00E+00	0.00E+00	0	1456	0.308	6.64E-01	3.01E-06	0.00E+00	0
1382	0.359	3.13E+01	0.00E+00	0.00E+00	0	1457	0.31	3.65E-01	1.46E-06	0.00E+00	0
1383	0.359	6.73E+01	0.00E+00	0.00E+00	0	1458	0.312	3.42E-01	8.23E-07	0.00E+00	0
1384	0.359	3.31E+01	0.00E+00	0.00E+00	0	1459	0.314	1.55E-01	3.09E-07	0.00E+00	0
1385	0.359	4.00E+01	0.00E+00	0.00E+00	0	1460	0.316	8.67E-01	3.09E-07	0.00E+00	0
1386	0.358	2.34E+01	0.00E+00	0.00E+00	0	1461	0.315	4.93E-01	0.00E+00	0.00E+00	0
1387	0.357	8.81E+00	0.00E+00	0.00E+00	0	1462	0.314	3.15E-01	0.00E+00	0.00E+00	0
1388	0.356	2.65E+01	0.00E+00	0.00E+00	0	1463	0.313	1.45E+00	0.00E+00	0.00E+00	0

1464	0.312	2.24E-01	0.00E+00	0.00E+00	0	1539	0.2778	3.66E-04	1.95E-04	0.00E+00	0
1465	0.311	7.58E-01	0.00E+00	0.00E+00	0	1540	0.278	8.26E-05	3.77E-04	0.00E+00	0
1466	0.311	1.06E+00	0.00E+00	0.00E+00	0	1541	0.2778	1.53E-04	2.98E-04	0.00E+00	0
1467	0.311	1.99E+00	0.00E+00	0.00E+00	0	1542	0.2776	5.29E-04	2.10E-04	0.00E+00	0
1468	0.311	6.82E-01	0.00E+00	0.00E+00	0	1543	0.2774	1.70E-04	1.66E-04	0.00E+00	0
1469	0.311	4.68E-01	0.00E+00	0.00E+00	0	1544	0.2772	6.19E-04	6.96E-05	0.00E+00	0
1470	0.311	1.88E+00	0.00E+00	0.00E+00	0	1545	0.277	8.44E-05	3.62E-05	0.00E+00	0
1471	0.3102	2.87E+00	2.77E-05	0.00E+00	0	1546	0.2768	3.06E-04	2.14E-05	0.00E+00	0
1472	0.3094	1.63E+00	1.61E-04	0.00E+00	0	1547	0.2766	1.19E-04	4.84E-06	0.00E+00	0
1473	0.3086	8.14E-01	1.06E-04	0.00E+00	0	1548	0.2764	1.12E-04	1.46E-06	0.00E+00	0
1474	0.3078	5.52E-01	4.92E-05	0.00E+00	0	1549	0.2762	4.82E-05	3.09E-07	0.00E+00	0
1475	0.307	1.01E-01	8.02E-06	0.00E+00	0	1550	0.276	8.07E-05	3.09E-07	0.00E+00	0
1476	0.3062	9.16E-01	2.94E-05	0.00E+00	0	1551	0.2758	1.16E-04	0.00E+00	0.00E+00	0
1477	0.3054	1.01E+00	5.31E-05	0.00E+00	0	1552	0.2756	3.48E-04	0.00E+00	0.00E+00	0
1478	0.3046	1.06E+00	3.27E-05	0.00E+00	0	1553	0.2754	7.36E-05	0.00E+00	0.00E+00	0
1479	0.3038	3.74E-01	4.92E-05	0.00E+00	0	1554	0.2752	1.21E-04	0.00E+00	0.00E+00	0
1480	0.303	1.05E+00	2.77E-05	0.00E+00	0	1555	0.275	7.01E-05	0.00E+00	0.00E+00	0
1481	0.3022	4.92E-01	1.99E-05	0.00E+00	0	1556	0.2746	9.18E-05	0.00E+00	0.00E+00	0
1482	0.3014	1.04E+00	1.16E-05	0.00E+00	0	1557	0.2742	7.18E-05	0.00E+00	0.00E+00	0
1483	0.3006	1.76E-01	4.84E-06	0.00E+00	0	1558	0.2738	7.35E-05	3.09E-07	0.00E+00	0
1484	0.2998	2.66E-01	3.01E-06	0.00E+00	0	1559	0.2734	8.61E-05	3.09E-07	0.00E+00	0
1485	0.299	2.94E-01	3.01E-06	0.00E+00	0	1560	0.273	9.18E-05	3.09E-07	0.00E+00	0
1486	0.3	2.89E-01	1.46E-06	0.00E+00	0	1561	0.2718	8.43E-05	3.09E-07	0.00E+00	0
1487	0.301	9.36E-01	1.46E-06	0.00E+00	0	1562	0.2706	1.83E-04	3.09E-07	0.00E+00	0
1488	0.302	3.63E-01	3.09E-07	0.00E+00	0	1563	0.2694	1.39E-04	0.00E+00	0.00E+00	0
1489	0.303	1.04E-01	3.09E-07	0.00E+00	0	1564	0.2682	1.55E-04	0.00E+00	0.00E+00	0
1490	0.304	1.21E-01	3.09E-07	0.00E+00	0	1565	0.267	8.06E-05	8.23E-07	0.00E+00	0
1491	0.3034	9.17E-02	0.00E+00	0.00E+00	0	1566	0.2664	1.18E-04	4.84E-06	0.00E+00	0
1492	0.3028	1.41E-01	3.09E-07	0.00E+00	0	1567	0.2658	8.61E-05	3.62E-05	0.00E+00	0
1493	0.3022	9.31E-02	2.19E-06	0.00E+00	0	1568	0.2652	1.23E-04	2.37E-04	0.00E+00	0
1494	0.3016	5.47E-02	3.01E-06	0.00E+00	0	1569	0.2646	5.87E-05	1.03E-03	0.00E+00	0
1495	0.301	1.02E-01	3.01E-06	0.00E+00	0	1570	0.264	7.01E-05	3.29E-03	0.00E+00	0
1496	0.3002	1.21E-01	8.23E-07	0.00E+00	0	1571	0.2638	7.35E-05	6.78E-03	0.00E+00	0
1497	0.2994	3.86E-02	9.18E-06	0.00E+00	0	1572	0.2636	6.50E-05	6.03E-03	0.00E+00	0
1498	0.2986	7.56E-02	4.84E-06	0.00E+00	0	1573	0.2634	7.18E-05	5.88E-03	0.00E+00	0
1499	0.2978	3.80E-02	8.23E-07	0.00E+00	0	1574	0.2632	7.52E-05	3.59E-03	0.00E+00	0
1500	0.297	1.57E-02	3.09E-07	0.00E+00	0	1575	0.263	6.02E-05	7.79E-04	0.00E+00	0
1501	0.2968	7.18E-03	3.09E-07	0.00E+00	0	1576	0.2622	9.37E-05	1.63E-03	0.00E+00	0
1502	0.2966	2.37E-02	3.09E-07	0.00E+00	0	1577	0.2614	6.18E-05	3.75E-03	0.00E+00	0
1503	0.2964	5.66E-02	0.00E+00	0.00E+00	0	1578	0.2606	5.55E-05	3.13E-03	0.00E+00	0
1504	0.2962	1.22E-01	0.00E+00	0.00E+00	0	1579	0.2598	1.27E-04	3.82E-03	0.00E+00	0
1505	0.296	5.77E-02	0.00E+00	0.00E+00	0	1580	0.259	5.86E-05	2.48E-03	0.00E+00	0
1506	0.2952	4.69E-03	0.00E+00	0.00E+00	0	1581	0.2584	6.50E-05	1.99E-03	0.00E+00	0
1507	0.2944	8.66E-03	0.00E+00	0.00E+00	0	1582	0.2578	7.00E-05	1.31E-03	0.00E+00	0
1508	0.2936	1.76E-02	0.00E+00	0.00E+00	0	1583	0.2572	1.99E-04	7.70E-04	0.00E+00	0
1509	0.2928	7.08E-02	0.00E+00	0.00E+00	0	1584	0.2566	5.55E-05	3.98E-04	0.00E+00	0
1510	0.292	4.02E-03	0.00E+00	0.00E+00	0	1585	0.256	7.00E-05	1.83E-04	0.00E+00	0
1511	0.292	5.51E-03	0.00E+00	0.00E+00	0	1586	0.2548	1.65E-04	6.54E-05	0.00E+00	0
1512	0.292	5.44E-03	0.00E+00	0.00E+00	0	1587	0.2536	2.19E-04	3.45E-05	0.00E+00	0
1513	0.292	1.30E-02	0.00E+00	0.00E+00	0	1588	0.2524	6.02E-05	9.18E-06	0.00E+00	0
1514	0.292	2.07E-02	0.00E+00	0.00E+00	0	1589	0.2512	5.55E-05	6.91E-06	0.00E+00	0
1515	0.292	3.80E-03	0.00E+00	0.00E+00	0	1590	0.25	1.18E-04	3.01E-06	0.00E+00	0
1516	0.2912	6.26E-03	0.00E+00	0.00E+00	0	1591	0.2502	9.36E-05	1.46E-06	0.00E+00	0
1517	0.2904	8.91E-03	0.00E+00	0.00E+00	0	1592	0.2504	2.33E-04	8.23E-07	0.00E+00	0
1518	0.2896	8.83E-03	0.00E+00	0.00E+00	0	1593	0.2506	8.41E-05	8.23E-07	0.00E+00	0
1519	0.2888	9.94E-03	0.00E+00	0.00E+00	0	1594	0.2508	1.80E-04	1.46E-06	0.00E+00	0
1520	0.288	4.05E-03	0.00E+00	0.00E+00	0	1595	0.251	1.02E-04	3.01E-06	0.00E+00	0
1521	0.2888	7.66E-04	0.00E+00	0.00E+00	0	1596	0.2512	1.45E-04	8.02E-06	0.00E+00	0
1522	0.2896	2.38E-03	0.00E+00	0.00E+00	0	1597	0.2514	2.79E-04	3.80E-05	0.00E+00	0
1523	0.2904	6.01E-04	3.09E-07	0.00E+00	0	1598	0.2516	9.35E-05	2.22E-04	0.00E+00	0
1524	0.2912	1.34E-03	1.46E-06	0.00E+00	0	1599	0.2518	9.16E-05	1.09E-03	0.00E+00	0
1525	0.292	2.97E-03	6.91E-06	0.00E+00	0	1600	0.252	5.85E-05	2.60E-03	0.00E+00	0
1526	0.2904	2.77E-03	1.16E-05	0.00E+00	0	1601	0.251	9.94E-05	4.87E-03	0.00E+00	0
1527	0.2888	3.03E-03	1.29E-05	0.00E+00	0	1602	0.25	1.70E-04	5.34E-03	0.00E+00	0
1528	0.2872	7.01E-04	1.16E-05	0.00E+00	0	1603	0.249	6.33E-05	5.90E-03	0.00E+00	0
1529	0.2856	1.58E-03	8.02E-06	0.00E+00	0	1604	0.248	6.99E-05	4.70E-03	0.00E+00	0
1530	0.284	2.33E-03	2.14E-05	0.00E+00	0	1605	0.247	6.01E-05	1.73E-03	0.00E+00	0
1531	0.2826	2.47E-03	4.92E-05	0.00E+00	0	1606	0.2474	6.66E-05	8.93E-04	0.00E+00	0
1532	0.2812	3.55E-04	1.39E-04	0.00E+00	0	1607	0.2478	6.33E-05	2.12E-03	0.00E+00	0
1533	0.2798	1.04E-04	3.08E-04	0.00E+00	0	1608	0.2482	1.48E-04	3.73E-03	0.00E+00	0
1534	0.2784	2.97E-04	5.04E-04	0.00E+00	0	1609	0.2486	8.41E-05	4.31E-03	0.00E+00	0
1535	0.277	9.33E-04	5.63E-04	0.00E+00	0	1610	0.249	8.59E-05	2.86E-03	0.00E+00	0
1536	0.2772	3.37E-04	3.18E-04	0.00E+00	0	1611	0.2488	1.14E-04	2.55E-03	0.00E+00	0
1537	0.2774	8.18E-04	1.81E-04	0.00E+00	0	1612	0.2486	6.33E-05	1.94E-03	0.00E+00	0
1538	0.2776	1.30E-04	4.92E-05	0.00E+00	0	1613	0.2484	1.36E-04	1.24E-03	0.00E+00	0

1614	0.2482	9.54E-05	7.00E-04	0.00E+00	0	1689	0.223	2.57E-04	4.92E-05	0.00E+00	0
1615	0.248	7.51E-05	4.43E-04	0.00E+00	0	1690	0.223	5.53E-04	9.20E-05	0.00E+00	0
1616	0.2474	8.96E-05	2.62E-04	0.00E+00	0	1691	0.222	3.59E-03	4.92E-04	0.00E+00	0
1617	0.2468	1.45E-04	1.72E-04	0.00E+00	0	1692	0.221	9.17E-04	1.50E-04	0.00E+00	0
1618	0.2462	6.99E-05	1.39E-04	0.00E+00	0	1693	0.22	1.33E-04	3.98E-05	0.00E+00	0
1619	0.2456	1.80E-04	8.97E-05	0.00E+00	0	1694	0.219	6.63E-04	5.11E-04	0.00E+00	0
1620	0.245	6.65E-05	5.11E-05	0.00E+00	0	1695	0.218	1.38E-04	1.45E-04	0.00E+00	0
1621	0.2458	6.65E-05	5.31E-05	0.00E+00	0	1696	0.2186	2.69E-04	1.04E-05	0.00E+00	0
1622	0.2466	7.16E-05	4.16E-05	0.00E+00	0	1697	0.2192	8.13E-03	3.88E-04	0.00E+00	0
1623	0.2474	6.99E-05	2.45E-05	0.00E+00	0	1698	0.2198	1.72E-04	1.69E-04	0.00E+00	0
1624	0.2482	7.16E-05	6.75E-05	0.00E+00	0	1699	0.2204	5.66E-04	5.92E-05	0.00E+00	0
1625	0.249	1.25E-04	1.56E-05	0.00E+00	0	1700	0.221	8.41E-04	2.72E-04	0.00E+00	0
1626	0.2484	7.16E-05	8.29E-05	0.00E+00	0	1702	0.219	1.45E-04	1.98E-04	0.00E+00	0
1627	0.2478	6.82E-05	6.12E-05	0.00E+00	0	1705	0.216	2.20E-03	3.93E-04	0.00E+00	0
1628	0.2472	7.16E-05	1.21E-04	0.00E+00	0	1710	0.207	2.25E-03	2.74E-04	0.00E+00	0
1629	0.2466	6.99E-05	7.40E-05	0.00E+00	0	1715	0.216	3.38E-03	7.67E-05	0.00E+00	0
1630	0.246	7.16E-05	1.02E-04	0.00E+00	0	1720	0.209	2.60E-03	1.09E-04	0.00E+00	0
1631	0.2452	7.50E-05	2.40E-04	0.00E+00	0	1725	0.2	5.67E-03	3.23E-04	0.00E+00	0
1632	0.2444	1.83E-04	5.51E-05	0.00E+00	0	1730	0.194	6.07E-03	2.38E-04	0.00E+00	0
1633	0.2436	1.52E-04	4.09E-04	0.00E+00	0	1735	0.193	9.18E-03	9.36E-05	0.00E+00	0
1634	0.2428	7.68E-05	8.97E-05	0.00E+00	0	1740	0.195	9.86E-03	8.04E-05	0.00E+00	0
1635	0.242	1.55E-04	4.73E-04	0.00E+00	0	1745	0.189	1.76E-02	3.87E-05	0.00E+00	0
1636	0.2408	7.68E-05	2.46E-04	0.00E+00	0	1750	0.191	1.01E-02	2.09E-05	0.00E+00	0
1637	0.2396	1.01E-04	1.06E-04	0.00E+00	0	1755	0.193	2.11E-02	1.50E-05	0.00E+00	0
1638	0.2384	7.67E-05	1.30E-03	0.00E+00	0	1760	0.188	1.35E-02	1.73E-05	0.00E+00	0
1639	0.2372	1.50E-04	1.89E-04	0.00E+00	0	1765	0.186	4.87E-02	4.32E-05	0.00E+00	0
1640	0.236	3.22E-04	1.66E-03	0.00E+00	0	1770	0.18	3.33E-02	9.36E-05	0.00E+00	0
1641	0.2366	8.21E-05	7.13E-04	0.00E+00	0	1775	0.176	8.28E-02	1.39E-04	0.00E+00	0
1642	0.2372	1.40E-04	4.02E-04	0.00E+00	0	1780	0.174	1.35E-01	5.43E-05	0.00E+00	0
1643	0.2378	8.96E-05	2.78E-03	0.00E+00	0	1785	0.173	2.67E-01	6.44E-05	0.00E+00	0
1644	0.2384	7.85E-05	3.52E-04	0.00E+00	0	1790	0.172	1.77E-01	2.72E-04	0.00E+00	0
1645	0.239	2.33E-04	9.63E-04	0.00E+00	0	1795	0.176	9.59E-01	6.09E-05	0.00E+00	0
1646	0.2384	3.53E-04	1.83E-03	0.00E+00	0	1800	0.172	1.36E+00	1.97E-05	0.00E+00	0
1647	0.2378	9.93E-05	2.19E-04	0.00E+00	0	1805	0.171	2.61E+00	4.47E-05	0.00E+00	0
1648	0.2372	1.29E-04	2.45E-03	0.00E+00	0	1810	0.163	3.62E+00	3.72E-05	0.00E+00	0
1649	0.2366	1.52E-04	7.17E-04	0.00E+00	0	1815	0.163	5.15E+00	2.47E-05	0.00E+00	0
1650	0.236	1.88E-04	3.56E-04	0.00E+00	0	1820	0.162	1.19E+01	6.22E-07	0.00E+00	0
1651	0.2364	1.16E-04	3.30E-03	0.00E+00	0	1825	0.159	7.36E+00	0.00E+00	0.00E+00	0
1652	0.2368	6.68E-04	1.34E-04	0.00E+00	0	1830	0.159	1.89E+01	0.00E+00	0.00E+00	0
1653	0.2372	3.57E-04	1.39E-04	0.00E+00	0	1835	0.153	3.52E+01	0.00E+00	0.00E+00	0
1654	0.2376	1.88E-04	1.89E-03	0.00E+00	0	1840	0.156	5.87E+01	0.00E+00	0.00E+00	0
1655	0.238	1.90E-04	1.66E-04	0.00E+00	0	1845	0.154	2.23E+01	0.00E+00	0.00E+00	0
1656	0.2378	2.85E-04	5.99E-04	0.00E+00	0	1850	0.151	3.58E+01	0.00E+00	0.00E+00	0
1657	0.2376	3.39E-04	2.49E-04	0.00E+00	0	1855	0.148	3.94E+01	0.00E+00	0.00E+00	0
1658	0.2374	2.39E-04	1.42E-05	0.00E+00	0	1860	0.146	2.70E+01	0.00E+00	0.00E+00	0
1659	0.2372	1.22E-04	1.61E-04	0.00E+00	0	1865	0.146	1.21E+01	0.00E+00	0.00E+00	0
1660	0.237	1.57E-04	1.09E-04	0.00E+00	0	1870	0.138	7.89E+01	0.00E+00	0.00E+00	0
1661	0.2362	4.01E-04	1.16E-05	0.00E+00	0	1875	0.138	7.01E+01	2.61E-05	0.00E+00	0
1662	0.2354	7.02E-04	2.65E-04	0.00E+00	0	1880	0.143	1.04E+01	1.09E-04	0.00E+00	0
1663	0.2346	1.70E-04	3.27E-05	0.00E+00	0	1885	0.141	1.28E+01	3.57E-05	0.00E+00	0
1664	0.2338	3.75E-04	2.29E-05	0.00E+00	0	1890	0.14	1.29E+01	8.79E-06	0.00E+00	0
1665	0.233	1.45E-04	1.79E-03	0.00E+00	0	1895	0.141	8.14E+00	1.10E-06	0.00E+00	0
1666	0.2328	5.53E-04	1.34E-02	0.00E+00	0	1900	0.136	4.03E+01	1.10E-06	0.00E+00	0
1667	0.2326	1.36E-04	1.84E-03	0.00E+00	0	1905	0.139	5.54E+01	1.10E-06	0.00E+00	0
1668	0.2324	9.33E-05	3.05E-04	0.00E+00	0	1910	0.141	1.18E+01	1.66E-06	0.00E+00	0
1669	0.2322	5.79E-04	6.96E-05	0.00E+00	0	1915	0.139	2.50E+01	6.22E-07	0.00E+00	0
1670	0.232	1.85E-04	4.92E-05	0.00E+00	0	1920	0.137	1.95E+01	6.22E-07	0.00E+00	0
1671	0.2304	2.39E-04	1.92E-04	0.00E+00	0	1925	0.135	7.28E+00	6.22E-07	0.00E+00	0
1672	0.2288	2.24E-04	3.98E-05	0.00E+00	0	1930	0.135	7.49E+00	2.33E-07	0.00E+00	0
1673	0.2272	1.59E-04	1.42E-05	0.00E+00	0	1935	0.134	2.79E+00	1.29E-05	0.00E+00	0
1674	0.2256	2.54E-04	3.42E-04	0.00E+00	0	1940	0.132	3.39E+00	5.89E-04	0.00E+00	0
1675	0.224	2.51E-04	2.37E-04	0.00E+00	0	1945	0.13	2.68E+00	7.10E-03	0.00E+00	0
1676	0.2242	5.18E-04	4.84E-06	0.00E+00	0	1950	0.129	9.47E-01	2.69E-02	0.00E+00	0
1677	0.2244	3.94E-04	2.10E-04	0.00E+00	0	1955	0.124	1.31E+00	9.53E-02	0.00E+00	0
1678	0.2246	5.79E-04	6.49E-04	0.00E+00	0	1960	0.128	8.17E-01	5.21E-02	0.00E+00	0
1679	0.2248	1.90E-04	8.02E-06	0.00E+00	0	1965	0.128	3.17E-01	6.35E-02	0.00E+00	0
1680	0.225	2.88E-04	2.45E-05	0.00E+00	0	1970	0.127	1.45E-01	3.35E-02	0.00E+00	0
1681	0.2246	1.38E-04	6.87E-04	0.00E+00	0	1975	0.132	1.04E-01	8.00E-03	0.00E+00	0
1682	0.2242	1.27E-04	3.10E-05	0.00E+00	0	1980	0.127	9.98E-02	1.33E-03	0.00E+00	0
1683	0.2238	1.75E-04	1.16E-05	0.00E+00	0	1985	0.125	6.08E-02	2.28E-04	0.00E+00	0
1684	0.2234	1.61E-03	1.34E-03	0.00E+00	0	1990	0.123	6.16E-02	2.30E-04	0.00E+00	0
1685	0.223	1.33E-04	4.16E-05	0.00E+00	0	1995	0.125	4.08E-02	5.78E-03	0.00E+00	0
1686	0.223	1.72E-04	2.29E-05	0.00E+00	0	2000	0.118	2.54E-02	1.41E-01	0.00E+00	0
1687	0.223	5.31E-04	6.70E-04	0.00E+00	0	2005	0.112	5.94E-02	2.67E-01	0.00E+00	0
1688	0.223	1.47E-04	1.11E-04	0.00E+00	0	2010	0.116	5.96E-03	1.36E-01	0.00E+00	0

2015	0.114	2.70E-02	1.73E-01	0.00E+00	0	2390	0.06	9.02E-02	3.17E-03	0.00E+00	0
2020	0.115	1.47E-02	9.04E-02	0.00E+00	0	2395	0.059	5.52E-02	4.15E-03	0.00E+00	0
2025	0.115	5.71E-03	2.63E-02	0.00E+00	0	2400	0.055	4.75E-02	2.31E-03	0.00E+00	0
2030	0.112	1.10E-02	6.90E-03	0.00E+00	0	2405	0.056	1.43E-01	2.21E-03	0.00E+00	0
2035	0.109	2.72E-03	3.79E-03	0.00E+00	0	2410	0.057	1.40E-01	9.30E-04	0.00E+00	0
2040	0.109	5.76E-03	4.25E-03	0.00E+00	0	2415	0.054	3.75E-01	6.30E-04	0.00E+00	0
2045	0.11	3.69E-03	5.92E-03	0.00E+00	0	2420	0.058	3.19E-01	5.92E-04	0.00E+00	0
2050	0.106	4.10E-03	3.73E-02	0.00E+00	0	2425	0.055	1.53E-01	1.19E-03	0.00E+00	0
2055	0.104	4.06E-03	6.50E-02	0.00E+00	0	2430	0.059	6.21E-02	4.63E-04	0.00E+00	0
2060	0.102	5.01E-03	3.14E-02	0.00E+00	0	2435	0.055	1.11E+00	4.69E-04	0.00E+00	0
2065	0.097	3.27E-03	4.68E-02	0.00E+00	0	2440	0.052	7.18E-02	2.96E-04	0.00E+00	0
2070	0.101	3.88E-03	3.41E-02	0.00E+00	0	2445	0.05	5.47E-01	2.35E-04	0.00E+00	0
2075	0.103	4.42E-03	1.55E-02	0.00E+00	0	2450	0.051	9.98E-01	2.23E-04	0.00E+00	0
2080	0.099	2.31E-03	4.75E-03	0.00E+00	0	2455	0.052	3.92E-01	1.24E-04	0.00E+00	0
2085	0.098	2.29E-03	5.64E-03	0.00E+00	0	2460	0.049	1.95E-01	8.60E-05	0.00E+00	0
2090	0.1	2.55E-03	3.41E-03	0.00E+00	0	2465	0.054	4.71E-01	5.26E-05	0.00E+00	0
2095	0.093	3.74E-03	1.38E-03	0.00E+00	0	2470	0.049	1.06E+00	5.93E-05	0.00E+00	0
2100	0.095	6.94E-03	5.89E-04	0.00E+00	0	2475	0.054	9.07E-01	1.85E-05	0.00E+00	0
2105	0.095	2.06E-03	4.66E-04	0.00E+00	0	2480	0.051	1.50E+00	2.35E-05	0.00E+00	0
2110	0.089	3.49E-03	5.89E-04	0.00E+00	0	2485	0.048	2.87E+00	8.04E-05	0.00E+00	0
2115	0.092	2.55E-03	2.58E-04	0.00E+00	0	2490	0.055	3.87E+00	5.26E-05	0.00E+00	0
2120	0.089	3.63E-03	2.23E-04	0.00E+00	0	2495	0.047	4.10E+00	2.35E-05	0.00E+00	0
2125	0.089	2.36E-03	9.17E-05	0.00E+00	0	2500	0.0512	1.80E+00	4.32E-05	0.00E+00	0
2130	0.089	2.46E-03	3.01E-05	0.00E+00	0	2505	0.0505	3.16E+00	1.50E-05	0.00E+00	0
2135	0.087	2.00E-03	7.85E-06	0.00E+00	0	2510	0.0491	3.28E+00	1.85E-05	0.00E+00	0
2140	0.092	1.35E-03	6.94E-06	0.00E+00	0	2515	0.0478	9.45E+00	2.47E-05	0.00E+00	0
2145	0.084	1.33E-03	3.43E-05	0.00E+00	0	2520	0.0469	3.72E+00	2.35E-05	0.00E+00	0
2150	0.083	3.69E-03	1.70E-04	0.00E+00	0	2525	0.0463	9.35E+00	1.97E-05	0.00E+00	0
2155	0.081	2.95E-03	1.47E-04	0.00E+00	0	2530	0.0466	3.29E+01	1.85E-05	0.00E+00	0
2160	0.084	4.51E-03	2.48E-04	0.00E+00	0	2535	0.046	3.08E+01	2.61E-05	0.00E+00	0
2165	0.082	4.18E-03	2.10E-04	0.00E+00	0	2540	0.0461	1.84E+01	1.29E-05	0.00E+00	0
2170	0.084	3.83E-03	1.79E-04	0.00E+00	0	2545	0.0458	8.71E+01	1.18E-05	0.00E+00	0
2175	0.079	4.23E-03	1.26E-04	0.00E+00	0	2550	0.0455	9.26E+01	3.72E-05	0.00E+00	0
2180	0.077	3.48E-03	2.03E-04	0.00E+00	0	2555	0.0452	3.16E+01	9.94E-05	0.00E+00	0
2185	0.069	1.10E-02	8.79E-05	0.00E+00	0	2560	0.0445	1.54E+02	4.16E-04	0.00E+00	0
2190	0.074	3.38E-03	3.43E-05	0.00E+00	0	2565	0.0443	2.21E+02	4.85E-04	0.00E+00	0
2195	0.075	4.15E-03	4.94E-05	0.00E+00	0	2570	0.0439	2.80E+02	4.69E-04	0.00E+00	0
2200	0.084	4.87E-03	3.66E-03	0.00E+00	0	2575	0.0433	3.97E+02	4.01E-04	0.00E+00	0
2205	0.077	4.45E-03	8.50E-04	0.00E+00	0	2580	0.043	2.37E+02	1.18E-04	0.00E+00	0
2210	0.077	2.78E-03	5.76E-05	0.00E+00	0	2585	0.0425	6.95E+02	5.20E-04	0.00E+00	0
2215	0.074	2.74E-03	2.53E-04	0.00E+00	0	2590	0.0422	4.44E+02	1.28E-03	0.00E+00	0
2220	0.079	2.01E-03	5.59E-04	0.00E+00	0	2595	0.0419	1.53E+03	8.57E-04	0.00E+00	0
2225	0.077	3.19E-03	6.82E-04	0.00E+00	0	2600	0.0417	3.43E+02	1.05E-03	0.00E+00	0
2230	0.077	1.20E-03	1.12E-03	0.00E+00	0	2605	0.0416	1.63E+03	5.13E-04	0.00E+00	0
2235	0.066	1.96E-03	1.43E-03	0.00E+00	0	2610	0.0413	6.78E+02	7.64E-04	0.00E+00	0
2240	0.061	1.20E-03	1.62E-03	0.00E+00	0	2615	0.0411	8.77E+02	1.00E-03	0.00E+00	0
2245	0.073	1.68E-03	2.65E-03	0.00E+00	0	2620	0.0409	1.01E+03	5.16E-04	0.00E+00	0
2250	0.077	1.28E-03	1.80E-03	0.00E+00	0	2625	0.0404	3.24E+02	3.37E-04	0.00E+00	0
2255	0.077	1.42E-03	4.11E-03	0.00E+00	0	2630	0.04	1.21E+03	2.96E-04	0.00E+00	0
2260	0.072	1.48E-03	4.13E-03	0.00E+00	0	2635	0.0396	2.84E+02	1.91E-04	0.00E+00	0
2265	0.073	1.35E-03	3.24E-03	0.00E+00	0	2640	0.0391	9.65E+01	7.67E-05	0.00E+00	0
2270	0.066	1.45E-03	6.13E-03	0.00E+00	0	2645	0.0389	2.46E+02	4.17E-05	0.00E+00	0
2275	0.065	1.46E-03	6.25E-03	0.00E+00	0	2650	0.0387	1.34E+02	6.61E-05	0.00E+00	0
2280	0.07	1.55E-03	3.02E-03	0.00E+00	0	2655	0.0386	4.19E+02	3.55E-04	0.00E+00	0
2285	0.067	1.56E-03	4.75E-03	0.00E+00	0	2660	0.0384	6.67E+02	9.78E-03	0.00E+00	0
2290	0.067	1.66E-03	6.30E-03	0.00E+00	0	2665	0.0383	1.80E+03	1.76E-01	0.00E+00	0
2295	0.066	1.76E-03	6.38E-03	0.00E+00	0	2670	0.0382	2.13E+03	9.39E-01	0.00E+00	0
2300	0.067	3.22E-03	9.38E-03	0.00E+00	0	2675	0.0378	1.16E+03	4.49E+00	0.00E+00	0
2305	0.064	3.69E-03	8.10E-03	0.00E+00	0	2680	0.0375	9.36E+02	8.68E+00	0.00E+00	0
2310	0.063	5.66E-03	1.50E-03	0.00E+00	0	2685	0.0372	5.81E+02	1.30E+01	0.00E+00	0
2315	0.059	5.47E-03	6.87E-03	0.00E+00	0	2690	0.0368	2.53E+02	4.10E+00	0.00E+00	0
2320	0.054	5.73E-03	1.28E-02	0.00E+00	0	2695	0.0365	1.10E+03	5.03E+00	0.00E+00	0
2325	0.056	7.71E-03	2.70E-03	0.00E+00	0	2700	0.036	3.18E+02	1.05E+01	0.00E+00	0
2330	0.056	4.95E-03	4.03E-03	0.00E+00	0	2705	0.0359	1.46E+02	6.72E+00	0.00E+00	0
2335	0.06	3.38E-03	4.45E-03	0.00E+00	0	2710	0.0357	1.31E+03	3.57E+00	0.00E+00	0
2340	0.059	2.15E-02	9.94E-03	0.00E+00	0	2715	0.0356	2.23E+02	1.55E+00	0.00E+00	0
2345	0.061	8.36E-03	9.66E-03	0.00E+00	0	2720	0.0355	1.44E+03	4.73E-01	0.00E+00	0
2350	0.062	3.15E-02	1.27E-02	0.00E+00	0	2725	0.0353	8.64E+02	2.93E-01	0.00E+00	0
2355	0.064	1.36E-02	9.19E-03	0.00E+00	0	2730	0.0352	7.84E+01	1.84E-01	0.00E+00	0
2360	0.066	1.11E-02	6.81E-03	0.00E+00	0	2735	0.0349	3.19E+02	2.26E-01	0.00E+00	0
2365	0.062	1.86E-02	2.99E-03	0.00E+00	0	2740	0.0348	1.49E+03	3.54E-01	0.00E+00	0
2370	0.062	6.29E-02	2.78E-02	0.00E+00	0	2745	0.0346	2.20E+02	1.06E+00	0.00E+00	0
2375	0.058	2.71E-02	9.35E-03	0.00E+00	0	2750	0.0345	1.80E+02	2.49E+00	0.00E+00	0
2380	0.056	6.31E-02	2.61E-03	0.00E+00	0	2755	0.0343	7.90E+02	6.76E+00	0.00E+00	0
2385	0.061	1.41E-01	4.72E-03	0.00E+00	0	2760	0.0341	2.65E+02	8.20E+00	0.00E+00	0

2765	0.0338	6.35E+02	3.40E+00	0.00E+00	0	3140	0.0206	1.03E+00	6.57E-04	3.89E-03	0
2770	0.0336	3.86E+02	2.32E+00	0.00E+00	0	3145	0.0205	1.20E+00	2.99E-04	4.67E-03	0
2775	0.0333	1.61E+02	6.55E+00	0.00E+00	0	3150	0.0204	4.80E-01	2.32E-03	4.87E-03	0
2780	0.0329	3.02E+02	6.05E+00	0.00E+00	0	3155	0.0203	6.06E-01	7.68E-04	4.48E-03	0
2785	0.0327	2.19E+02	3.59E+00	0.00E+00	0	3160	0.0202	2.31E-01	4.86E-03	3.70E-03	0
2790	0.0324	1.40E+02	1.97E+00	0.00E+00	0	3165	0.0202	5.31E-02	7.91E-03	2.72E-03	0
2795	0.0321	7.74E+01	1.26E+00	0.00E+00	0	3170	0.0201	1.10E-01	2.66E-03	2.14E-03	0
2800	0.032	8.41E+01	7.50E-01	0.00E+00	0	3175	0.02	1.91E-01	1.36E-02	1.56E-03	0
2805	0.0318	3.35E+02	6.35E-01	0.00E+00	0	3180	0.0199	2.00E-01	2.77E-03	1.36E-03	0
2810	0.0317	4.24E+01	4.38E-01	0.00E+00	0	3185	0.0198	1.93E-01	3.16E-02	1.17E-03	0
2815	0.0316	6.13E+01	3.48E-01	0.00E+00	0	3190	0.0198	7.35E-01	5.06E-03	1.17E-03	0
2820	0.0314	1.39E+02	2.56E-01	0.00E+00	0	3195	0.0197	1.28E+00	3.35E-02	1.17E-03	0
2825	0.0312	1.66E+01	1.61E-01	0.00E+00	0	3200	0.0196	6.08E+00	1.48E-02	1.56E-03	0
2830	0.0311	1.54E+01	1.05E-01	0.00E+00	0	3205	0.0195	9.09E+00	2.69E-02	1.36E-03	0
2835	0.0308	1.05E+02	4.89E-02	0.00E+00	0	3210	0.0194	8.22E+00	3.62E-02	1.75E-03	0
2840	0.0306	3.76E+01	5.88E-02	0.00E+00	0	3215	0.0193	4.44E+00	1.48E-02	1.17E-03	0
2845	0.0303	9.18E+00	6.01E-02	0.00E+00	0	3220	0.0192	1.75E+00	6.38E-02	1.36E-03	0
2850	0.03	3.83E+01	5.71E-02	0.00E+00	0	3225	0.0191	7.16E+00	8.02E-03	1.95E-03	0
2855	0.0297	5.57E+01	5.16E-02	0.00E+00	0	3230	0.0191	5.05E+00	4.93E-02	8.96E-03	0
2860	0.0294	1.14E+01	5.35E-02	0.00E+00	0	3235	0.019	3.56E-01	7.72E-03	3.70E-03	0
2865	0.0292	4.89E+00	5.56E-02	0.00E+00	0	3240	0.019	5.79E-01	6.78E-02	1.56E-03	0
2870	0.029	2.00E+01	3.21E-02	0.00E+00	0	3245	0.0189	4.54E+00	6.55E-03	1.17E-03	0
2875	0.0288	7.31E+00	2.07E-02	0.00E+00	0	3250	0.0189	6.83E-01	5.50E-02	1.75E-03	0
2880	0.0287	4.38E+00	2.31E-02	0.00E+00	0	3255	0.0187	1.90E-01	6.92E-03	2.33E-03	0
2885	0.0285	5.09E+00	2.12E-02	0.00E+00	0	3260	0.0186	1.22E+00	6.59E-02	2.33E-03	0
2890	0.0284	8.42E+00	1.68E-02	0.00E+00	0	3265	0.0185	1.90E+00	6.18E-03	2.53E-03	0
2895	0.0283	2.31E+00	8.56E-03	0.00E+00	0	3270	0.0184	1.55E+00	5.30E-02	8.62E-02	0
2900	0.0282	1.54E+01	5.26E-03	0.00E+00	0	3275	0.0183	5.71E-01	2.57E-03	1.68E-01	0
2905	0.0281	1.10E+01	2.41E-03	0.00E+00	0	3280	0.0182	7.67E-01	2.88E-02	7.75E-02	0
2910	0.0279	2.31E+00	9.89E-04	0.00E+00	0	3285	0.0182	1.36E-01	2.13E-03	4.82E-02	0
2915	0.0276	4.65E+00	3.93E-04	0.00E+00	0	3290	0.0182	1.50E-01	1.67E-02	6.22E-02	0
2920	0.0274	2.05E+00	1.75E-04	0.00E+00	0	3295	0.0181	1.73E+00	2.85E-03	6.66E-02	0
2925	0.0272	4.73E+00	9.36E-05	0.00E+00	0	3300	0.0179	1.36E+00	1.59E-02	6.72E-02	0
2930	0.0269	1.16E+00	5.10E-05	0.00E+00	0	3305	0.0177	8.18E-01	6.28E-03	5.64E-02	0
2935	0.0266	1.03E+00	2.22E-05	0.00E+00	0	3310	0.0175	3.84E-01	7.12E-02	4.58E-02	0
2940	0.0264	2.49E+00	1.08E-05	0.00E+00	0	3315	0.0174	5.10E-01	0.00E+00	3.75E-02	0
2945	0.0261	5.02E+00	3.57E-05	0.00E+00	0	3320	0.0172	5.71E+00	2.57E-01	2.58E-02	0
2950	0.0259	1.28E+00	1.52E-04	0.00E+00	0	3325	0.017	4.05E-01	8.28E-02	1.91E-02	0
2955	0.0258	1.97E+00	4.66E-04	0.00E+00	0	3330	0.0168	4.31E-01	9.67E-03	1.31E-02	0
2960	0.0256	1.06E+00	8.76E-04	0.00E+00	0	3335	0.0167	7.95E-02	2.27E-02	8.77E-03	0
2965	0.0255	6.10E-01	1.12E-03	0.00E+00	0	3340	0.0165	6.03E-01	1.71E-03	5.84E-03	0
2970	0.0254	8.81E+00	1.05E-03	0.00E+00	0	3345	0.0164	5.57E-01	3.99E-02	3.89E-03	0
2975	0.0253	4.43E+00	1.44E-03	0.00E+00	0	3350	0.0162	1.85E-01	3.35E-03	2.33E-03	0
2980	0.0251	2.14E+00	1.97E-03	0.00E+00	0	3355	0.0161	4.50E-01	3.84E-02	1.56E-03	0
2985	0.025	5.39E-01	1.26E-03	0.00E+00	0	3360	0.0159	3.79E-01	7.85E-03	9.72E-04	0
2990	0.0249	3.50E-01	6.64E-04	0.00E+00	0	3365	0.0159	2.36E-01	7.33E-03	5.83E-04	0
2995	0.0248	1.45E+00	6.30E-04	0.00E+00	0	3370	0.0158	2.32E-01	6.90E-02	3.89E-04	0
3000	0.0247	6.20E-01	1.28E-04	0.00E+00	0	3375	0.0157	1.36E-01	5.48E-03	1.94E-04	0
3005	0.0245	1.48E+00	1.41E-04	0.00E+00	0	3380	0.0156	8.31E-02	9.12E-02	1.94E-04	0
3010	0.0244	6.58E-01	2.48E-04	0.00E+00	0	3385	0.0156	1.35E-01	9.42E-03	1.94E-04	0
3015	0.0243	7.83E-01	2.64E-04	0.00E+00	0	3390	0.0155	1.35E-02	3.06E-02	1.94E-04	0
3020	0.0241	7.03E+00	1.72E-04	0.00E+00	0	3395	0.0155	3.18E-02	1.69E-02	1.94E-04	0
3025	0.024	5.61E-01	1.05E-04	0.00E+00	0	3400	0.0154	1.45E-02	6.13E-03	1.94E-04	0
3030	0.0239	9.23E-01	3.87E-05	0.00E+00	0	3405	0.0153	1.15E-01	7.63E-02	1.94E-04	0
3035	0.0238	1.63E+00	1.29E-05	0.00E+00	0	3410	0.0152	1.69E-01	5.99E-03	1.94E-04	0
3040	0.0237	2.44E+00	4.42E-06	0.00E+00	0	3415	0.0152	1.95E-02	5.55E-02	1.94E-04	0
3045	0.0236	1.34E+00	1.66E-06	0.00E+00	0	3420	0.0151	7.18E-03	7.23E-03	1.94E-04	0
3050	0.0235	4.95E+00	6.22E-07	0.00E+00	0	3425	0.015	7.88E-03	2.55E-02	1.94E-04	0
3055	0.0235	7.01E+00	3.66E-06	0.00E+00	0	3430	0.0149	3.94E-03	4.31E-02	1.94E-04	0
3060	0.0234	7.16E-01	2.33E-07	0.00E+00	0	3435	0.0148	1.93E-02	3.77E-03	3.89E-04	0
3065	0.0232	1.38E+00	2.33E-07	0.00E+00	0	3440	0.0147	1.23E-02	4.14E-02	3.89E-04	0
3070	0.0231	2.94E+00	2.33E-07	0.00E+00	0	3445	0.0147	2.01E-02	5.44E-03	3.89E-04	0
3075	0.023	7.80E-01	1.10E-06	0.00E+00	0	3450	0.0146	3.83E-03	1.50E-02	1.94E-04	0
3080	0.0228	1.17E+00	6.22E-07	0.00E+00	0	3455	0.0146	2.84E-02	2.36E-02	1.94E-04	0
3085	0.0226	2.54E+00	0.00E+00	0.00E+00	0	3460	0.0145	1.21E-02	1.71E-03	1.94E-04	0
3090	0.0224	1.95E+00	1.66E-06	0.00E+00	0	3465	0.0145	3.92E-03	2.73E-02	1.94E-04	0
3095	0.0222	5.11E+00	2.27E-06	0.00E+00	0	3470	0.0144	8.82E-03	4.39E-03	1.94E-04	0
3100	0.022	1.04E+00	1.66E-06	0.00E+00	0	3475	0.0143	1.07E-02	9.26E-03	1.94E-04	0
3105	0.0218	4.13E+00	1.08E-05	0.00E+00	0	3480	0.0142	5.46E-03	1.22E-02	1.94E-04	0
3110	0.0216	5.11E+00	2.35E-05	0.00E+00	0	3485	0.0142	7.60E-03	3.84E-03	1.94E-04	0
3115	0.0214	1.81E+00	3.87E-05	0.00E+00	0	3490	0.0141	1.33E-02	1.16E-02	1.94E-04	0
3120	0.0212	3.28E-01	4.94E-05	7.78E-04	0	3495	0.0141	6.92E-03	3.84E-03	1.94E-04	0
3125	0.021	1.22E+00	2.25E-04	8.77E-03	0	3500	0.014	8.63E-03	3.22E-03	1.94E-04	0
3130	0.0209	6.47E-01	1.39E-04	9.55E-03	0	3505	0.0139	7.94E-03	3.89E-03	1.94E-04	0
3135	0.0208	2.28E-01	2.90E-04	3.31E-03	0	3510	0.0138	1.00E-02	1.75E-03	1.94E-04	0

3515	0.0138	2.07E-02	9.26E-04	1.94E-04	0
3520	0.0137	1.06E-02	1.11E-03	0.00E+00	0
3525	0.0137	1.57E-02	1.46E-03	0.00E+00	0
3530	0.0136	1.41E-02	3.31E-03	0.00E+00	0
3535	0.0136	2.15E-02	9.37E-03	0.00E+00	0
3540	0.0135	2.70E-02	1.22E-02	0.00E+00	0
3545	0.0135	2.00E-02	1.04E-02	0.00E+00	0
3550	0.0134	2.02E-02	3.37E-03	0.00E+00	0
3555	0.0133	4.49E-02	3.10E-03	0.00E+00	0
3560	0.0132	1.34E-02	2.52E-03	0.00E+00	0
3565	0.0132	8.16E-03	6.45E-03	2.92E-03	0
3570	0.0131	5.64E-02	3.81E-03	1.84E-02	0
3575	0.013	3.18E-02	1.01E-02	2.78E-02	0
3580	0.0129	1.22E-02	4.63E-03	2.03E-02	0
3585	0.0129	2.61E-02	6.97E-03	8.18E-03	0
3590	0.0128	2.99E-02	3.14E-03	1.62E-02	0
3595	0.0128	2.38E-02	1.83E-03	9.74E-03	0
3600	0.0127	1.54E-02	1.23E-03	1.13E-02	0
3605	0.0127	6.92E-03	5.89E-03	1.48E-02	0
3610	0.0126	2.58E-02	2.84E-03	1.41E-02	0
3615	0.0126	2.74E-02	7.24E-04	1.19E-02	0
3620	0.0125	4.05E-03	6.33E-04	8.96E-03	0
3625	0.0125	1.04E-02	3.02E-03	7.60E-03	0
3630	0.0124	1.82E-02	1.39E-03	5.06E-03	0
3635	0.0124	1.51E-02	6.96E-04	3.70E-03	0
3640	0.0123	4.00E-03	6.61E-04	2.53E-03	0
3645	0.0123	3.71E-03	3.99E-03	1.95E-03	0
3650	0.0122	9.80E-03	2.46E-03	1.95E-03	0
3655	0.0122	8.59E-03	2.96E-04	3.89E-03	0
3660	0.0121	7.28E-03	2.03E-04	1.17E-03	0
3665	0.0121	9.42E-03	2.40E-03	5.83E-04	0
3670	0.012	5.88E-02	1.76E-03	1.94E-04	0
3675	0.012	2.51E-01	1.30E-04	5.83E-04	0
3680	0.0119	6.60E-02	2.20E-04	5.83E-04	0
3685	0.0118	2.35E-02	1.57E-03	5.83E-04	0
3690	0.0117	1.53E-02	1.77E-03	5.83E-04	0
3695	0.0117	1.24E-02	2.53E-04	3.89E-04	0
3700	0.0116	3.59E-03	2.53E-04	3.89E-04	0
3705	0.0116	3.55E-03	6.82E-04	3.89E-04	0
3710	0.0115	1.43E-02	1.94E-03	3.89E-04	0
3715	0.0115	1.59E-02	6.30E-04	3.89E-04	0
3720	0.0114	6.53E-03	1.11E-04	1.94E-04	0
3725	0.0114	6.53E-03	6.92E-04	1.94E-04	0
3730	0.0113	1.32E-02	9.81E-04	1.94E-04	0
3735	0.0113	2.89E-02	6.89E-04	1.94E-04	0
3740	0.0112	1.88E-02	3.09E-04	1.94E-04	0
3745	0.0112	8.34E-03	4.29E-04	1.94E-04	0
3750	0.011	1.16E-02	5.76E-04	1.94E-04	0
3755	0.011	1.90E-02	2.38E-04	0.00E+00	0
3760	0.0109	2.03E-02	9.94E-05	0.00E+00	0
3765	0.0109	2.11E-02	6.30E-04	0.00E+00	0
3770	0.0108	1.63E-02	2.96E-04	0.00E+00	0
3775	0.0108	1.25E-02	3.09E-04	0.00E+00	0
3780	0.0107	7.53E-03	3.37E-04	0.00E+00	0
3785	0.0107	2.12E-02	4.04E-04	0.00E+00	0
3790	0.0106	3.16E-02	5.36E-04	0.00E+00	0
3795	0.0106	1.31E-02	6.57E-04	0.00E+00	0
3800	0.0105	3.75E-03	7.68E-04	0.00E+00	0
3805	0.0105	7.66E-03	4.88E-04	0.00E+00	0
3810	0.0104	2.44E-02	3.87E-04	0.00E+00	0
3815	0.0104	3.22E-02	2.99E-04	0.00E+00	0
3820	0.0103	5.12E-03	5.26E-04	0.00E+00	0
3825	0.0103	3.42E-03	2.10E-04	0.00E+00	0
3830	0.0102	7.85E-03	1.63E-04	0.00E+00	0
3835	0.0102	3.15E-02	4.26E-04	0.00E+00	0
3840	0.0101	6.62E-03	1.12E-03	0.00E+00	0
3845	0.0101	4.03E-03	2.42E-03	0.00E+00	0
3850	0.01	3.37E-03	2.53E-03	0.00E+00	0
3855	0.01	7.58E-03	2.37E-03	0.00E+00	0
3860	0.0099	1.01E-02	6.30E-03	0.00E+00	0
3865	0.0099	6.21E-03	1.09E-02	0.00E+00	0
3870	0.0098	3.18E-03	1.70E-02	0.00E+00	0
3875	0.0098	6.74E-03	2.02E-02	0.00E+00	0
3880	0.0097	4.34E-03	2.38E-02	0.00E+00	0
3885	0.0097	5.03E-03	2.23E-02	0.00E+00	0
3890	0.0097	2.88E-03	2.09E-02	0.00E+00	0
3895	0.0096	3.87E-03	1.57E-02	0.00E+00	0
3900	0.0096	6.96E-03	3.82E-03	0.00E+00	0
3905	0.0096	3.46E-03	1.01E-02	0.00E+00	0
3910	0.0095	2.72E-03	1.81E-02	0.00E+00	0
3915	0.0095	3.57E-03	1.84E-02	0.00E+00	0
3920	0.0094	5.09E-03	1.72E-02	0.00E+00	0
3925	0.0094	2.99E-03	1.74E-02	0.00E+00	0
3930	0.0093	3.37E-03	1.60E-02	0.00E+00	0
3935	0.0093	2.26E-03	1.30E-02	0.00E+00	0
3940	0.0092	2.61E-03	1.24E-02	0.00E+00	0
3945	0.0092	3.85E-03	1.04E-02	0.00E+00	0
3950	0.0091	3.78E-03	8.49E-03	0.00E+00	0
3955	0.0091	2.35E-03	7.91E-03	0.00E+00	0
3960	0.009	2.31E-03	6.89E-03	0.00E+00	0
3965	0.009	2.52E-03	6.12E-03	0.00E+00	0
3970	0.0089	2.91E-03	6.30E-03	0.00E+00	0
3975	0.0089	2.87E-03	7.86E-03	0.00E+00	0
3980	0.0088	2.38E-03	8.81E-03	0.00E+00	0
3985	0.0088	2.23E-03	7.69E-03	2.00E-04	0
3990	0.0088	2.37E-03	8.03E-03	2.00E-04	0
3995	0.0087	2.41E-03	8.98E-03	2.00E-04	0
4000	0.0087	2.38E-03	1.41E-04	2.00E-04	0
4005	0.00866	1.53E-02	1.70E-04	2.00E-04	0
4010	0.00862	1.24E-02	2.61E-04	2.00E-04	0
4015	0.00858	3.59E-03	1.68E-04	0.00E+00	0
4020	0.00854	3.55E-03	1.77E-04	0.00E+00	0